# Horns Rev 3 offshore wind farm: hydrography, sediment spill, water quality, geomorphology and coastal morphology

**Technical Report** · April 2014



David Brew
Royal HaskoningDHV, Peterborough, United Kingdom



N.T. Hoan
National University of Civil Engineering



Keming Hu
Royal HaskoningDHV

Energinet.dk

# Horns Rev 3 Offshore Wind Farm

Technical report no. 3

## HYDROGRAPHY, SEDIMENT SPILL, WATER QUALITY, GEOMORPHOLOGY AND COASTAL MORPHOLOGY

APRIL 2014

Energinet.dk

# Horns Rev 3 Offshore Wind Farm

## HYDROGRAPHY, SEDIMENT SPILL, WATER QUALITY, GEOMORPHOLOGY AND COASTAL MORPHOLOGY

---

| | |
|---|---|
| **Client** | Energinet.dk<br>Att. Indkøb<br>Tonne Kjærsvej 65<br>DK-7000 Fredericia |
| **Consultant** | Orbicon A/S<br>Ringstedvej 20<br>DK-4000 Roskilde |
| **Sub-consultant** | Royal HaskoningDHV<br>Rightwell House, Bretton<br>Peterborough, PE3 8DW<br>United Kingdom |
| **Project no.** | 3621200091 |
| **Document no.** | HR-TR-035 |
| **Version** | 05 |
| **Prepared by** | DR. David S. Brew, Hoan Nguyen, DR. Keming Hu,<br>DR. Christa Page |
| **Reviewed by** | DR. Nick Cooper |
| **Approved by** | Kristian Nehring Madsen |
| **Cover photo** | Scott Wischhof |
| **Photos** | Unless specified © Orbicon A/S – Energinet.dk |
| **Published** | April 2014 |

## TABLE OF CONTENTS

## SUMMARY

This report provides an assessment of the potential impacts of the proposed Horns Rev 3 offshore wind farm development on hydrography, sediment spill, water quality, geomorphology and coastal morphology both offshore and along the nearest shore line of Denmark. In order to assess the potential impacts of the wind farm (including all associated infrastructure), the export cable corridor and the landfall site, relative to baseline (existing) conditions, a combination of detailed numerical modelling and expert assessment has been employed. These impacts have been assessed using the worst case characteristics of the proposed development as provided by the project and presented as the Technical Project Description (Energinet.dk, 2014). Considerations of the proposed impacts upon the wave, tidal current, sediment transport and water quality regimes have been made for the construction, operation and decommissioning phases of the development.

### Pressures during Construction

Over the period of construction there is the likelihood for discrete short-term disturbances of the offshore seabed as the wind turbine foundations are installed and the export and inter-array cables are installed sequentially across the development site. Seabed sediments have the potential to be released into the water column resulting in the formation and distribution of sediment plumes. At the landfall site, construction activities may result in short-term changes to the sediment budget, as infrastructure causes temporary blockages to alongshore sediment transport.

In this assessment, the worst case scenario regarding sediment spill and transport was considered to be seabed preparation for concrete GBS foundations and jetting for inter-array cable installation and was consequently modelled together over a 30-day installation period. A worst case total of nine foundations in four blocks were assumed to be installed synchronously followed by the laying of six inter-array cables per block. In the modelled worst case scenario foundations were located around the perimeter of the pre-investigation area to provide an indication of the worst geographical spread of sediment released into the water column.

The results show that the worst case sediment plume attains suspended sediment concentrations of greater than 200mg/l but only in small local patches. Concentrations reduce to zero within 500m of the foundations and cable transects in all directions. Across the majority of each block of nine foundations, suspended sediment concentrations are generally less than 100mg/l. Maximum concentrations quickly reduce until they are zero up to 500m from the foundations in all directions. Suspended sediment concentrations greater than 10mg/l are only exceeded up to 0.5% of the simulation period. Maximum bed thickness change (sediment deposition from the plume) throughout the 30-day simulation period was predicted to be about 50mm locally around the foundations, decreasing to zero less than 200m from the foundations.

The effect on sediment transport of jetting the export cable and seabed preparation for substation installation was modelled over a 15-day simulation period. Along the export cable, the suspended sediment concentration was predicted to reach a maximum of greater than 200mg/l along the line of the jet, reducing to zero up to 2km to the north and south. Suspended sediment concentrations greater than 10mg/l are only exceeded up to 1.5% of the simulation period. Maximum bed thickness change throughout the simulation period was predicted to be up to 30mm near the coast, decreasing to less than 15mm along the majority of the cable route, decreasing to zero up to 200m away.

Concentrations of chemical contaminants within the offshore sediments were shown to be low in the sediment sampling undertaken during baseline mapping. Hence, changes to concentrations of chemical contaminants in the water column are not anticipated. Samples were not collected along the export cable route but the re-suspension of sediments is so short lived during cable installation that large changes to chemical concentrations in the water column are not anticipated.

At the coastal landfall site, sediment transport has the potential to be affected by the temporary construction of infrastructure. The worst case scenario is considered to be construction, over a continuous period of two weeks, of an open trench across the intertidal (beach) zone. The trench would offer a partial barrier to alongshore sediment transport, which is to the south. The results of expert assessment showed that the magnitude of change will be temporary and the presence of the trench will not have a longer term effect on natural coastal processes.

### Pressures during Operation

The greatest potential for changes in tidal current and wave regimes occurs during the operational stage of the wind farm. In this assessment, the effect of operation on these processes was modelled using a worst case layout of 3MW foundations across the western half of the pre-investigation area (the shallowest water). No potential effects are considered for the inter-array and export cables because, during operation, they will be buried.

The results show predicted changes to both tidal currents and waves would be relatively small. The maximum change to depth-averaged current velocity is predicted to be +/-0.008m/s with the greatest reductions and increases predicted to occur along and between, respectively, the north-south lines of foundations. Predicted changes in significant wave height were simulated for one-year and 50-year waves approaching from the northwest, west and southwest. Significant wave heights are predicted to change by a maximum of +/-0.007m adjacent to each of the foundation locations.

The predicted changes in tidal current velocities and wave heights are so small that they would not translate into changes to sediment transport pathways and morphology.

No changes to the existing water quality are anticipated during the operation of Horns Rev 3.

### Pressures during Decommissioning

The decommissioning phase is generally considered to incur similar or lesser changes to tidal, wave and sediment spill and transport than the construction phase.

### Cumulative Effects

Cumulative effects with Horns Rev 1 and Horns Rev 2 offshore wind farms have been considered with respect to interaction of hydrography and water quality. It is unlikely that the construction plumes or the changes to tidal currents and waves caused by development of Horns Rev 3 will interact with the operational effects of Horns Rev 1 and Horns Rev 2.

### Impact Assessment

The table below describes the impact significance for the environmental factors related to hydrography and water quality during construction, operation and decommissioning of the wind farm.

*Horns Rev 2 Offshore Wind Farm*

| Phase | Environmental Factor | Impact Significance |
|---|---|---|
| Construction | Suspended sediment concentrations and deposition (foundations and cables) | Negligible Negative |
| | Water quality associated with re-suspension of contaminated sediments (foundations and cables) | No Impact |
| | Water quality associated with re-suspension of nutrients (foundations and cables) | No Impact |
| | Water quality associated with use of construction materials | Negligible Negative |
| | Natura 2000 sites | No Impact |
| Operation | Changes to tidal currents (foundations) | No Impact |
| | Changes to waves (foundations) | No Impact |
| | Water quality associated with use of maintenance materials | Negligible Negative |
| | Natura 2000 sites | No Impact |
| Decommissioning | Suspended sediment concentrations and deposition (foundations and cables) | Negligible Negative |
| | Hydrography and water quality (foundations and cables) | Negligible Negative |
| | Hydrography and water quality (turbine components and ancillary structures) | Negligible Negative |
| | Natura 2000 sites | No Impact |

## 1. INTRODUCTION

### 1.1. Horns Rev 3 Offshore Wind Farm

The proposed Horns Rev 3 Offshore Wind Farm is located north of Horns Rev (Horns Reef) in a shallow area in the eastern North Sea (Figure 1.1). Horns Rev is a geomorphological feature that extends approximately 40km into the North Sea west of Blåvands Huk, the westernmost point of Denmark. The area outlined for development (pre-investigation area) occupies approximately 160km$^2$ about 20-30km west-northwest of Blåvands Huk. Horns Rev 3 is located to the immediate northeast of the existing Horns Rev 2 Offshore Wind Farm and approximately 20km north-northwest of the existing Horns Rev 1 Offshore Wind Farm (Figure 1.1). Energinet.dk has agreed with the Danish Energy Agency for a target capacity of 400 Megawatt (MW) for Horns Rev 3.

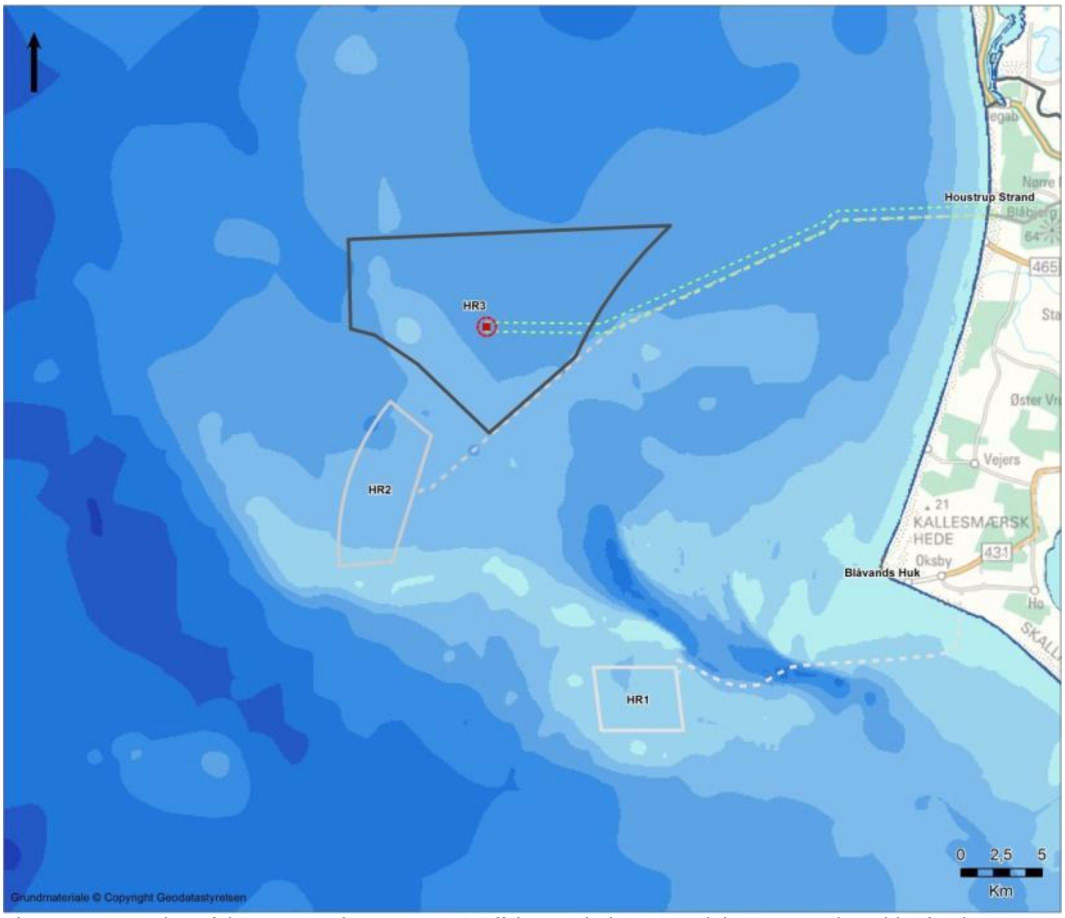


Figure 1.1. Location of the proposed Horns Rev 3 Offshore Wind Farm and the proposed corridor for the export cables towards shore.

Electricity from Horns Rev 3 will be transferred to shore by an export cable, which will be routed to a landfall site across the beach and dunes at Houstrup Strand (Figure 1.1). The proposed works to install the cable will be both offshore and onshore, as the cable runs from the wind farm to the coast. An export cable corridor has been delineated which is 1,000m wide from the platform to shore, with the flexibility to place the cable anywhere within the corridor. The corridor exits from a substation in the centre of the pre-investigation area and is approximately 34km long from its offshore connection to the beach at Houstrup Strand. The location of the landfall corridor is shown in Figure 1.2.


Figure 1.2. Landfall location of the Horns Rev 3 export cable at Houstrup Strand.

## 1.2. Objectives

This report provides an assessment of the potential changes to prevailing hydrodynamic, geomorphological, coastal morphology and water quality conditions arising as a result of the construction, operation and decommissioning of Horns Rev 3, both alone and cumulatively with Horns Rev 1 and Horns Rev 2. The assessment of effects, in turn, informs the assessment of direct, indirect and cumulative impacts on a range of parameters (e.g. benthic ecology, fisheries) that will be studied as separate parts of the EIA process.

This report presents an understanding of the existing coastal and marine physical processes across the Horns Rev 3 pre investigation area, the associated export cable corridor and the landfall site. This is followed by the definition of worst case scenarios for each element of the development in terms of their potential effects on hydrography, sediment spill, water quality, geomorphology and coastal morphology which are then compared to the existing conditions through expert judgment and numerical modelling.

The potential effects have been assessed conservatively using worst case characteristics for the proposed Horns Rev 3 project. This is because the specific details of the project have not been resolved and there are still a number of alternatives available in the choice of, for example, turbine type, foundation type and layout prior to application. The use of worst case is an acknowledged EIA approach where the details of the whole project are not available when the application is submitted. The worst case scenario for each individual impact is used so that it can be safely assumed that all lesser options will have less potential impact.

## 1.3. Project Description

The key components of the Horns Rev 3 offshore wind farm development, in the context of potential effects on hydrography, sediment spill and water quality, are the type and size of foundations and their layout pattern, the installation approach and duration of foundations, export and inter-array cables as well as construction works at the landfall site.

### 1.3.1 Foundation Type and Layout

A number of wind turbine foundation types are being considered, including concrete gravity base structures (GBS), driven steel monopiles, jackets and suction buckets (Energinet.dk, 2014). A range of different foundation types and sizes could be combined to create the 400MW capacity for Horns Rev 3. Energinet.dk is considering three wind turbine sizes:

- a minimum size 3MW of which 134-136 foundations could be installed to reach the 400MW capacity;
- an 8MW wind turbine where 50-52 foundations would provide 400MW of power; and
- a maximum size 10MW with installation of 40-42 foundations.

The 3MW and 10MW wind turbines are the minimum and maximum sizes being considered so that any turbine between these two sizes will be covered by the assessment of effects. Energinet.dk has tested several layouts of 3MW, 8MW and 10MW wind turbines in terms of derived annual energy production. As the size of the pre-investigation area is spacious relative to installation of 400MW of power, the turbines may potentially be installed in various sectors of the area. To encompass likely scenarios, three different locations across the pre-investigation area have been established for each turbine size. These layouts, shown in Figures 1.3 to 1.5, are:

- western side of the pre-investigation area furthest from the shore (Figure 1.3).
- centre of the pre-investigation area (Figure 1.4); and
- eastern side of the pre-investigation area closest to the shore (Figure 1.5).

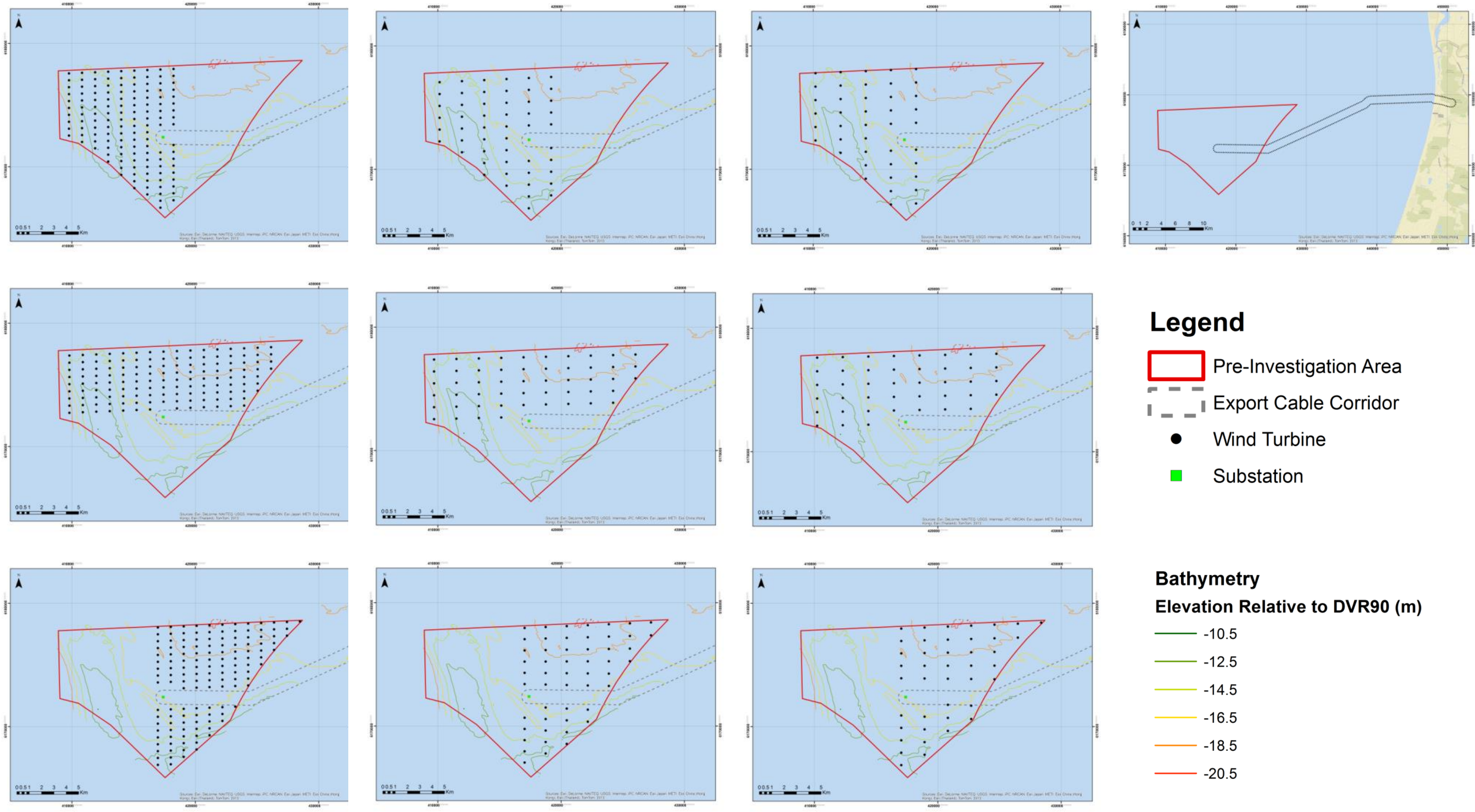


Figure 1.3. Potential layouts for 3MW (left column), 8MW (middle column) and 10MW (right column) for wind turbines across the pre-investigation area. Bathymetry was collected by Energinet.dk in July and August 2012 (Ramboll, 2013a, b)

### 1.3.2 Substation

The maximum number of each size of turbine excludes the substation, which is located towards the centre of the pre-investigation area (Figure 1.3). Foundation options for the platform are a jacket with four legs piled into the seabed or a hybrid four-legged structure built on top of a solid concrete caisson on the seabed (Energint.dk, 2013).

### 1.3.3 Installation of Foundations

The greatest effect on hydrography and water quality during the construction phase of the development will depend on the installation method used; different installation methods are required for different foundation types. Concrete GBS foundations rely on their mass including ballast to withstand the loads generated by the offshore environment and the wind turbine. For GBS foundations, an area of seabed may need to be dredged in order to provide a levelled surface upon which they are installed. Seabed preparation may also be needed for installation of a concrete caisson for the substation. No seabed preparation is necessary for any other foundation type; however, jackets may need pre-dredging prior to piling for each jacket leg.

### 1.3.4 Installation of Cables

The Horns Rev 3 export and inter-array cables will be installed using jetting (Energinet.dk, 2014). Jetting works by fluidising the seabed using a combination of high-flow, low pressure and low flow, high pressure water jets to cut into sands, gravels and low to medium strength clays. For Horns Rev 3, the seabed consists of predominantly sand (Section 4). The jetting to the desired depth (maximum 2m offshore increasing to 3-5m into the beach) will take place from the landfall and seawards.

## 1.4. Potential Impacts during Construction

During the construction phase of the proposed Horns Rev 3 offshore wind farm, there is potential for turbine, foundation and cable installation activities to cause water and sediment disturbance effects, potentially resulting in changes in water quality, suspended sediment concentrations and/or sea bed or shoreline levels due to deposition or erosion. These potential impacts include:

- Changes in suspended sediment concentrations and associated water quality due to foundation installation;
- Changes in sea bed levels due to foundation installation;
- Changes in water quality associated with re-suspension of nutrients due to foundation installation;
- Changes in suspended sediment concentrations and associated water quality due to inter-array cable installation;
- Changes in sea bed levels due to inter-array cable installation;
- Changes in water quality associated with re-suspension of nutrients due to inter-array cable installation;
- Changes in suspended sediment concentrations due to export cable installation;
- Changes in sea bed levels due to export cable installation;

- Changes in water quality associated with re-suspension of nutrients due to export cable installation;
- Changes in water quality associated with use of construction materials; and
- Changes to suspended sediment concentrations and coastal morphology at the export cable landfall.

## 1.5. Potential Impacts during Operation

During the operational phase of the proposed Horns Rev 3 offshore wind farm, there is potential for the presence of the foundations to cause changes to the tidal and wave regimes due to physical blockage effects and to water quality. These potential impacts include:

- Changes to the tidal regime due to the presence of foundation structures;
- Changes to the wave regime due to the presence of foundation structures; and
- Changes in water quality associated with use of maintenance materials

## 1.6. Potential Impacts during Decommissioning

During the decommissioning phase, there is potential for turbine, foundation and cable removal activities to cause changes in water quality and suspended sediment concentrations and/or sea bed or shoreline levels as a result of water and sediment disturbance effects.  The types of effect will be comparable to those identified for the construction phase:

- Changes in suspended sediment concentrations and associated water quality due to foundation removal;
- Changes in sea bed levels due to foundation removal;
- Changes in water quality associated with re-suspension of nutrients due to foundation removal;
- Changes in suspended sediment concentrations and associated water quality due to inter-array cable removal;
- Changes in sea bed levels due to inter-array cable removal;
- Changes in water quality associated with re-suspension of nutrients due to inter-array cable removal;
- Changes in suspended sediment concentrations due to export cable removal;
- Changes in sea bed levels due to export cable removal;
- Changes in water quality associated with re-suspension of nutrients due to export cable removal;
- Changes in water quality associated with use of decommissioning materials; and
- Changes to suspended sediment concentrations and coastal morphology at the export cable landfall.

## 1.7. Environmental Designations

The proposed Horns Rev 3 Offshore Wind Farm is located north of Horns Rev (Horns Reef) in a shallow area in the eastern North Sea in a region with several internationally protected Natura 2000 sites.  The aim of the Natura 2000 network is to assure the long-term survival of Europe's most valuable and threatened species and habitats. The network is comprised of Special Areas of Conservation (SAC) designated by Member States under the Habitats Directive and Special Protection Areas (SPAs) which were designated under the 1979 Birds Directive.

Five Natura 2000 sites (Figure 1.4), one marine site and four terrestrial sites are located within approximately 40km of the proposed wind farm area. Each of the sites is composed of one or more SPA´s or SAC's:

- Natura 2000 site 246 is a marine site located about 25km south of the proposed wind farm area. The site includes SPA 113 Sydlige Nordsø.
- Natura 2000 site 69 is situated on land about 35km east of the proposed wind farm. The site includes SPA 43 Ringkøbing Fjord and SAC 62 Ringkøbing Fjord og Nymindestrømmen.
- Natura 2000 site 83 is situated on land about 40km east of the proposed wind farm. The site includes SAC 72 Blåbjerg Egekrat, Lyngbos Hede og Hennegårds Klitter.
- Natura 2000 site 84 is situated on land about 35km east of the proposed wind farm area. The site includes SPA 50 Kallesmærsk Hede og Grærup Langsø and SAC 73 Kallesmærsk Hede, Grærup Langsø, Fiilsø og Kærgård Klitplantage.
- Natura 2000 site 89 is situated on land about 35km east of the proposed wind farm. The site includes SPA 57 Vadehavet and SAC 78 Vadehavet med Ribe Å, Tved Å og Varde Å vest for Varde.

Each Natura 2000 site is designated in order to protect specific species and habitats. All EU Member States are committed to carry out appropriate conservation measures to maintain and restore the species and habitats, for which the site has been designated, to a favourable conservation status. All activities that could significantly disturb these species or deteriorate the habitats of the protected species or habitat types must be avoided and cannot be approved by the authorities.


*Figure 1.4. Natura 2000 areas*

## 1.8. Assessment Methodology

The generic assessment methodology adopted to understand impacts of Horns Rev 3 follows the methods for EIA published by Orbicon (2013) (Figure 1.4). In this method the overall goal is to describe the Severity of Impact caused by Horns Rev 3. The assessment begins with two steps; to define the magnitude of the pressure and the sensitivity of the environmental factor. Combining the magnitude of the pressure and sensitivity gives the Degree of Impact, which, in turn is combined with the importance to give the Severity of Impact. It may be necessary to consider the risk of a certain impact occurring, and in these cases, the Severity of Impact is considered against the Likelihood of the occurrence, giving the Degree of Risk.

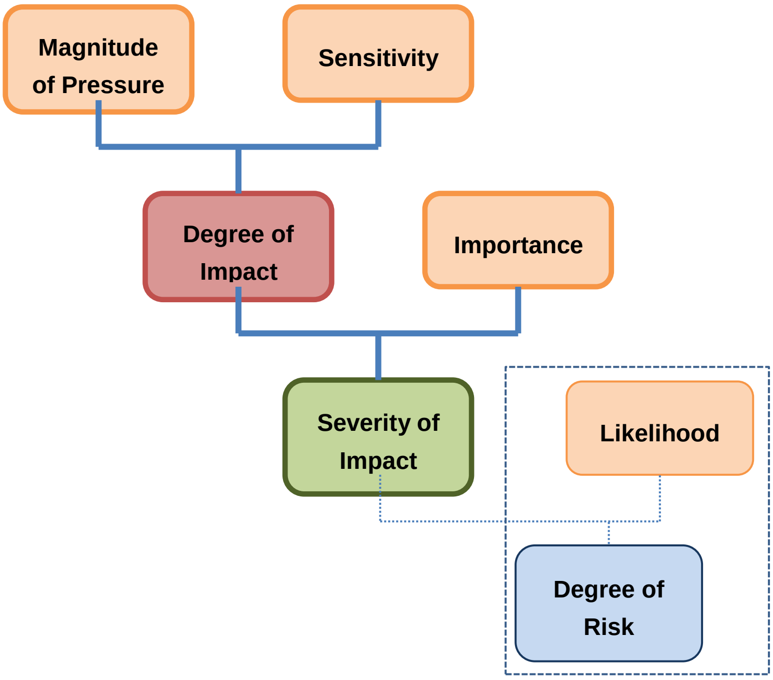


Figure 1.5. Generic methodology used for impact assessment of Horns Rev 3.

The methodology adopted to understand changes to hydrography and water quality caused by Horns Rev 3 is initially taken to the level of Magnitude of Pressure (Figure 1.5). The magnitude of pressure is defined by pressure indicators (Table 1.1). These indicators are based on the effects on hydrography, sediment spill and water quality in order to achieve the most optimal description of pressure; for example; millimeters of sediment deposited within a certain period and area in excess of natural deposition values. The magnitude of pressure is defined as low, medium, high or very high and is defined by its duration and range (spatial extent) (Table 1.1).

Table 1.1. Definition of the magnitude of pressure.

| Magnitude | Duration | Range |
|---|---|---|
| Very High | Recovery takes longer than ten years or is permanent | International |
| High | Recovered within ten years after end of construction | National |
| Medium | Recovered within five years after end of construction | Regional |
| Low | Recovered within two years after end of construction | Local |

Sensitivity to a pressure varies between environmental factors. For hydrology, sediment spill and water quality, the sensitivity of the receptor is a function of its capacity to accommodate change and reflects its ability to recover if it is affected. Table 1.2 sets out the generic criteria used to define the sensitivity of the physical marine environment to change.

Table 1.2. Criteria to determine the sensitivity of the marine environment to change.

| Sensitivity | Criteria |
|---|---|
| Very High | The marine environment has a very low capacity to accommodate any change to hydrology (such as wave height), sediment spill and/or water quality, compared to baseline conditions |
| High | The marine environment has a low capacity to accommodate any change to hydrology, sediment spill and/or water quality compared to baseline conditions |
| Medium | The marine environment has a high capacity to accommodate changes to hydrology, sediment spill and water quality due, for example to, large size of water body, location away from sensitive habitats and a high capacity for dilution. Small changes to baseline conditions are, however, likely. |
| Low | Physical conditions are such that they are likely to tolerate proposed changes with little or no impact on baseline conditions. |

Horns Rev 3 has a large physical scale and a high degree of temporal and spatial variance for all hydrological, sediment spill and water quality parameters considered. As a result, the marine environment in relation to hydrology, sediment spill and water quality is considered to be of medium sensitivity.

In order to determine the degree of impact; the magnitude of pressure and sensitivity are combined in a matrix (Table 1.3). The degree of impact is the description of an impact to a given environmental factor without putting it into a broader perspective (the latter is acheived by including importance in the evaluation, Table 1.4).

Table 1.3. Matrix for the assessment of the degree of impact.

| Magnitude of Pressure | Sensitivity | | | |
|---|---|---|---|---|
| | **Very High** | **High** | **Medium** | **Low** |
| **Very High** | Very High | Very High | High | High |
| **High** | Very High | High | High | Medium |
| **Medium** | High | High | Medium | Low |
| **Low** | Medium | Medium | Low | Low |

Table 1.4. Definition of importance to an environmental component.

| Importance Level | Description |
|---|---|
| Very High | Components protected by international legislation/conventions (Annex I, II and IV of the Habitats Directive, Annex I of the Birds Directive), or of international ecological importance. Components of critical importance for wider ecosystem functions. |
| High | Components protected by national or local legislation, or adapted on national “Red Lists”. Components of importance for far-reaching ecosystem functions. |
| Medium | Components with specific value for the region, and of importance for local ecosystem functions |
| Low | Other components of no special value, or of negative value |

The importance of the environmental factor is assessed for each environmental sub-factor. Some sub-factors are assessed as a whole, but in most cases, the importance assessment is broken down into components and/or sub-components in order to conduct an environmental impact assessment. The importance criteria are graded into four tiers (Table 1.4).

The severity of impact is assessed from the grading of the degree of impact and importance of the environmental factor, using the matrix shown in Table 1.5. If it is not possible to grade the degree of impact and/or importance, an assessment is given based on expert judgement.

Table 1.5. Matrix for the assessment of the severity of impact.

| Degree of Impact | Importance of the Environmental Component | | | |
|---|---|---|---|---|
| | **Very High** | **High** | **Medium** | **Low** |
| **Very High** | Very High | High | Medium | Low |
| **High** | High | High | Medium | Low |
| **Medium** | Medium | Medium | Medium | Low |
| **Low** | Low | Low | Low | Low |

Based on the severity of impact, the significance of the impact can be determined through the phrases described in Table 1.6. The contents of the table have been defined by Energinet.dk.

Table 1.6. Definition of significance of impact.

| Severity of Impact | Significance of Impact | Dominant Effects |
|---|---|---|
| **Very High** | Significant Negative | Impacts are large in extent and/or duration. Recurrence or likelihood is high, and irreversible impacts are possible |
| **High** | Moderate Negative | Impacts occur, which are either relatively large in extent or are long term in nature (lifetime of the project). The occurrence is recurring, or the likelihood for recurrence is relatively high. Irreversible impact may occur, but will be strictly local, on, for example, cultural or natural conservation heritage. |
| **Medium** | Minor Negative | Impacts occur, which may have a certain extent or complexity. Duration is longer than short term. There is some likelihood of an occurrence but a high likelihood that the impacts are reversible |
| **Low** | Negligible Negative | Small impacts occur, which are only local, uncomplicated, short term or without long term effects, and without irreversible effects |
| **Low** | Neutral / No Impact | No impact compared to status quo |
| | Positive Impacts | Positive impact occurring in one or more of the above statements |

# 2. GEOLOGY

## 2.1. Data Collection

Energinet.dk has supplied geological data across the Horns Rev 3 pre-investigation area and part-way along the export cable corridor, which have been surveyed by GEMS Survey between 10th July 2012 and 25th August 2012 (Ramboll, 2013a, b). Pinger, sparker and mini-gun sub-bottom profilers were deployed along east-west lines spaced 100m apart with 1,000m spaced north-south cross lines (Figure 2.1). A geotechnical survey was completed by GEO (Danish Geotechnical Institute) between 9th June 2013 and 27th August 2013. Cone penetration tests (CPT) were carried out at 28 locations; at 12 of these locations a borehole was recovered (GEO, 2013) (Figure 2.1).

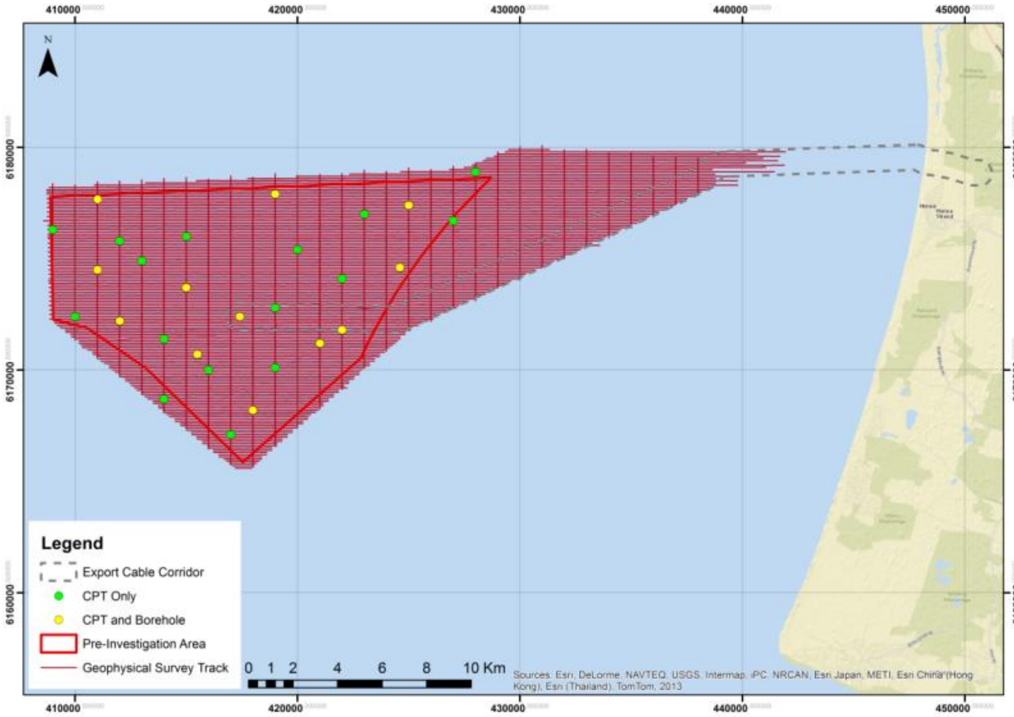


Figure 2.1. Geophysical survey lines and location of geotechnical data recovery for Horns Rev 3.

Ramboll (2013a, b) interpreted the geology across the pre-investigation area using the results of the 2012 geophysical survey (Section 1.4). Their stratigraphic classification is summarised in Table 2.1 and Figure 2.2 and used the nomenclature of Larsen and Andersen (2005) who divided the Quaternary of Horns Rev into two major sequences separated by an erosional unconformity (Reflector C) (Figure 2.3). GEO (2013) presented an interpretation of the geology using the borehole and CPT data that, in general, had several similarities to that using the geophysical results. However, the stratigraphic unit boundaries and their ages recovered at the borehole locations often showed a poor correlation with the geophysical model. For example, sediments of Holocene age were found to much greater depths in the boreholes than in the geophysical model.

Table 2.1. Main geological units across Horns Rev 3 (Ramboll, 2013a, b).

| Unit | Summary Description | Depth (m) to Base below Seabed |
|---|---|---|
| Holocene Marine 1 | Blanket cover of fine-medium sand | 0-7 |
| Holocene Marine 2 | Blanket cover of fine sand | 1-20 |
| Holocene Freshwater | Local channel fill of silt / clay | 1-25 |
| Horns Rev Valley | Channel fill of interbedded sand and silt /clay | 5-30 |
| Weichselian Meltwater | Planar deposits of fine sand, silt and clay | 2-30 |
| Eemian Marine | Silt and clay | 2-40 |
| Eemian Freshwater | Planar deposits of fine sand, silt and clay | 6-35 |
| Saalian Meltwater | Fine sand, silt and clay | 20-50 |
| Saalian Glacial Infill | Chaotic mix of sediment filling tunnel valley | 0-330 |
| Saalian Glacial | Clay diamict | 100-280 |

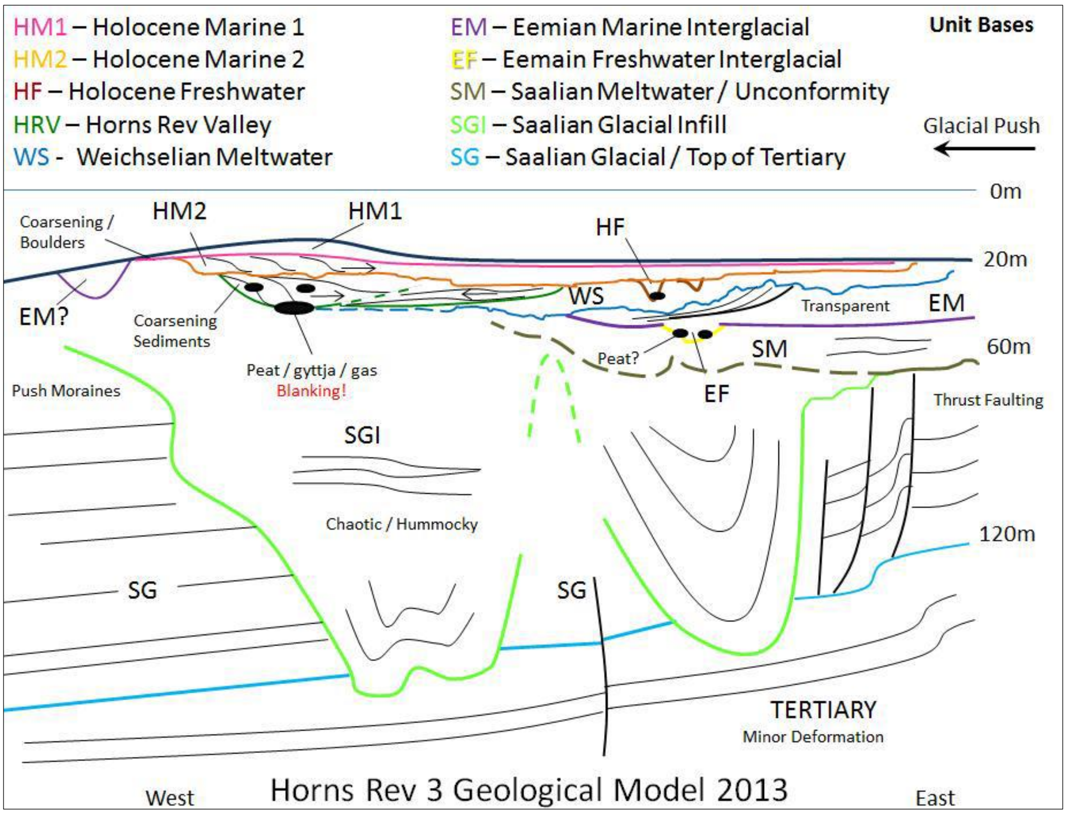

Figure 2.2. A geological model of Horns Rev 3 (Ramboll, 2013a, b).

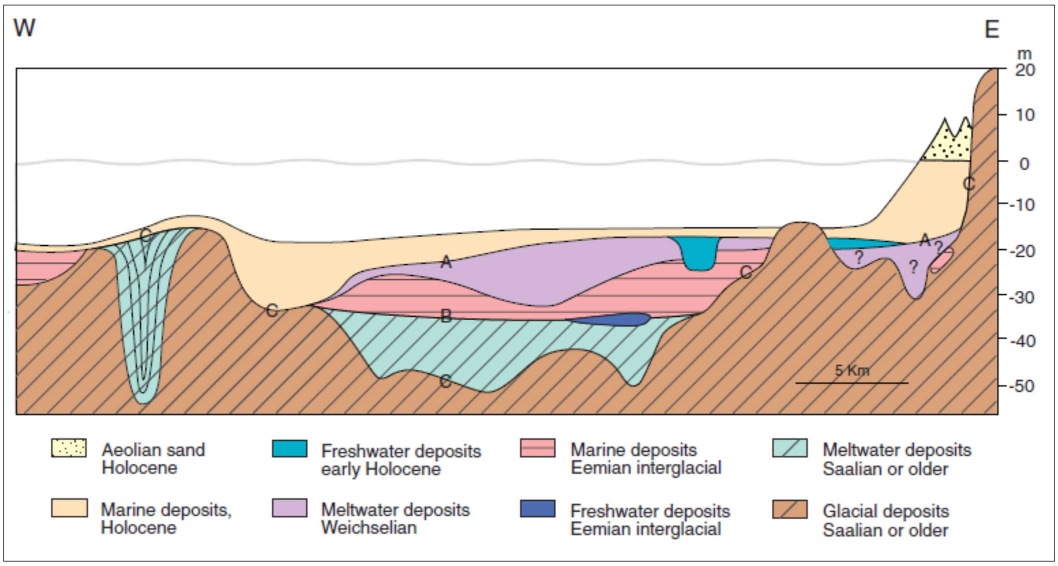


Figure 2.3. Schematic east-west section approximately along 55°45' N immediately north of Horns Rev 3 and the export cable corridor (Larsen and Anderson, 2005).

## 2.2. Pleistocene Evolution

### 2.2.1 Saalian

The oldest Pleistocene sequence is a glacial sequence of Saalian age composed of various tills (Larsen and Anderson, 2005) defined by Ramboll (2013a, b) as the Saalian Glacial unit. Ramboll (2013a, b) also identified infilled tunnel valleys (Saalian Glacial Infill unit) cut into the Saalian Glacial Unit (Figure 2.2). Ramboll (2013a, b) noted that the base of the Saalian sequence is greater than 100m below the seabed, but GEO (2013) identified Tertiary deposits in two boreholes between 36 and 46m below the seabed.

Larsen and Anderson (2005) defined Reflector C, which marks the top of the Saalian glacial sequence in the form of a 30-40km wide basin which is the seaward extension of the so-called *Bakke-ø* landscape on land. Along the coast, the elevation of this landscape is approximately 20-30m high dropping offshore to about 40m below the seabed at the bottom of the basin, before rising close to the sea bed in the west of Horns Rev 3 (Figures 2.2 and 2.3). Where the surface rises towards the seabed, the bathymetry forms a ridge along the southwest and southeast extremities of Horns Rev 3 (Section 3). This ridge is part of a relatively high standing area of glacial deposits west of Horns Rev called *Vovov Bakke-ø* (Larsen and Anderson, 2005).

Above Reflector C is a series of glacial and interglacial units which fill the basin including (in order of decreasing age) Saalian meltwater deposits, Eemian interglacial deposits, Weichselian glacial deposits and Holocene interglacial deposits (Figures 2.2 and 2.3). These deposits form the geological core of the pre-investigation area to the north and east of the ridge. Each unit is separated from the one above by an erosional unconformity.

According to Larsen and Anderson (2005), the Saalian deposits above Reflector C consist of glaciofluvial sands with occasional till. Ramboll (2013a, b) defined them as proglacial meltwater sediments (Saalian Meltwater unit) deposited after retreat of the ice sheet (with sediments up to 30m thick).

### 2.2.2 Eemian

Prior to marine inundation during the following Eemian interglacial, small channels were eroded into the Saalian meltwater plain and up to 20m of freshwater sediments (sand and mud with peat) were deposited (Eemian Freshwater unit) (Ramboll, 2013a, b). Once the area was inundated, a marine mud up to 40m thick was deposited (Eemian Marine unit). The boreholes did not recover sediments of Eemian age (GEO, 2013).

### 2.2.3 Weichselian

During the Weichselian glaciation, Horns Rev 3 was ice-free and covered by proglacial river plains, where up to 20m of glaciofluvial sand and mud was deposited (Weichselian Meltwater unit of Ramboll, 2013a, b). The base of the deposits across Horns Rev 3 deepens from around 20m below the seabed along central parts of the export cable corridor to almost 30m below the seabed across the pre-investigation area (Figure 2.4). The bulk of the Weichselian deposits across Horns Rev 3 were supplied with sediment from the Skjern River system outlet cut through the old Saalian landscape to the northeast (Houmark-Nielsen, 2003) (Figure 2.5). GEO (2013) recovered meltwater deposits in boreholes, but were unable to establish their age.

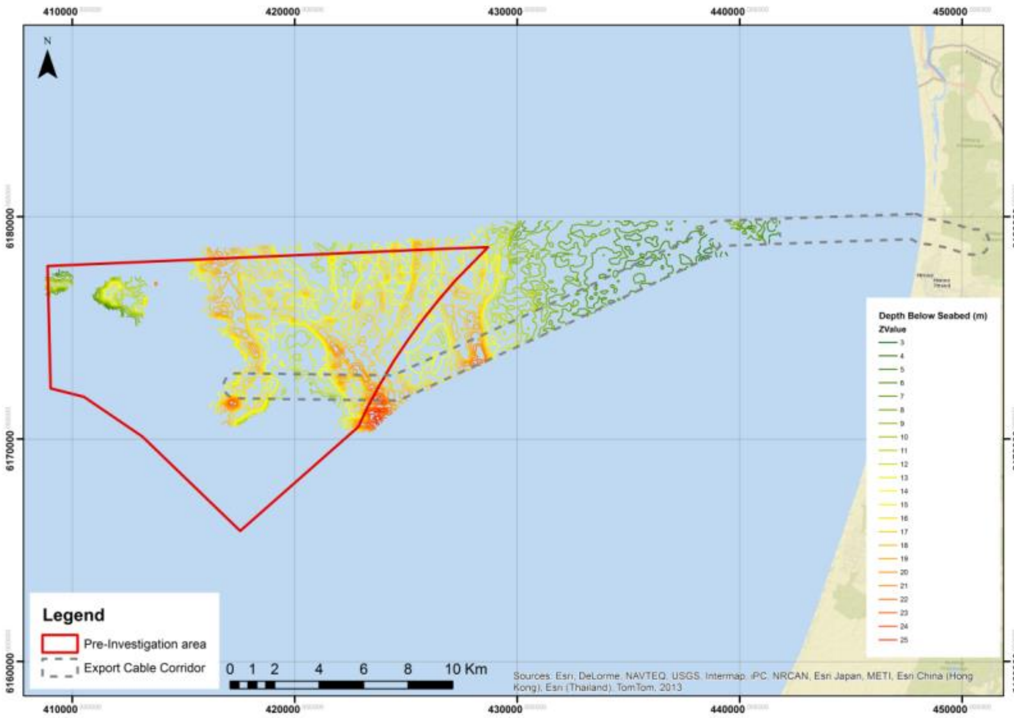


Figure 2.4. Interpreted depth below seabed to the base of the Weichselian Meltwater unit (Ramboll, 2013a).

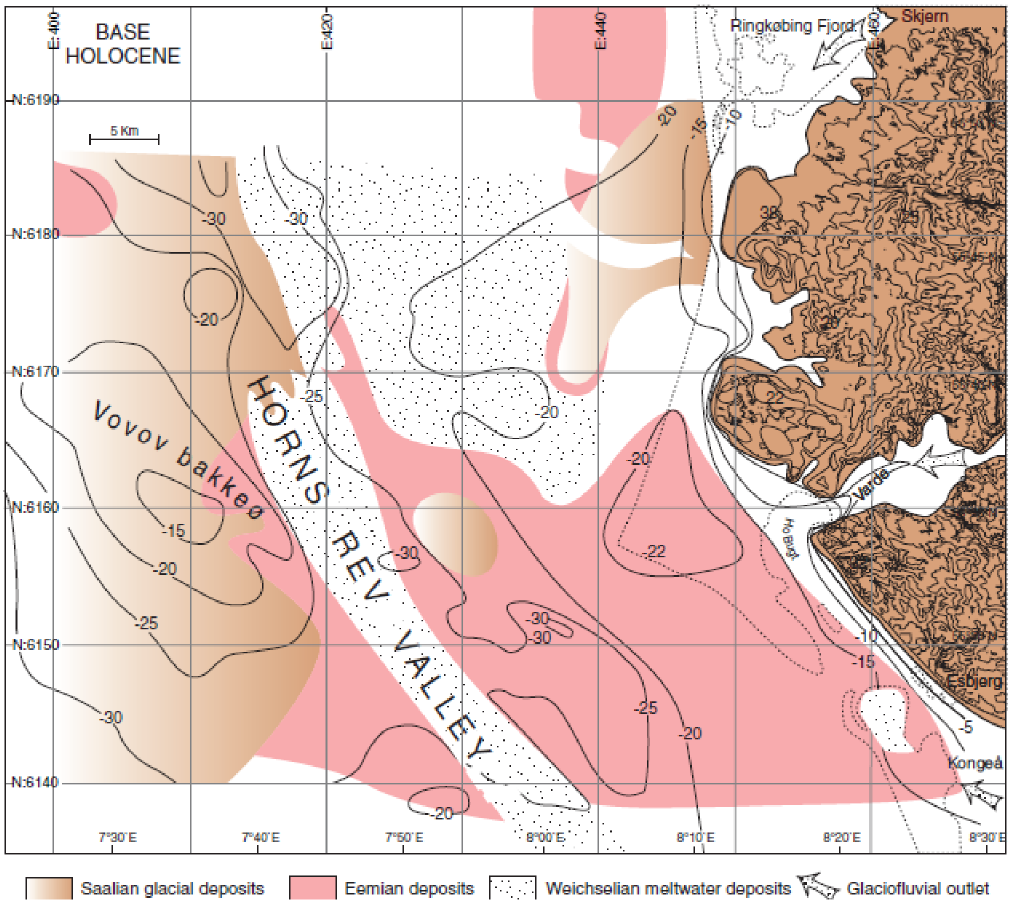


Figure 2.5. Map of the topography at the base of the Holocene and a subcrop geological map. The arrows mark the major outlets of meltwater streams during the Weichselian glaciation (Larsen and Anderson, 2005).

During the Weichselian, a valley (Horns Rev Valley) about 5km wide was cut to about 30m below the seabed through Eemian deposits and into the Saalian deposits (Figure 2.6). It is filled with up to 17m of sand and mud with possible peat at the base and was defined as the Horns Rev Valley unit by Ramboll (2013a, b). Larsen and Anderson (2005) suggested that the river plain across Horns Rev 3 was active during the main Weichselian glacial advance (24,000 to 19,000 years ago), while erosion and infilling of the Horns Rev Valley was related to a younger glacial phase between 19,000 and 17,000 years ago.

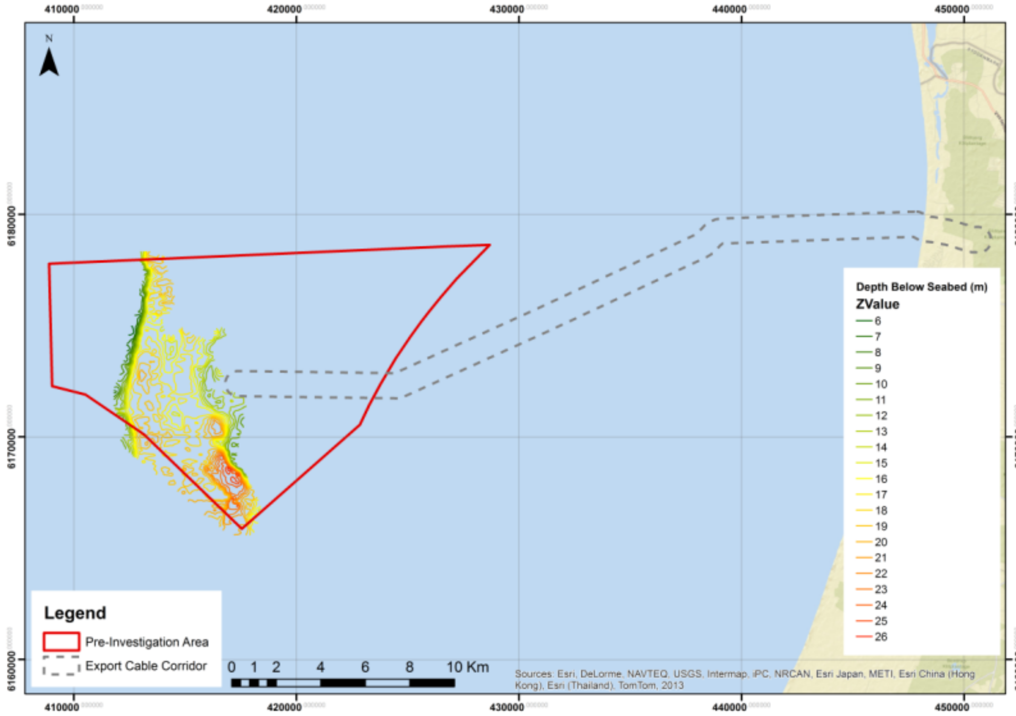


Figure 2.6. Interpreted depth below seabed to the base of the Horns Rev Valley unit (Ramboll, 2013a).

## 2.3. Holocene Evolution

The peak of the Weichselian glaciation occurred approximately 18,000 years ago. However, it wasn't until the start of the Holocene (10,000 years ago) that the glacial period ended and the northern hemisphere entered an interglacial. During the decline of the glaciation, increased melting of the ice sheets released large volumes of water causing global sea levels to rise. As this rise occurred, the North Sea Basin was slowly inundated and Horns Rev changed from being a land area to a marine area around 8,800 years ago (Ramboll, 2013a, b). At the base of the Holocene sediments is an erosional surface (caused by the inundation of marine waters across the area) cut into Saalian, Eemian and Weichselian deposits (Figure 2.5).

The nature of the transition from continental to fully marine conditions resulted in a number of different depositional environments acting across Horns Rev over a short space of time, from terrestrial and fluvial through brackish to fully marine. Early in this transition, up to 13m of freshwater sediments (sand and mud) were deposited in channels (Holocene Freshwater unit of Ramboll, 2013a, b) and as solifluction soils (GEO, 2013) (Figure 2.7). Following inundation, up to 20m of marine sand was deposited. The total thickness of Holocene sediments identified in the boreholes is up to about 35m (GEO, 2013). Ramboll (2013a, b) divided the sand into a lower Holocene Marine 2 unit deposited in nearshore environments and an upper Holocene Marine 1 unit deposited in deeper water (Figures 2.8 and 2.9).

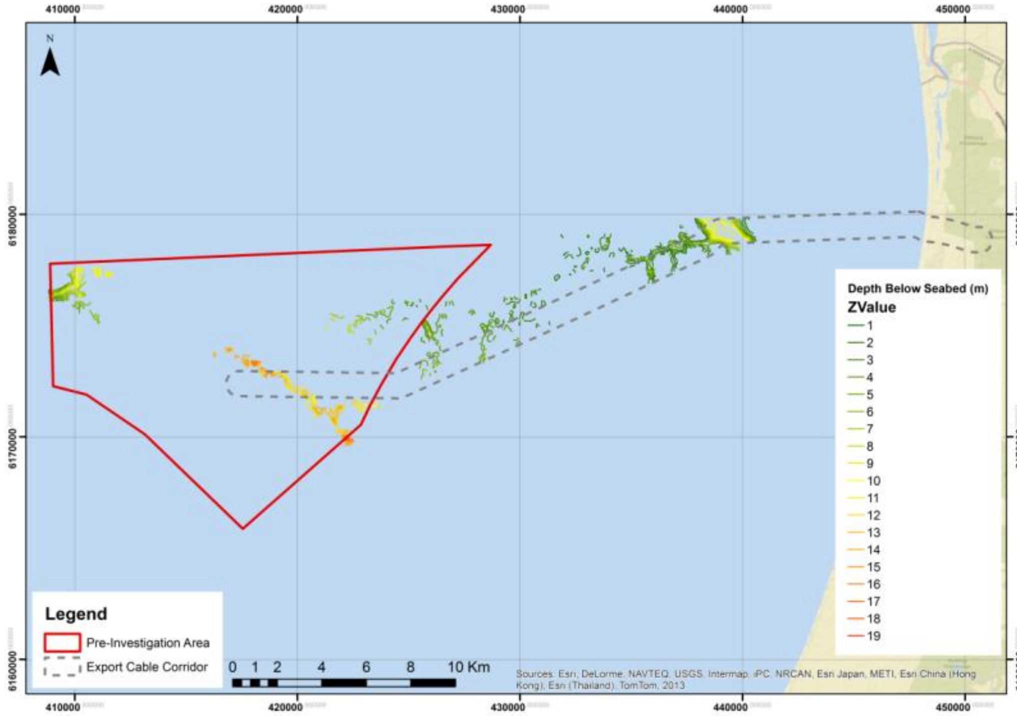


Figure 2.7. Interpreted depth below seabed to the base of the Holocene Freshwater unit (Ramboll, 2013a).

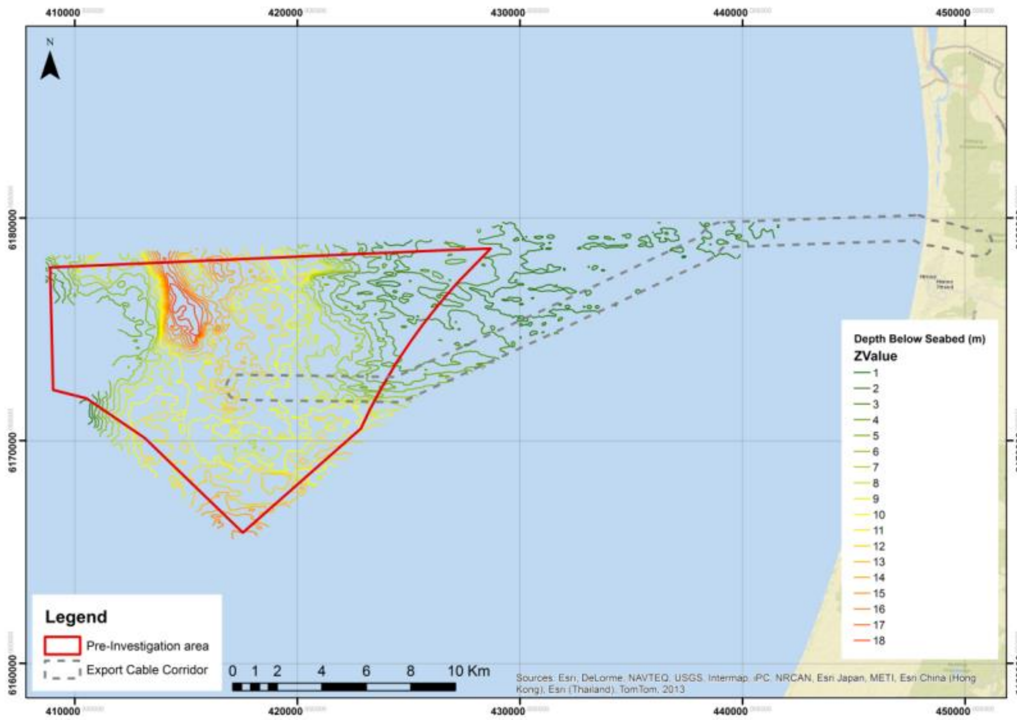


Figure 2.8. Interpreted depth below seabed to the base of the Holocene Marine 2 unit (Ramboll, 2013a).

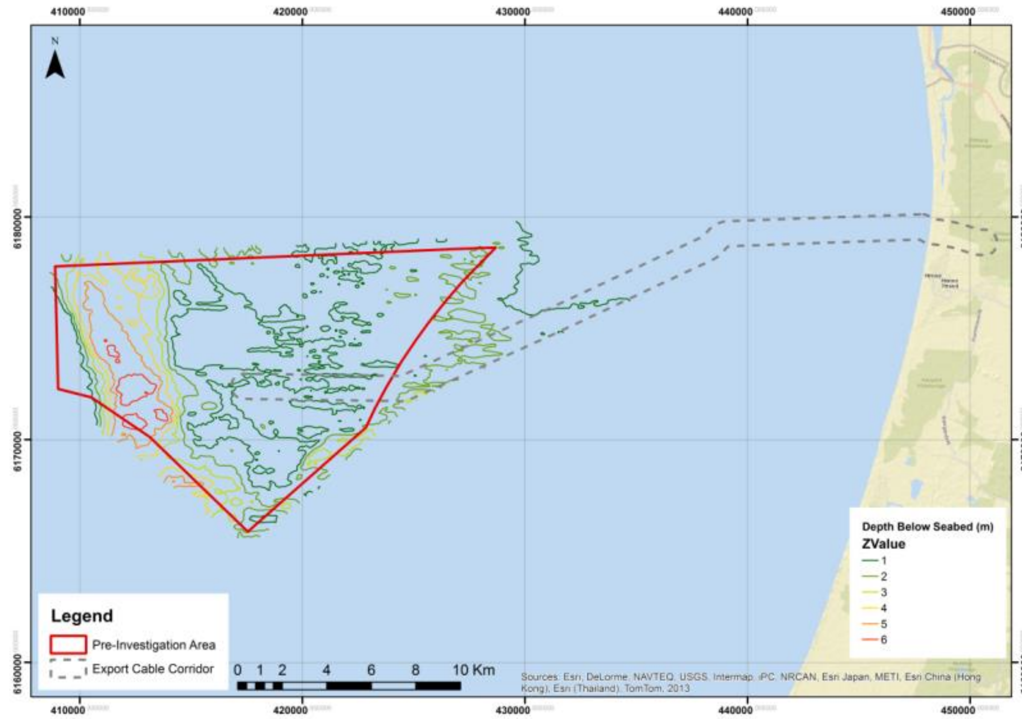


Figure 2.9. Interpreted depth below seabed to the base of the Holocene Marine 1 unit (Ramboll, 2013a).

GEO (2013) recovered a 5cm peat layer from the Holocene Freshwater unit, which contained a large piece of wood. Radiocarbon dating of the wood provided a date of 8211-7791 BC, from the early part of the Holocene.

*Sea bed samples*

# 3. HYDRODYNAMIC PROCESSES

## 3.1. Data Collection

Metocean data including water levels, tidal currents and waves has been collated from a variety of stations located in the North Sea near the Danish coastline (Figure 3.1 and Table 3.1). Wave and wind data between 2007 and 2012 has been forecasted at the Gorm offshore platform, located about 200km offshore from the Danish coastline. In the nearshore zone, wave data between 2007 and 2012 has been measured at Nymindegab. Measured water levels at the coast are available at Esbjerg and Hvide Sande from 2007 to 2013. One year of current data (2011), with a minimum of down time, has been recorded at the FINO3 platform approximately 80km from the Danish west coast. Regional current and water level data were also extracted from the International Hydrographic Organization (IHO) tidal stations along the coastlines of United Kingdom, France, Germany, Belgium, Spain, The Netherlands and Denmark.

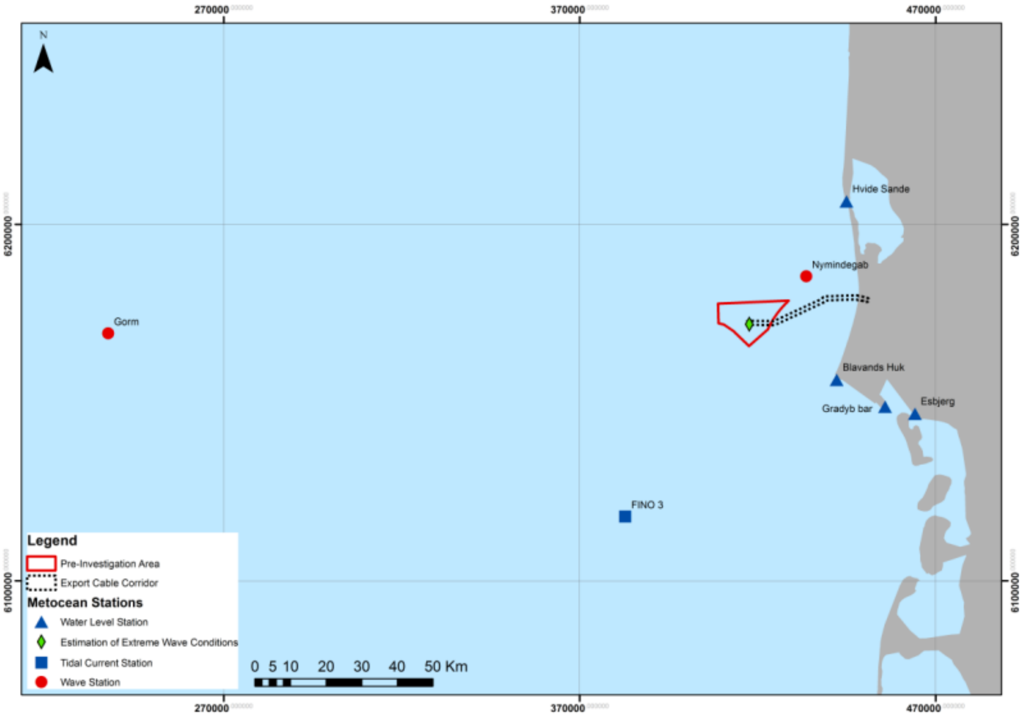


Figure 3.1. Metocean data stations for Horns Rev 3.

Table 3.1. Metocean data recorded at the stations shown in Figure 3.1.

| Location | Data Type | Period | |
|---|---|---|---|
| | | Start | End |
| Esbjerg | Measured water levels | 01/01/2007 | 02/01/2013 |
| Hvide Sande | Measured water levels | 01/01/2007 | 02/01/2013 |
| Gorm | Forecasted wave and wind data | 01/01/2007 | 26/12/2012 |
| Nymindegab | Measured wave data | 01/01/2007 | 26/12/2012 |
| FINO3 | Measured current data | 01/02/2011 | 06/12/2011 |

## 3.2. Astronomic Water Levels at the Coast

Due to the position of the amphidromic point offshore from Denmark the tidal range along the coast differs significantly from north to south. At Blåvands Huk and locations to its south (Grådyb Bar and Esbjerg) the spring tidal range is 1.5-1.8m (Table 3.2). At Hvide Sande, north of Blåvands Huk, the spring tidal range is 0.8m.

Table 3.2. Tidal datums at four coastal locations near to Horns Rev 3 (Admiralty Tide Tables, 2013). Locations are shown in Figure 3.1.

| Location | Tidal Datum (m above Chart Datum) | | | | Range (MHWS-MLWS) |
|---|---|---|---|---|---|
| | MHWS | MHWN | MLWN | MLWS | |
| *Hvide Sande | 0.8 | 0.7 | 0.2 | 0.0 | 0.8 |
| Blåvands Huk | 1.8 | 1.4 | 0.3 | 0.0 | 1.8 |
| Grådyb Bar | 1.5 | 1.2 | 0.3 | 0.0 | 1.5 |
| *Esbjerg | 1.9 | 1.5 | 0.5 | 0.1 | 1.8 |

*Chart Datum (CD) is about 0.8m below the Danish Vertical Reference 1990 (DVR90) at Esbjerg and about 0.25m below DVR90 at Hvide Sande.

Measured water levels relative to Danish Vertical Reference 1990 (DVR90 which is approximately mean sea level) were available at Esbjerg and Hvide Sande from 2007 to 2013. Water levels range from -1.2m to 1.1m DVR90 at Esbjerg and from -0.7 to 0.7m DVR90 at Hvide Sande. Water level data for two spring-neap tidal cycles at Esbjerg and Hvide Sande are presented in Figures 3.2 (April/May 2011) and 3.3 (September 2011). The water levels at Esbjerg are consistently higher on high tides and consistently lower on low tides than Hvide Sande.

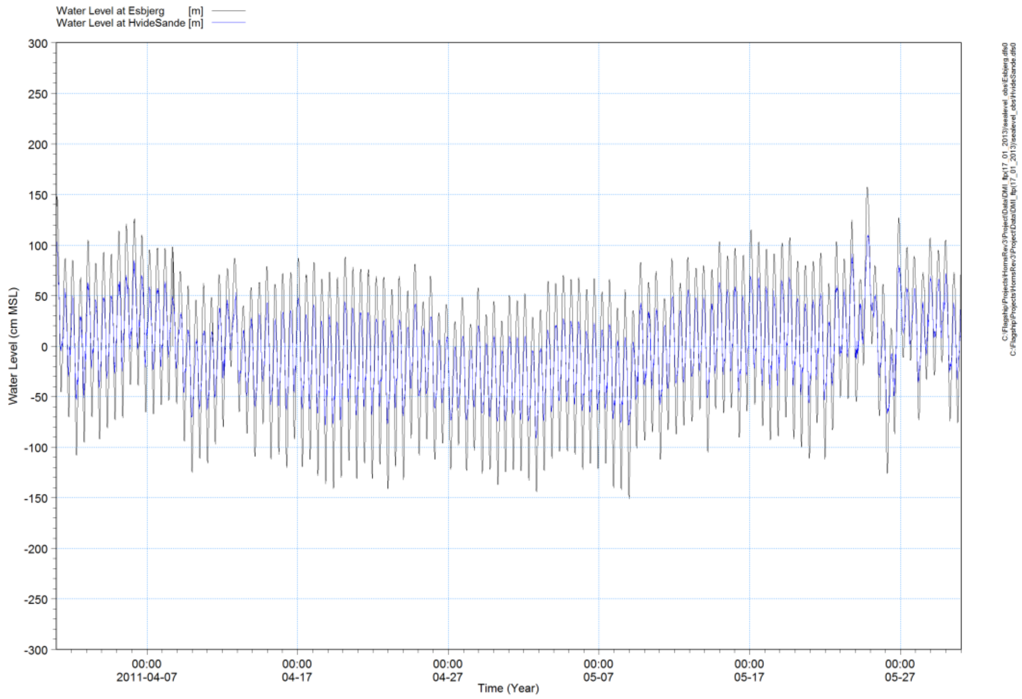


Figure 3.2. Water levels measured at Esbjerg and Hvide Sande tide gauges for April and May 2011.

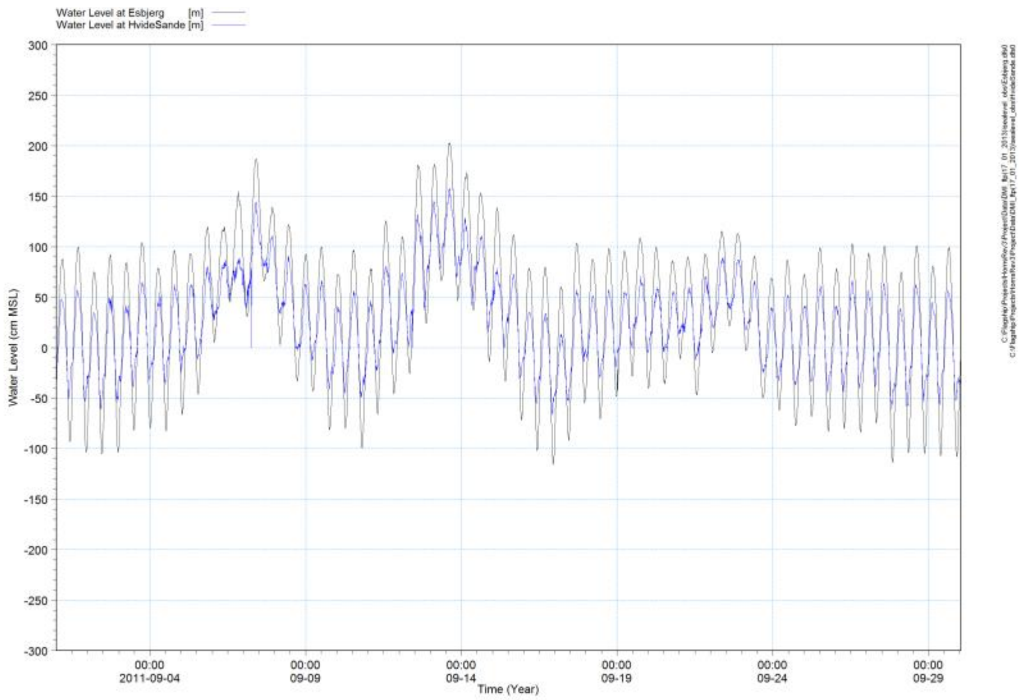


Figure 3.3. Water levels measured at Esbjerg and Hvide Sande tide gauges for September 2011.

## 3.3. Storm Surge and Extreme Water Levels

According to Sørensen et al. (2013) storm surge levels reach 3.11m and 3.19m above DVR90 once every 100 years at Hvide Sande Port and Hvide Sande (sea), respectively.

Table 3.3 and Figures 3.4 and 3.5 provide the statistics for 20-year, 50-year and 100-year events.

Table 3.3. Extreme water levels at Hvide Sande Port and Hvide Sande (sea) (Sørensen et al., 2013).

| Return Period (Years) | Extreme Water Level (m DVR90) | |
|---|---|---|
| | Hvide Sande Port | Hvide Sande (Sea) |
| 20 | 2.85+/-0.08 | 2.81+/-0.16 |
| 50 | 3.01+/-0.10 | 3.03+/-0.22 |
| 100 | 3.11+/-0.12 | 3.19+/-0.27 |

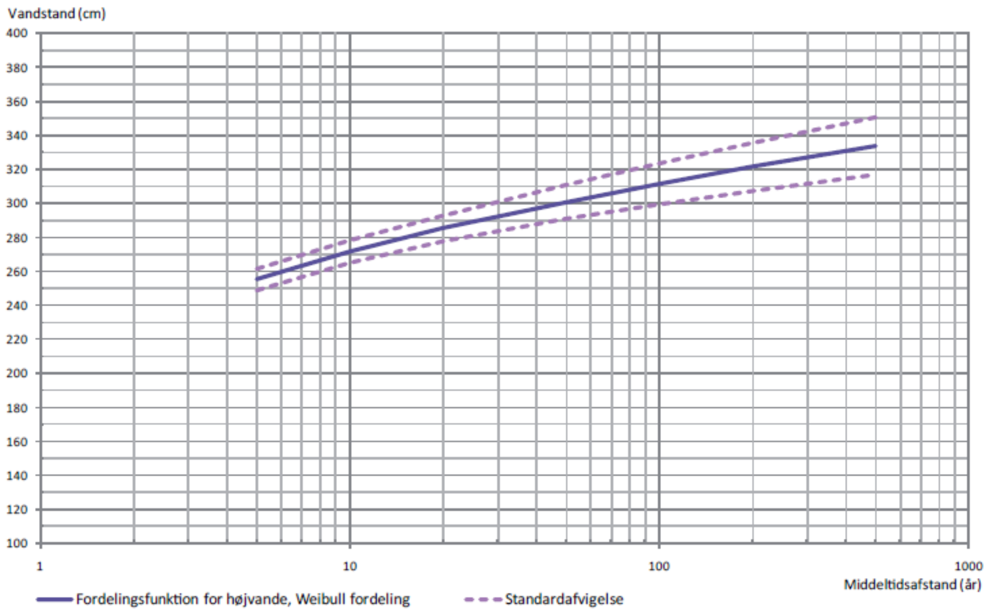


Figure 3.4. Extreme water levels at Hvide Sande Port (Sørensen et al., 2013).

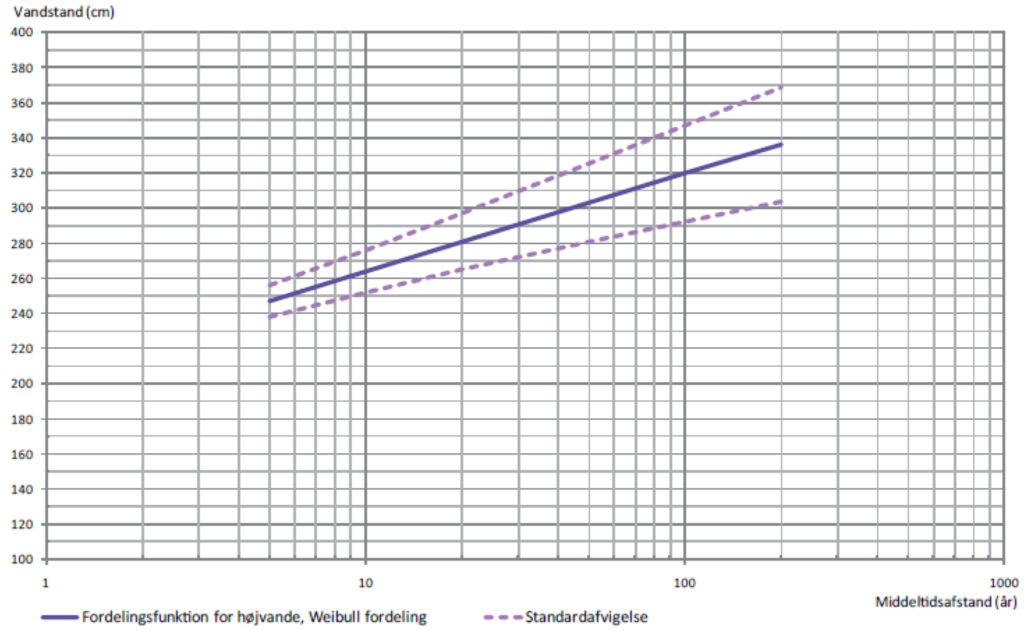


Figure 3.5. Extreme water levels at Hvide Sande (Sea) (Sørensen et al., 2013).

## 3.4. Tidal Currents

Measured tidal current data was available for 2011 at FINO3 in 23m of water. Discrete measurements were recorded for every 2m of water depth equating to 11 points from 2m to 22m. The velocity vectors at all points were summed and the resultant vectors were then divided by the number of points to define the depth-averaged current velocity vectors. The tidal current rose shows the dominant flows were towards the north-northwest with peak current velocities greater than 0.7m/s (Figure 3.6). Calm periods (less than 0.1m/s) occurred approximately 6.5% of the time.

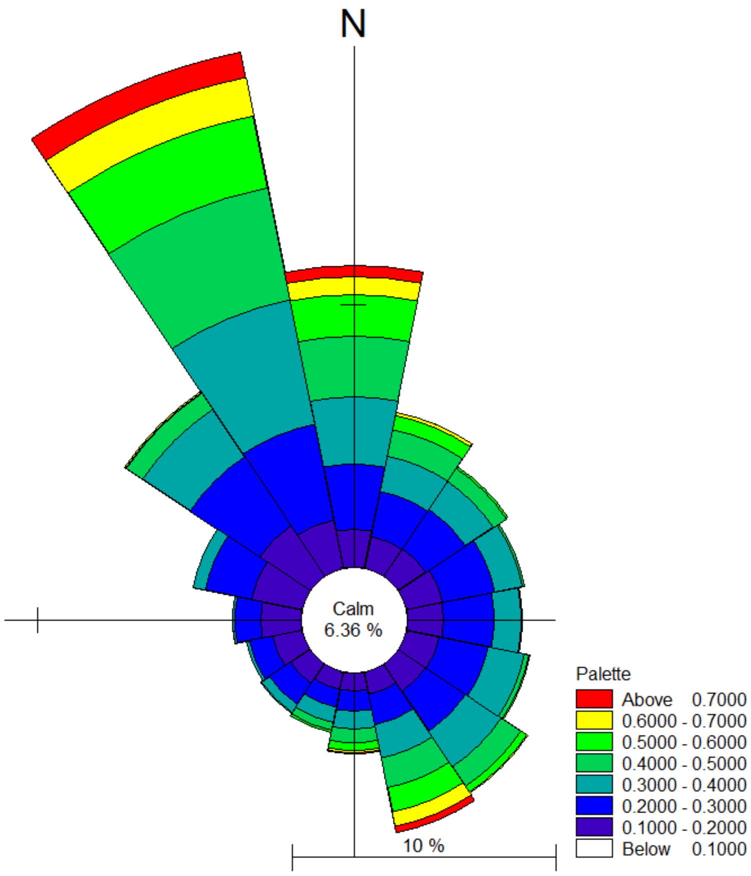


Figure 3.6. Depth-averaged tidal current distribution at FINO3 for 2011.

## 3.5. Wind

Offshore winds were forecast using StormGeo's Weather Research and Forecasting model (WRF) applied at Gorm. The average wind speed is about 4-8m/s mainly from the northwest to southwest sector (overall westerly) (Figure 3.7).

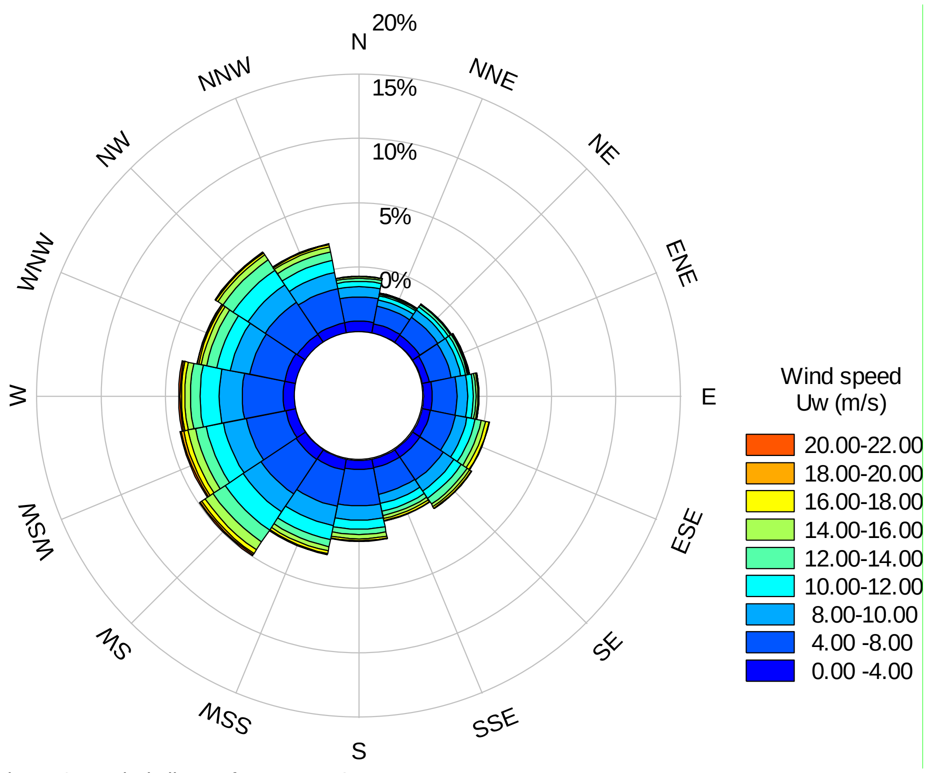

Figure 3.7. Wind climate forecast at Gorm.

## 3.6. Significant Wave Heights

Forecast time series wave data is available offshore at Gorm and measured wave data inshore is available between 2007 and 2012 at Nymindegab. Wave roses show the dominant wave directions are from the northwest and north-northwest at both locations (Figure 3.8). The average significant wave height ranges from 0.5m to 1.0m.

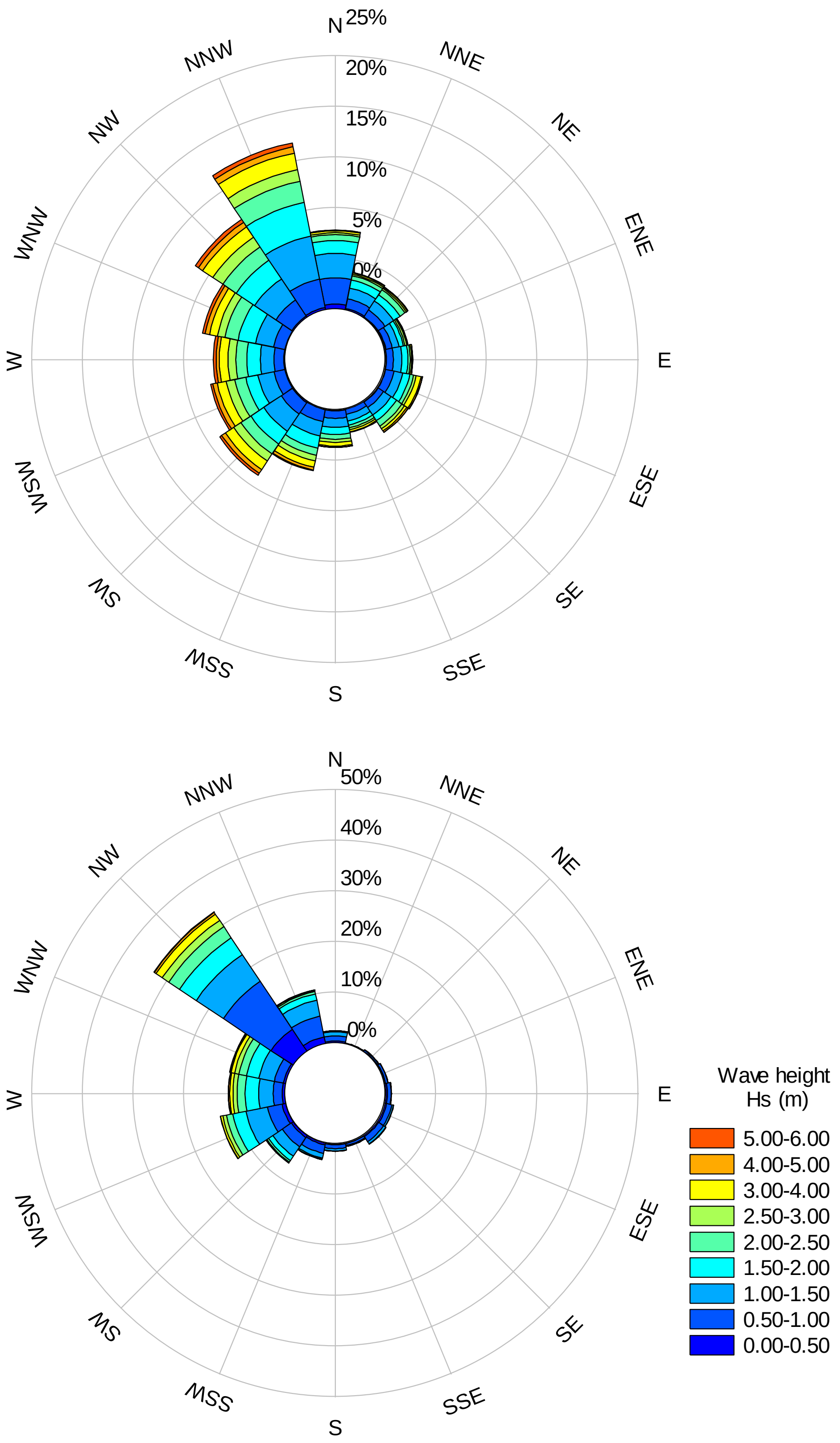


Figure 3.8. Significant wave height at the offshore Gorm platform (top) and the nearshore Nymindegab station (bottom).

## 3.7. Extreme Wave Heights and Periods

Praem-Larsen and Kofoed (2013) estimated extreme wave conditions at a single location (55°41'13''N, 07°41'24''E) within Horns Rev 3. The results show that extreme significant wave heights of 6m can be expected as often as once a year (Table 3.4). The 100-year extreme significant wave height is 8.7m.

Table 3.4. Extreme significant wave heights at Horns Rev 3 (Praem-Larsen and Kofoed, 2013).

| Return Period (years) | Significant Wave Height (m) |
|---|---|
| 1 | 6.0 |
| 5 | 7.0 |
| 10 | 7.4 |
| 20 | 7.8 |
| 40 | 8.2 |
| 50 | 8.3 |
| 100 | 8.7 |

Extreme wave conditions at Gorm for three directional sectors (northwest, west and southwest) are summarised in Table 3.5.

Table 3.5. Extreme significant wave heights at Gorm.

| Return Period (years) | Significant Wave Height (m) | | |
|---|---|---|---|
| | Northwest | West | Southwest |
| 1 | 12.0 | 12.4 | 9.5 |
| 5 | 14.3 | 13.8 | 10.5 |
| 10 | 15.0 | 13.9 | 10.7 |
| 20 | 15.7 | 13.9 | 10.8 |
| 40 | 16.2 | 13.9 | 10.9 |
| 50 | 16.4 | 13.9 | 11.0 |
| 100 | 16.9 | 13.9 | 11.0 |

## 3.8. Sea-level Rise

Global sea level is primarily controlled by three factors; thermal expansion of the ocean, melting of glaciers and change in the volume of the ice caps of Antarctica and Greenland. The Intergovernmental Panel on Climate Change (IPCC, 2013) estimated a global average sea-level rise of between 1.5 and 1.9mm/yr with an average value of 1.7mm/yr for the period 1901 to 2010. Between 1971 and 2010, the rate was estimated at 2.0mm/yr (1.7-2.3mm/yr) rising to 3.2mm/yr (2.8-3.6mm/yr) between 1993 and 2010.

Mean sea level has been recorded at Esbjerg since 1887. Aagaard and Sørensen (2013) estimated the mean rate of sea-level rise over the period 1887 to present has been 1.37mm/year, whereas from the late 1970's up to the present day, the rate of sea-level rise accelerated to 3.27mm/year. Knudsen et al. (2008) analysed tide gauge measurements at Esbjerg and showed an accelerated rate of sea-level rise of approximately 4 mm/yr between 1972 and 2007, and 5mm/yr from 1993 to 2003, compared to an average of 1.35mm/yr between 1889 and 2007.

*Houstrup Strand*

# 4. SEDIMENTARY PROCESSES AND WATER QUALITY

## 4.1. Bathymetry

Energinet.dk has supplied multibeam echosounder bathymetric data across the Horns Rev 3 pre-investigation area and part-way along the export cable corridor, which have been surveyed by GEMS Survey between 10th July 2012 and 25th August 2012 (Ramboll, 2013a, b). The main lines were run east-west with a spacing of 100m with 1,000m spaced north-south cross lines (Figure 2.1), achieving 100% coverage of bathymetry.

The water depths across Horns Rev 3 range from -10m to -21m DVR90 gradually deepening from southwest to northeast (Figure 4.1). The minimum water depths are defined as a ridge along the southwest of the pre-investigation area and the maximum water depths occur across the north and far west of the area.

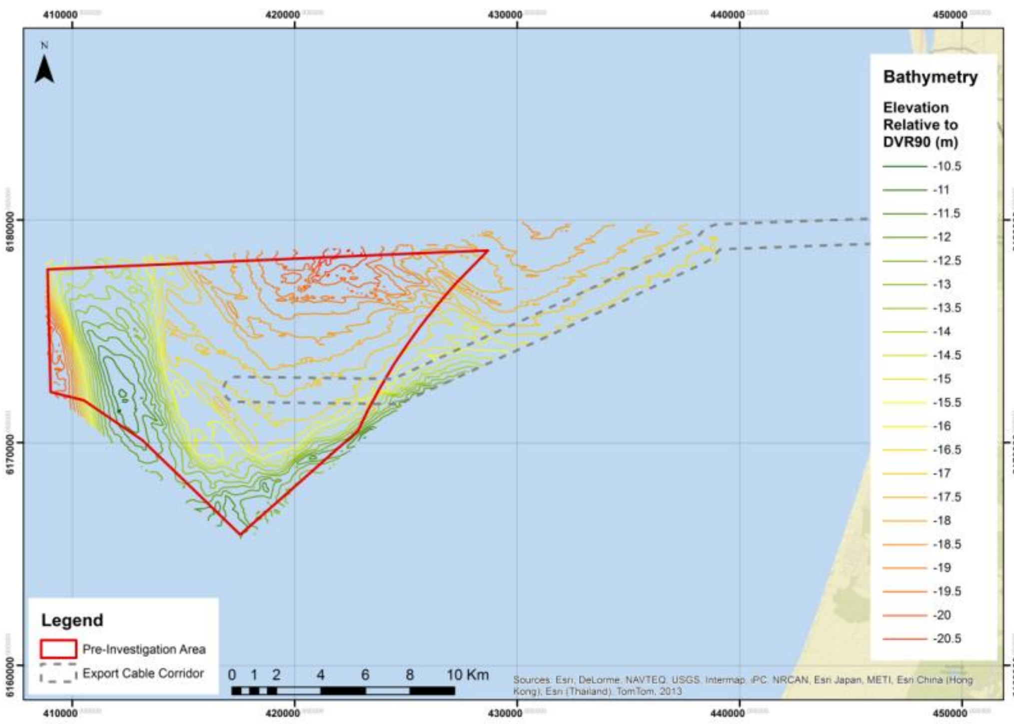


Figure 4.1. Bathymetry of Horns Rev 3 collected by Energinet.dk in July and August 2012 (Ramboll, 2013a, b)

Some areas of the seabed demonstrate a series of sub-parallel depressions oriented west-northwest to east-southeast (Ramboll, 2013a, b). They are present in the deepest northern part of the pre-investigation area and across the southwest-northeast oriented part of the ridge.

## 4.2. Seabed Sediment Distribution

GEMS Survey visited 50 sites for seabed sediment grab samples across Horns Rev 3 between 10th July 2012 and 25th August 2012 (Ramboll, 2013a, b). A further six grab samples were collected on 15th March 2013 as part of a POD survey for sediment contaminant analysis. The distribution of the seabed sediment samples is shown in Figure 4.2. All of the 56 recovered samples have been analysed for particle size distribution (Ramboll, 2013b). The seabed sediment grab samples were supported by collection of (100% coverage) side-scan sonar data across the pre-investigation area and part-way along the export cable corridor (surveyed by GEMS Survey between 10th July 2012 and 25th August 2012) (Figure 2.1).

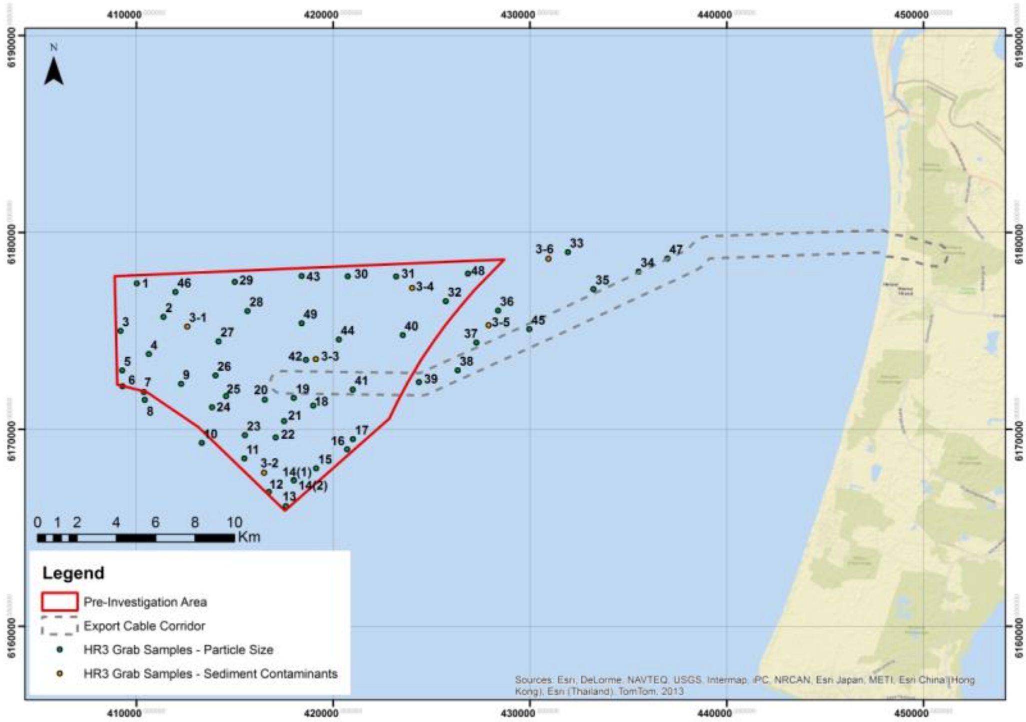


Figure 4.2. Location of grab samples for Horns Rev 3.

The seabed sediment distribution derived from the 2012 geophysical and grab sample data is summarised in Figure 4.3 (Ramboll, 2013a, b). The seabed across Horns Rev 3 is mainly medium sand in the west and south, and fine sand in the northeast.

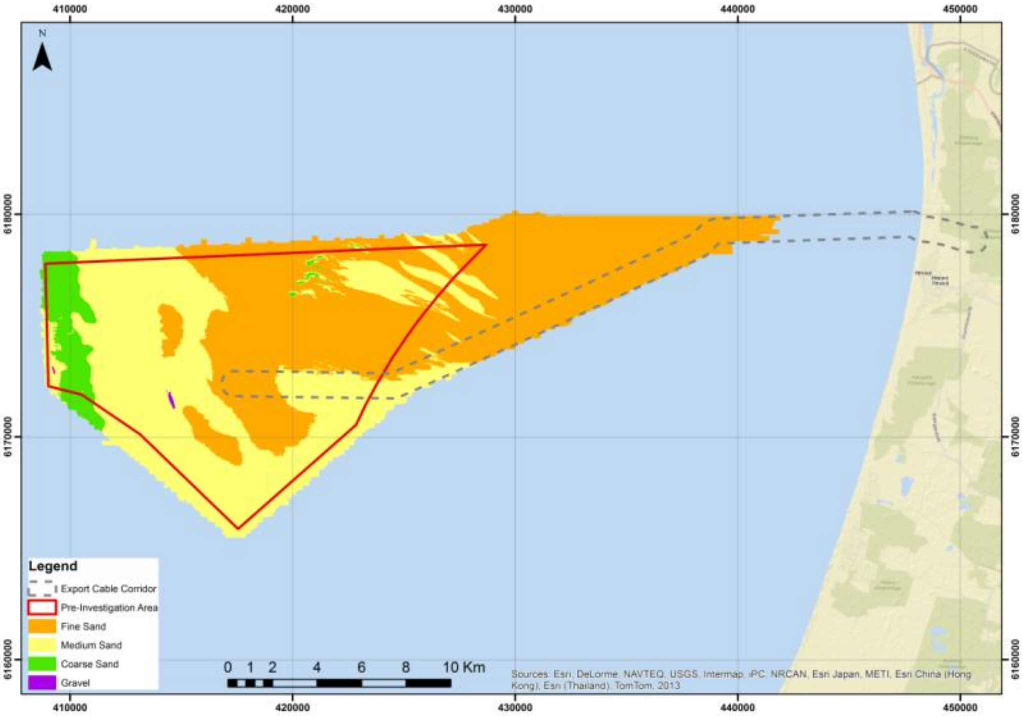


Figure 4.3. Seabed sediment characteristics across Horns Rev 3 (Ramboll, 2013a, b).

Particle size data from the 56 seabed sediment sample sites are summarised in Tables 4.1 and 4.2. Within the pre-investigation area boundary, 42 samples show that the sediments are dominated by sand (96-100%) with one sample containing gravel. The predominant sand is medium sand (diameter 0.20-0.60mm; using the DGF classification of 1988). Smaller patches of fine sand (0.063-0.20mm) and coarse sand (0.60-2.00mm) occur within the larger area of medium sand. All the samples within the pre-investigation area contain less than 3.4% mud. The average median particle size ($d_{50}$) for all the samples, excluding the gravel sample, is 0.43mm; including the gravel sample, the average $d_{50}$ increases to 0.54mm.

Table 4.1. Particle size distribution of seabed sediment samples across the pre-investigation area.

| Sample ID | % mud | % sand | % gravel | $d_{50}$ (mm) | DGF Sand Class |
|---|---|---|---|---|---|
| | <0.063mm | 0.063mm-2mm | >2mm | | |
| 1 | 0.25 | 93.71 | 6.04 | 0.96 | coarse |
| 2 | 0.62 | 97.40 | 1.99 | 0.48 | medium |
| 3 | 0.97 | 98.84 | 0.19 | 0.17 | fine |
| 4 | 0.39 | 99.05 | 0.56 | 0.79 | coarse |
| 5 | 0.59 | 49.90 | 49.51 | 1.99 | coarse |
| 7 | 0.66 | 96.65 | 2.69 | 0.92 | coarse |
| 9 | 0.51 | 99.19 | 0.30 | 0.49 | medium |
| 11 | 0.49 | 99.51 | 0.00 | 0.31 | medium |
| 12 | 0.56 | 98.83 | 0.61 | 0.47 | medium |
| 13 | 0.69 | 99.31 | 0.00 | 0.29 | medium |
| 14 (1) | 0.88 | 96.25 | 2.88 | 0.43 | medium |
| 14 (2) | 0.85 | 99.02 | 0.13 | 0.43 | medium |
| 15 | 0.77 | 95.47 | 3.76 | 0.51 | medium |
| 16 | 0.71 | 99.06 | 0.23 | 0.44 | medium |
| 17 | 0.56 | 99.44 | 0.00 | 0.28 | medium |
| 18 | 1.35 | 98.60 | 0.05 | 0.19 | fine |
| 19 | 0.91 | 99.02 | 0.07 | 0.19 | fine |
| 20 | 1.15 | 98.31 | 0.53 | 0.34 | medium |
| 21 | 0.95 | 93.63 | 5.42 | 0.46 | medium |
| 22 | 2.26 | 97.67 | 0.07 | 0.23 | medium |
| 23 | 0.41 | 99.55 | 0.04 | 0.34 | medium |
| 24 | 0.65 | 98.47 | 0.88 | 0.44 | medium |
| 25 | 0.43 | 31.04 | 68.53 | 5.19 | gravel |
| 26 | 0.51 | 99.49 | 0.00 | 0.30 | medium |
| 27 | 1.29 | 98.71 | 0.00 | 0.26 | medium |
| 28 | 1.85 | 98.15 | 0.00 | 0.20 | medium |
| 29 | 0.49 | 99.51 | 0.00 | 0.23 | medium |
| 30 | 0.48 | 91.91 | 7.62 | 1.55 | coarse |
| 31 | 1.37 | 96.57 | 2.06 | 0.47 | medium |
| 32 | 0.97 | 99.00 | 0.03 | 0.30 | medium |
| 40 | 3.34 | 96.66 | 0.00 | 0.16 | fine |
| 41 | 0.87 | 99.11 | 0.03 | 0.21 | medium |

| Sample ID | % mud | % sand | % gravel | $d_{50}$ (mm) | DGF Sand Class |
|---|---|---|---|---|---|
| | <0.063mm | 0.063mm-2mm | >2mm | | |
| 42 | 1.25 | 98.73 | 0.02 | 0.20 | fine |
| 43 | 2.10 | 97.87 | 0.03 | 0.17 | fine |
| 44 | 1.14 | 98.77 | 0.09 | 0.18 | fine |
| 46 | 0.60 | 95.38 | 4.02 | 0.45 | medium |
| 48 | 0.83 | 99.17 | 0.00 | 0.30 | medium |
| 49 | 2.06 | 97.70 | 0.24 | 0.16 | fine |
| 3-1 | 0.57 | 99.27 | 0.16 | 0.34 | medium |
| 3-2 | 0.58 | 99.42 | 0.00 | 0.29 | medium |
| 3-3 | 1.07 | 98.75 | 0.17 | 0.20 | fine |
| 3-4 | 0.42 | 99.32 | 0.27 | 0.42 | medium |

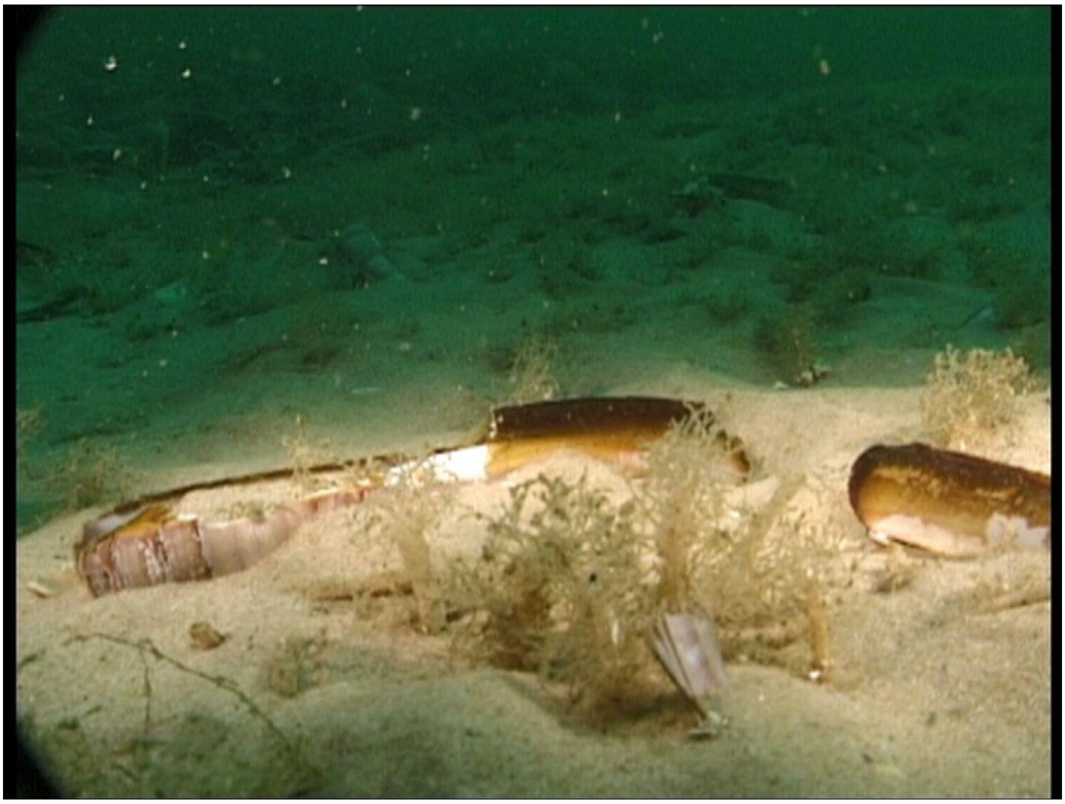

*Sea bed*

Table 4.2. Particle size distribution of seabed sediment samples outside but adjacent to the pre-investigation area (including the export cable corridor).

| Sample ID | % mud <0.063mm | % sand 0.063mm-2mm | % gravel >2mm | $d_{50}$ (mm) | DGF Sand Class |
|---|---|---|---|---|---|
| 6 | 1.32 | 98.60 | 0.08 | 0.32 | medium |
| 8 | 0.96 | 97.63 | 1.41 | 0.89 | coarse |
| 10 | 0.31 | 99.38 | 0.30 | 0.49 | medium |
| 33 | 1.83 | 98.16 | 0.01 | 0.13 | fine |
| 34 | 2.72 | 97.28 | 0.00 | 0.12 | fine |
| 35 | 2.59 | 96.11 | 1.30 | 0.13 | fine |
| 36 | 3.90 | 96.02 | 0.08 | 0.28 | medium |
| 37 | 0.43 | 99.50 | 0.07 | 0.42 | medium |
| 38 | 0.76 | 99.22 | 0.02 | 0.17 | fine |
| 39 | 0.57 | 99.14 | 0.29 | 0.48 | medium |
| 45 | 3.53 | 96.40 | 0.07 | 0.16 | fine |
| 47 | 1.65 | 98.31 | 0.04 | 0.14 | fine |
| 3-5 | 0.62 | 99.38 | 0.00 | 0.16 | fine |
| 3-6 | 1.36 | 98.61 | 0.03 | 0.13 | fine |

## 4.3. Bedforms

The majority of Horns Rev 3 is devoid of mobile bedforms and the seabed is generally planar. However, Ramboll (2013b) provided evidence for a solitary asymmetrical sand wave on the bathymetric high in the west of the pre-investigation area. The geometry of the bedform indicates migration towards the south-southwest.

## 4.4. Suspended Sediment

The pre-investigation area is characterised by relatively high concentrations of inorganic nutrients, low transparency due to high amounts of re-suspended material in the water column, total mixing of the water column and generally good oxygen conditions (Bio/consult, 2000). Concentrations of suspended solids are thought to be around 2-10mg/l in calm conditions, and predicted to rise to several hundred mg/l during storm conditions (Bio/consult, 2000).

## 4.5. Sediment Quality

Oil drilling activities have been considerably more intensive in the northern regions of the North Sea. Therefore, the total quantity of hydrocarbons and other inorganic contaminants such as Poly Aromatic Hydrocarbons (PAHs) and Polychlorinated Biphenols (PCBs) tend to show an increase from the southern North Sea to the northern North Sea. Cefas (2001) reported that, in general, North Sea coastal areas are more metal contaminated than offshore areas because coasts and rivers are the main sources of trace metals.

The seabed at Horns Rev 3 and along the export cable consists of relatively well sorted sediments of sand and gravel with a few pockets of fine-grained sediment, and low organic content (less than 1%, Table 4.3) (Bio/consult, 1999). Chemical pollutants are usually associated with the finer sediment fractions (less than 0.063mm) which act as a sink for many of the persisting, bio-accumulating and toxic contaminants, in particularly metals and hydrocarbons (Horowitz, 1991). Therefore, significant contamination is unlikely to be present across the pre-investigation area and along the export cable.

In order to provide more specific information on the concentration of metals, hydrocarbons and nutrients, six seabed sediment samples (3-1 to 3-6) were collected on 15$^{th}$ March 2013 (Figure 4.2). The six samples were analysed for the following contaminants:

- orthophosphate;
- nitrites/nitrates;
- total organic carbon;
- arsenic;
- cadmium;
- chromium;
- copper;
- mercury;
- lead;
- nickel;
- zinc;
- PAHs;
- PCBs; and
- organotins.

The sediments were sampled for analyses of contaminants and nutrients at six locations identical to the mammal POD stations. The sample locations were representative of the different seabed characteristics including parts of the export cable corridor. ROV video inspections of the seabed along the cable corridor close to shore showed no differences compared to the general sediment patterns represented by the samples. Hence, sediment characteristics along the cable corridor close to shore can be considered more or less identical with the sediment found at locations 3-3 to 3-6.

The context of the contamination found within the sediments of Horns Rev 3 can be established through the use of Action Levels for Dredged Material (OSPAR, 2008), which were adopted by the Ministry of Environment for Denmark in 2005 (Table 4.4). These Action Levels are used to assess the suitability of material for disposal at sea, but are not statutory standards. In addition, although they are generally used in relation to dredging activities, in the absence of sediment quality standards, they are a good indicator as to the potential contamination levels of *in situ* sediments and possible impact on the marine environment, since they take into account eco-toxicological data. Table 4.3 summarises the results from the contaminant analysis, which have been compared to these Action Level standards.

*Horns Rev 1 turbine*

Table 4.3. Contaminant data collected from the six seabed sediment sample sites across Horns Rev 3.

| Contaminant mg/kg (dry weight) unless otherwise stated | Sample ID | | | | | |
|---|---|---|---|---|---|---|
| | 3-1 | 3-2 | 3-3 | 3-4 | 3-5 | 3-6 |
| Arsenic(As) | 2.6 | 3.1 | 3.7 | 2.0 | <2 | 2.5 |
| Cadmium (Cd) | <0.05 | <0.05 | <0.05 | <0.05 | <0.05 | <0.05 |
| Chromium (Cr) | <1 | 1.2 | 1.2 | 2.2 | 3.4 | 4.4 |
| Copper (Cu) | <2 | <2 | <2 | <2 | <2 | <2 |
| Mercury (Hg) | <0.01 | <0.01 | <0.01 | <0.01 | <0.01 | <0.01 |
| Lead (Pb) | <3 | <3 | <3 | <3 | 3.6 | 4.2 |
| Nickel (Ni) | <1 | <1 | <1 | <1 | 1.1 | 1.6 |
| Zinc (Zn) | 1.6 | 4.0 | 2.5 | 5.0 | 8.9 | 16 |
| Tributyl Tin (TBT) | All below limit of detection (LOD) | | | | | |
| PCB (µg/kg) | All below limit of detection (LOD) | | | | | |
| PAH | All below LOD | All below LOD except phenanthrene at 0.0006 | | All below LOD | All below LOD | All below LOD except phenanthrene at 0.0011 |
| Orthophosphate | <5 | <5 | <5 | <5 | <5 | <5 |
| Nitrites/nitrates | 1.3 | 5.2 | 7.7 | 1.0 | 2.2 | 1.2 |
| Total Organic Carbon | 0.23 | 0.23 | 0.24 | 0.33 | 0.34 | 0.5 |

Table 4.4. Action levels for disposal of dredged material as adopted in October 2005 by the Ministry of the Environment for Denmark (OSPAR, 2008).

| Contaminant mg/kg (dry weight) if not otherwise stated | Action Level 1 | Action Level 2 |
|---|---|---|
| Arsenic (As) | 20 | 60 |
| Cadmium (Cd) | 0.4 | 2.5 |
| Chromium (Cr) | 50 | 270 |
| Copper (Cu) | 20 | 90 |
| Mercury (Hg) | 0.25 | 1 |
| Nickel (Ni) | 30 | 60 |
| Zinc (Zn) | 130 | 500 |
| Lead (Pb) | 40 | 200 |
| Tributyl Tin (TBT) | 7 | 200 |
| PCB (µg/kg) (sum of 7 PCBs) | 20 | 200 |
| PAH (sum of 9 PAHs) | 3 | 30 |

Table 4.3 shows that the baseline sediment quality within Horns Rev 3 is very good and concentrations are well below the specified Action Levels. Moreover, the predominantly well-sorted bed composition, comprising primarily sand and gravel significantly reduces the potential for any contaminants to accumulate.

## 4.6. Water Quality

The County of Ribe monitors water quality at three stations which are situated south of Blåvands Huk. The three stations are situated at different water depths (4m, 11m and 14m) and monitor nitrogen, phosphorous and silica in the surface water layer. The Blåvands Huk west station is in close proximity to the pre-investigation area and can be regarded as representative (Figure 4.4).

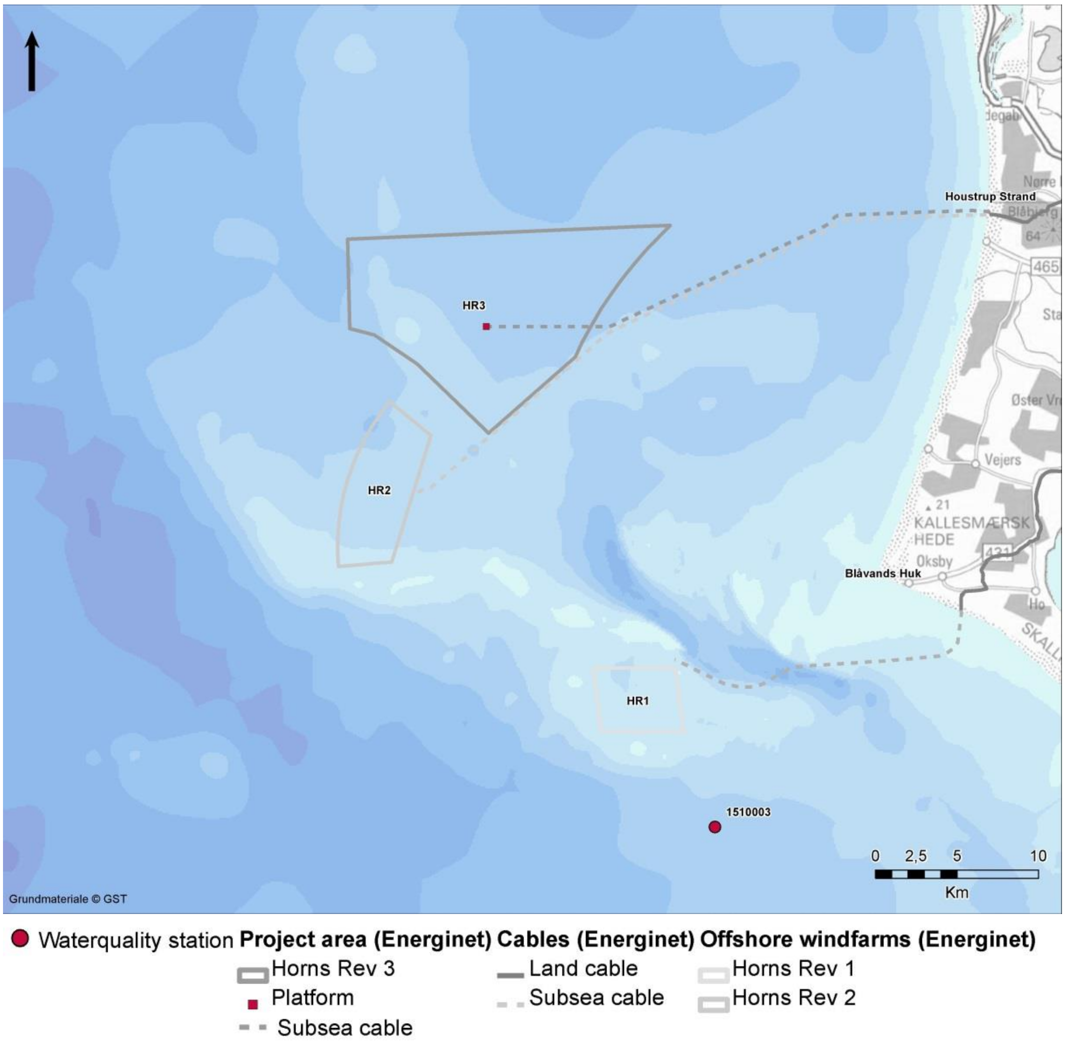


Figure 4.4. Location of Blåvands Huk west water quality station.

Environmental Impact Assessment water quality reports for Horns Rev 1 and Horns Rev 2 (Bio/consult, 2000, 2006) describe a general decrease in nutrients northwards from the Wadden Sea along the west coast of Denmark. The increased concentrations of nutrients and chlorophyll a in the most southerly part of the North Sea primarily reflect the discharge of nutrient-rich water from the German Rivers. In additional, regional runoff from land and atmospheric deposition over the North Sea contribute to increased nutrient levels in this region.

The OSPAR (Oslo/Paris Convention) Commission has evaluated the status of water quality in the northeast Atlantic during a 10 year monitoring and assessment programme (OSPAR, 2010). The Greater North Sea region summary, within which Horns Rev 3 is located, highlights that eutrophication caused by nutrient inputs is a problem along the east coast of the North Sea from Belgium to Norway. In addition, concentrations of metals (cadmium, mercury and lead) and Persistent Organic Pollutants are above typical background levels in some offshore waters and unacceptable in some coastal areas.

The North Sea can be considered as a mixing zone between runoff from land-based tributaries and the relatively 'clean' North Atlantic water entering from the north of Scotland and west via the English Channel. The location of several major rivers and water circulation patterns explain why river runoff from eastern United Kingdom is mainly discharged and confined to the southern North Sea. For this reason, most dissolved metals are more concentrated in the southern North Sea rather than in the northern North Sea, where Horns Rev 3 is located (Cefas, 2001).

Law et al. (1994) reported that in comparison to metal concentrations in estuaries, those observed in offshore sites were low. Many of the metals included in the survey had higher concentrations in the southern North Sea than in the northern North Sea with the exception of lead, which is attributed to the generally lower salinity in the southern North Sea, a consequence of the greater freshwater input from major rivers.

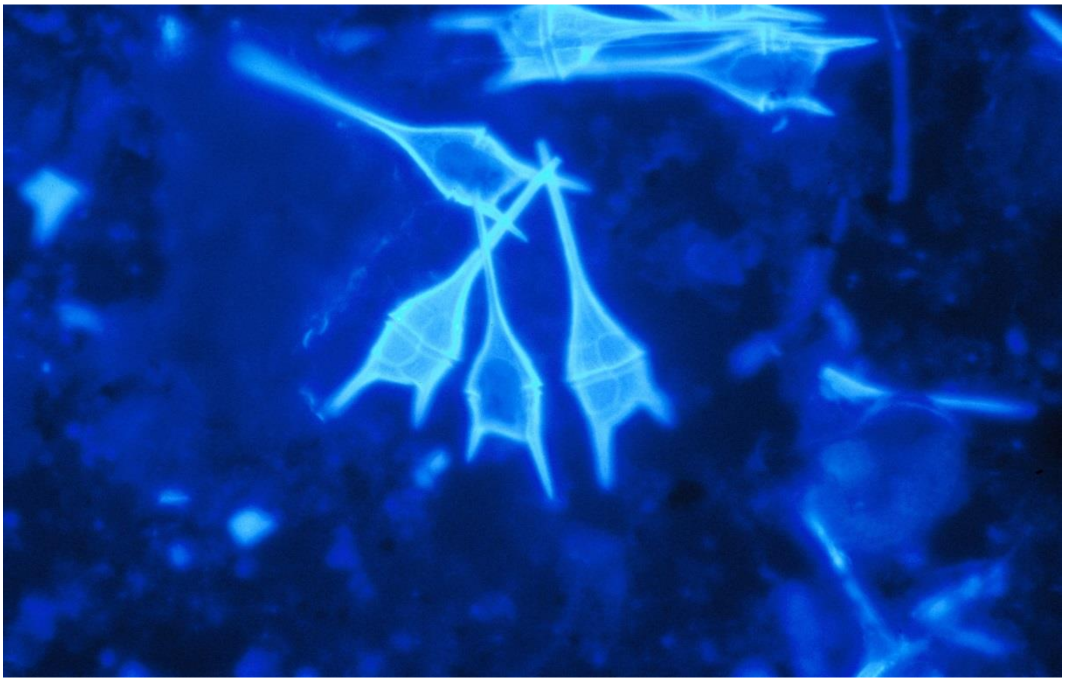

*Plankton*

# 5. COASTAL GEOMORPHOLOGY

The coastal geomorphology between Ringkøbing Fjord and Fanø Island is dominated by Holocene sediments forming a broad coastal plain comprised of several inter-related geomorphological elements (Figure 5.1) (Larsen, 2003). These include Blåvands Huk cuspate foreland, a strand plain of beach ridges north of the foreland (Henne-Vejers Strand, including the landfall at Houstrup Strand) and Skallingen barrier-spit south of the foreland. Immediately offshore from Blåvands Huk and comprising a westerly extension of the foreland is Inner Horns Rev, which itself is separated from Outer Horns Rev by Slugen channel. Located behind Skallingen barrier-spit is Ho Bugt lagoon and Skallingen saltmarsh fed by a tidal inlet (Grådyb inlet) that separates the spit from Fanø Island further south.

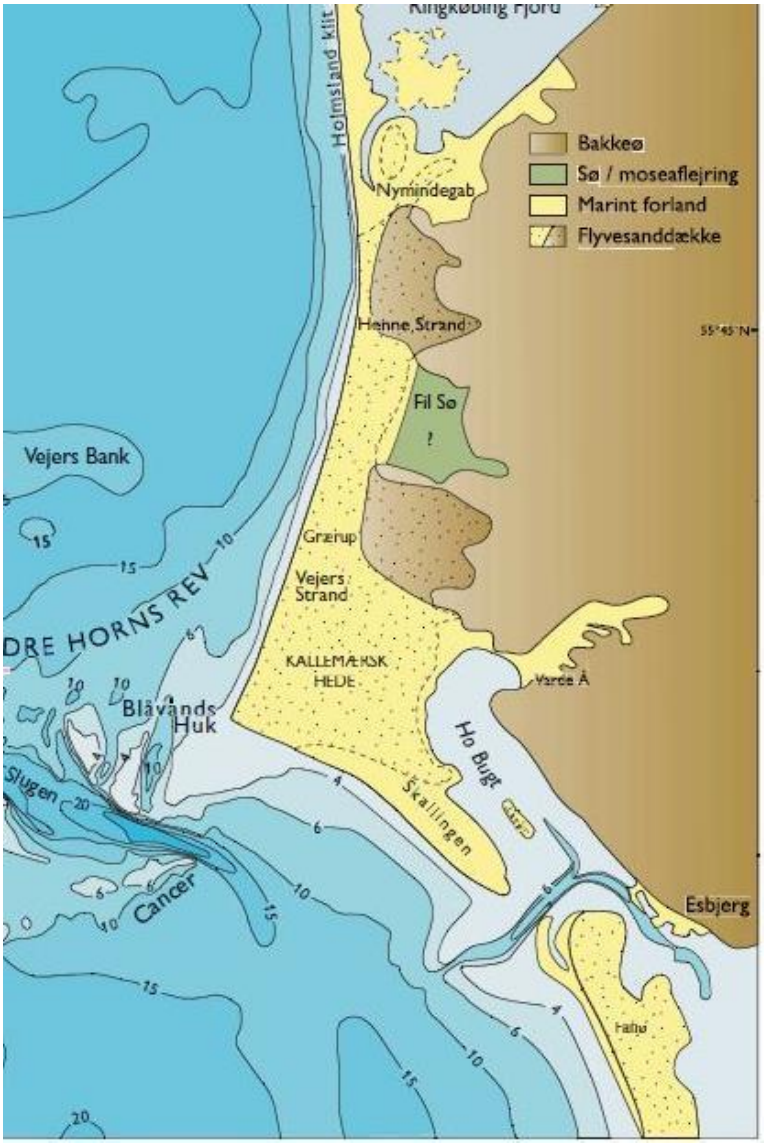


Figure 5.1. Geomorphology of the coastal region landward of Horns Rev 3. Legend: Bakkeø = erosional remnants of Saalian landscape; Sø / moseaflejring = lake and bog deposits; Marint forland = marine foreland; Flyvesanddække = wind deposit sand (Larsen, 2003).

## 5.1. Geomorphological Elements

### 5.1.1 Bakke-ø Landscape

The Pleistocene geology of the west coast of Denmark local to Horns Rev 3 is dominated by sediments deposited during the Saalian glaciation. The outcropping surface of these sediments is known as the *Bakke-ø* landscape, and is the elevated onshore equivalent of the surface that passes beneath Horns Rev 3 (Figure 2.2). The western edge of this landscape is located 0.5-10km inland from the coast between Ringkøbing Fjord and Fanø Island and is exposed in cliffs along the inner shore of Ho Bugt. Between the Saalian outcrop and the coastline, the geomorphology is dominated by sediments deposited during the Holocene (Figure 5.1).

### 5.1.2 Henne-Vejers Strand Plain, Blåvands Huk Cuspate Foreland and Inner Horns Rev

Henne-Vejers strand plain is a 0.5-2.5km wide coastal plain extending south from Ringkøbing Fjord before it widens into the cuspate foreland of Blåvands Huk (Nielsen et al., 1995). Blåvands Huk, which is the westernmost point in Denmark, is a cuspate foreland up to 10km wide and covered by 5-10m of wind-blown sand (especially in the Kallemærsk Hede area).

Both the strand plain and cuspate foreland originated during the Holocene (over the last 7,500 years since sea level reached close to its present level), when the sheltering effect of the shallow (2-6m) Outer Horns Rev caused a slowing of the southerly-directed sediment transport in the area around Blåvands Huk and Inner Horns Rev. This reduction in transport caused this part of the Danish coast to accrete laterally up to 10km westward (Figure 5.1). Overall, this area was a major Holocene sink for sediments transported south along the coast, as well as for sediment transported across the seabed. Currently, the coast north of Blåvands Huk to Nymindegab is prograding at about 0.5–2m/yr. However, the coast north of Nymindegab, in front of Ringkøbing Fjord (Holmsland dune-spit) is eroding at 2-5m/year (Leth et al., 2004).

The development of Inner Horns Rev, a 6km-wide system of shoals and channels protruding 16km into the North Sea west of Blåvands Huk, is an offshore extension of this system (Larsen and Andersen, 2005). The bank is a highly dynamic area with active sand-accumulation, and according to Larsen and Andersen (2005), the west end of the shoal has prograded about 3.5km west over the last 800 years. Slugen channel is a deep channel which separates Inner Horns Rev from Outer Horns Rev.

### 5.1.3 Skallingen Barrier-Spit and Grådyb Tidal Inlet

Skallingen is a 12km long, 2.5km wide barrier-spit, stretching southeast from Blåvands Huk. It is characterised by gentle cross-shore slopes caused by abundant supply of fine-grained sand from the Weichselian outwash plain. It comprises three geomorphological zones:

- 80-100m wide beach and intertidal zone;
- 0.3-1km wide dunes; and
- 1.5-2km wide back-barrier saltmarsh.

Skallingen barrier-spit partly originated from sand transported to the south around the Blåvands Huk foreland. However, given that only a small proportion of sediment passes round Blåvands Huk (DHI, 2006), then the spit is partly built by sand being transported landwards from the shallow subtidal area.

Skallingen barrier-spit is relatively young, documented on maps from the 17th century (Aagaard et al., 1995). A map from 1612 shows open water at the location of the current spit and the shoreline was further inland along another spit known as Langli (Fruergaard et al., 2013) (Figure 5.2). In 1650, the spit is represented by a linear shoal and Langli has become an island. In 1695, Skallingen was a supratidal sand shoal, which forms the basis for the current barrier-spit. Fruergaard et al. (2013) showed that the origin of the barrier-spit was an aggradational (raising elevation) storm shoal deposited rapidly by a 1,000 year storm event in October 1634. During this event, up to 8m of sand was deposited to form the shoal concurrent with 5m of sand in a prograding shoreface.

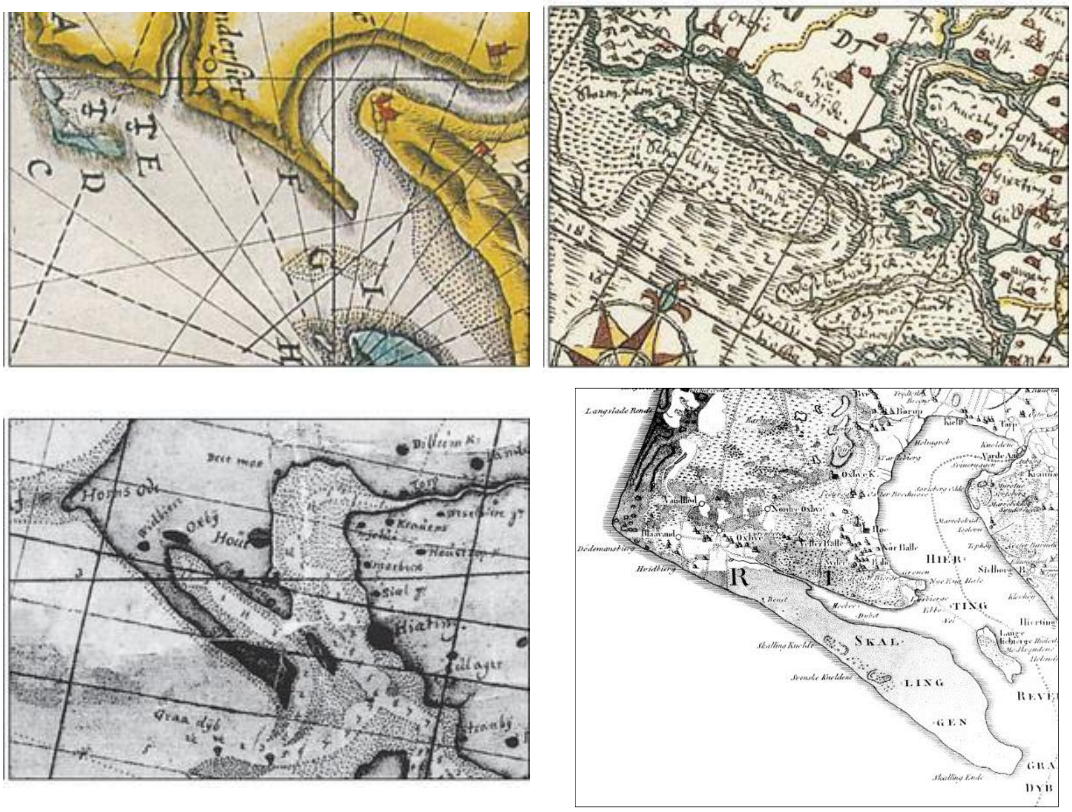


Figure 5.2. Historic maps of Skallingen barrier-spit; 1612 (top left), 1650 (top right), 1695 (bottom left) and 1804 (bottom right).

Re-distribution and continued deposition on these initial geomorphological features led to development of the modern barrier-spit. A map from 1804 describes Skallingen as a barrier generally without vegetation (Figure 5.2). During the 19th century, the surface elevation of the barrier increased due to accretion, and aeolian (wind-blown) processes became more important, leading to the formation and growth of dunes (Aagaard et al., 2007). In the 1930s, any remaining low points between the dunes were closed by construction of large sand dykes in recessed positions in order to prevent overwash. Following their construction, large (8-12m high) foredunes accreted seaward of the dykes.

Since 1804, the southwest facing shoreline migrated landward (eroded) at an average rate of 3-5m/year synchronous with accretion on the barrier-spit itself (Aagaard et al., 1995; Christiansen et al., 2004) (Figure 5.3). Figure 5.4 shows cross-sectional profiles between 1972 and 2012 spaced 2km apart across the central part of Skallingen (Aagaard and Sorensen, 2013). They describe erosion over the past 40 years with a mean rate of about 4.2m/yr. Erosional scarps in the dune front are the main indicator of this erosion. The erosion of the seaward dune face occurs mainly during large storm surges when water levels are elevated. Major dune front erosion has been linked to storms in 1981, 1990 and 1999. Maximum erosion occurred during the 1990s surges when dune recession was up to 44m (Aagaard et al., 1995).

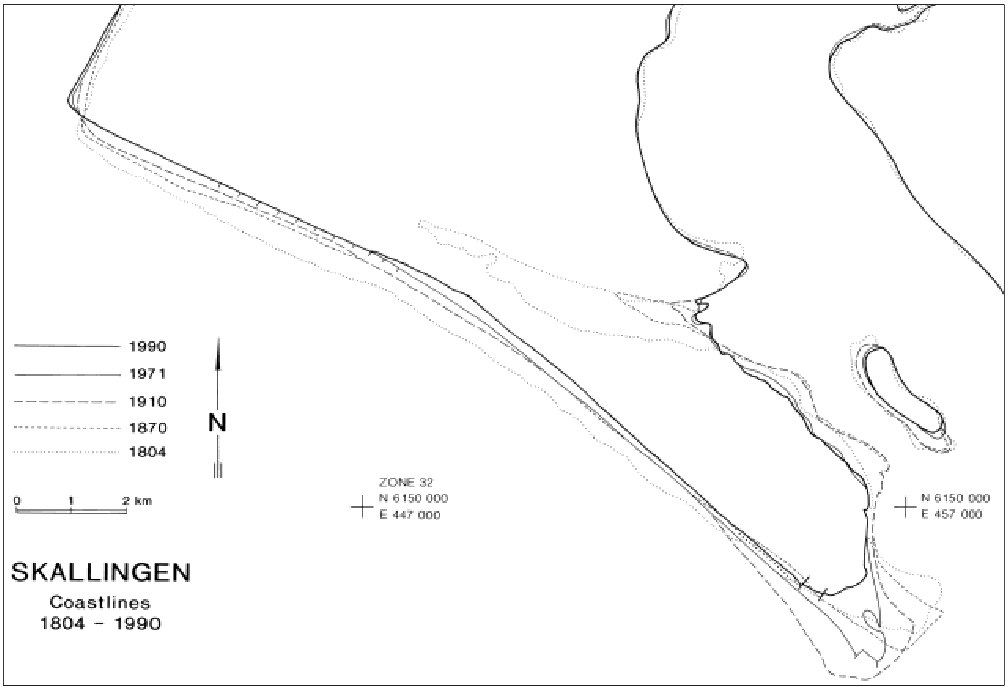


Figure 5.3. Evolution of south Blåvands Huk and Skallingen barrier-spit between 1804 and 1990 (Aagaard et al., 1995).

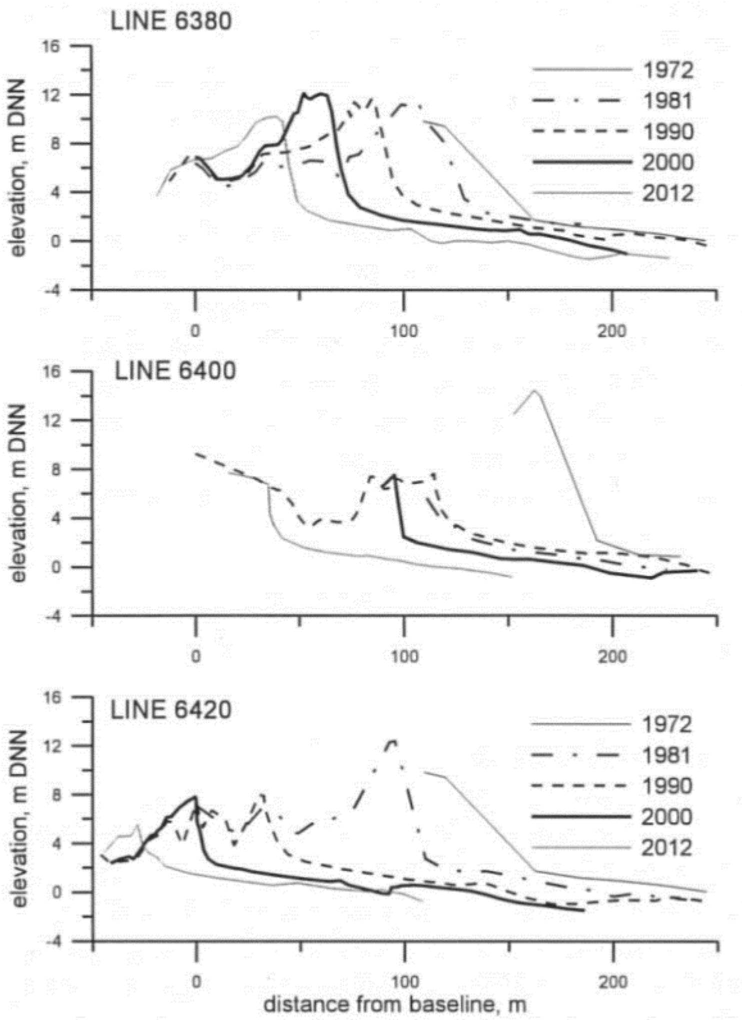


Figure 5.4. Profiles across Skallingen barrier-spit between 1972 and 2012 (Aagaard and Sorensen, 2013).

Figure 5.3 also shows that the tip of Blåvands Huk has moved northwest by approximately 500m between 1804 and 1990 and the tip of the spit receded by about 1.5km in the 1970s. The end of the barrier-spit has eroded approximately 1950m between 1945 and 2000 with maximum erosion rates of 250m/year (Christiansen et al., 2004).

### 5.1.4 Outer Horns Rev

Horns Rev 3 is located in deeper water approximately 10-15km north of the bathymetric high of Outer Horns Rev (Figure 1.1). Outer Horns Rev is about 35km long and comprises southeast and northwest shoals (Figure 5.5). The southeast shoal is approximately 15km long and 1km wide (at the 6m contour) and oriented east-northeast to west-southwest. It consists of two 'sub-shoals'; eastern shoal (Cancer) with water depths less than 5m and western shoal (Vyl) with water depths less than 4m. The northwest shoal is approximately 30km long and 1.5km wide (at the 6m contour) and oriented west-northwest to east-southeast between Munk and Tuxen and east-west between Tuxen and Vovov. It contains three 'sub-shoals'; eastern shoal (Munk) with depths less than 2m, middle shoal (Tuxen) with depths less than 3m and western shoal (Vovov) with depths less than 4m.

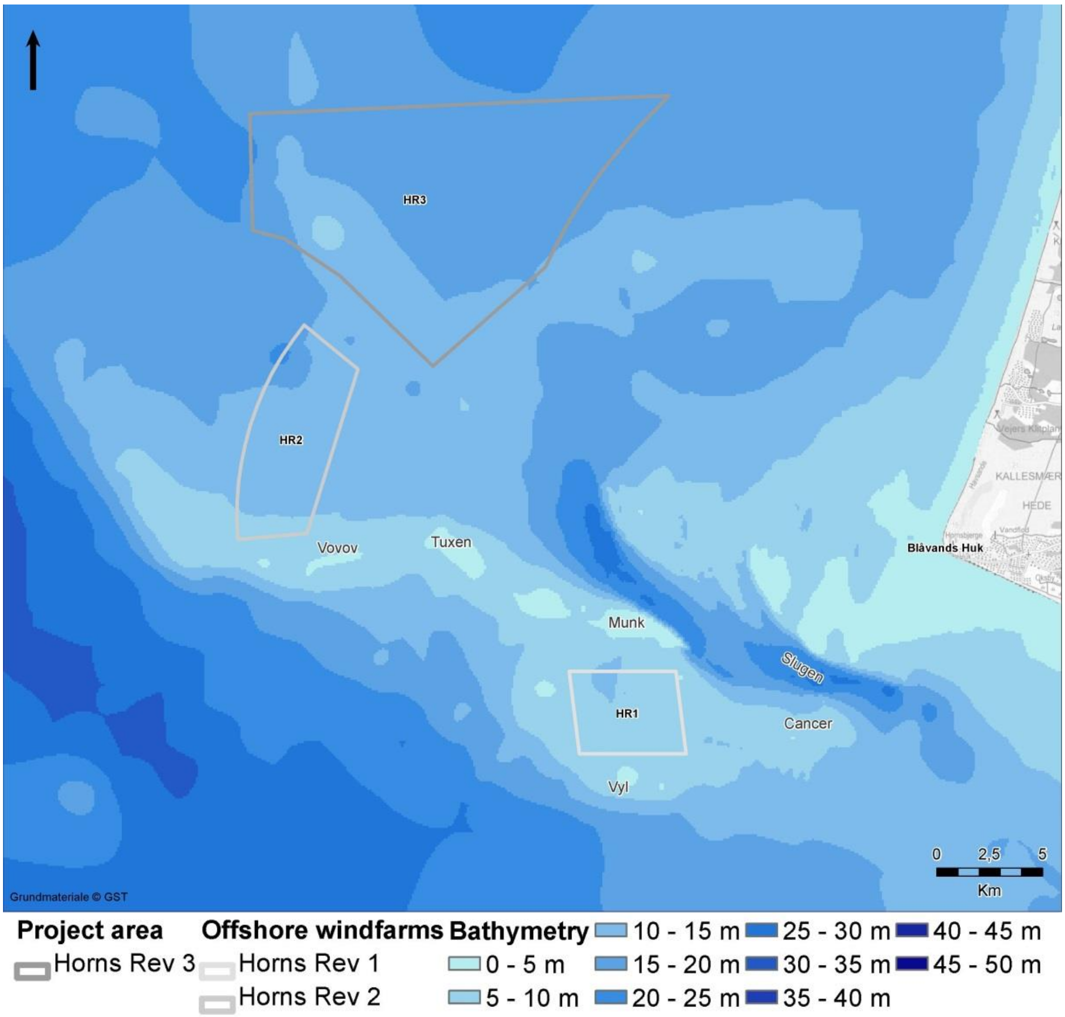


Figure 5.5. Bathymetry of Outer Horns Rev.

### 5.1.5 Ho Bugt Lagoon and Skallingen Saltmarsh

Skallingen saltmarsh in Ho Bugt Lagoon is one of the largest undiked saltmarsh areas in Europe. It covers an area of 31km$^2$ and is located on the lagoon side of Skallingen barrier-spit.

The process of overwash across the Skallingen dunes deposited washover fans of sand in the back-barrier area and at the beginning of the 20th century initial colonisation of saltmarsh vegetation began on these lower-lying sandy areas. The salt marsh developed in two phases, starting around 1900 and in the 1950s (Bartholdy and Madsen, 1985; Aagaard et al., 1995). Artificial sand dykes were constructed in 1933, sheltering the existing marsh from the North Sea and blocking overwash channels (Aagaard et al., 1995). Bartholdy et al. (2004) measured saltmarsh accretion rates of 2-4mm/year since 1933. Bartholdy and Madsen (1985) estimated that approximately 85% of the fine-grained sediment deposited in the back-barrier area has been imported from the North Sea through Grådyb tidal inlet.

## 5.2. Sediment Transport and Budget along the coastline

DHI (2006) modelled the longshore sediment transport along the coast north of Blåvands Huk driven by the predominant waves from the northwest (Figure 3.7). They predicted a net potential southward transport near Nymindegab of about 1Mm$^3$/year. The potential transport rate decreases towards Blåvands Huk caused by the sheltering effect of Outer Horns Rev. This decrease in rate has led to the historical accretion of Blåvands Huk (Section 5.1). The shoreline south of Blåvands Huk is eroding, and this process in combination with the accretion to the north has resulted in the northwest movement of the cuspate foreland (Figure 5.3).

DHI (2006) showed that there is only limited exchange of sediment between areas to the north and south of Blåvands Huk (Figure 5.6). This is because Inner Horns Rev shoal extending west from Blåvands Huk causes wave attenuation and traps sediment transported from the north, and only a small fraction continues south along the coast. Hence, the longshore sediment supply to Skallingen barrier-spit from sources north of Blåvands Huk is limited.

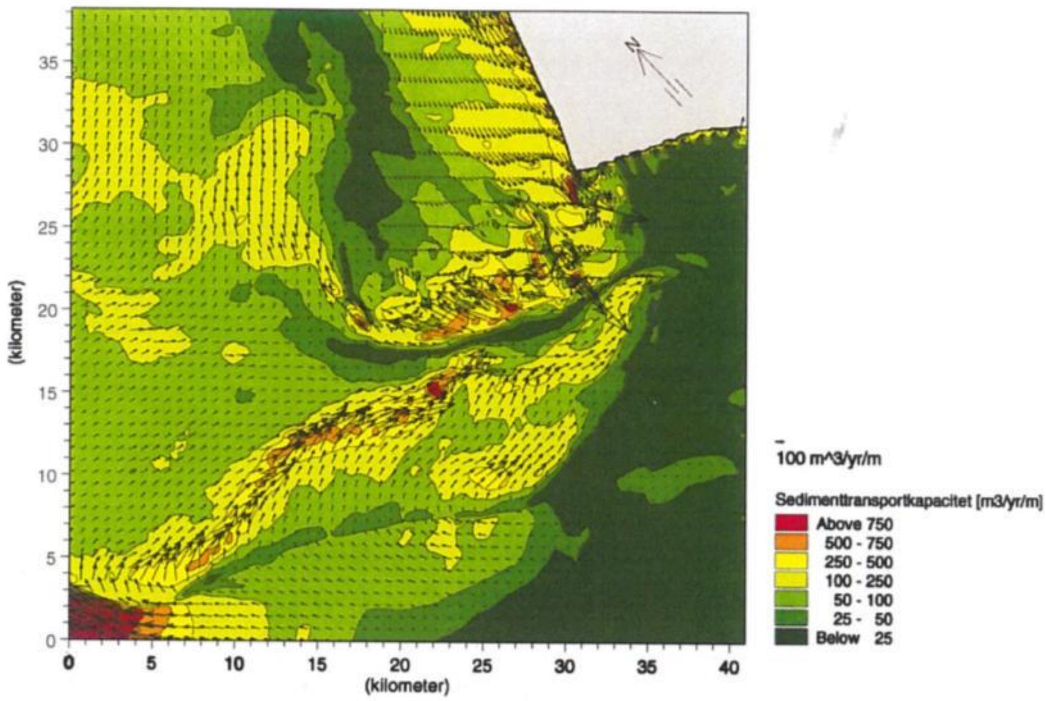


Figure 5.6. Sediment transport patterns across Inner Horns Rev (DHI, 2006).

The sediment budget of Skallingen barrier-spit has been estimated by Christiansen et al. 2004). Given that there is little sediment supply to Skallingen from northerly sources (DHI, 2006), and it is highly unlikely that sand from southerly sources will be able to cross the greater than 10m deep dredged navigation channel of Grådyb tidal inlet, the beach and shoreface are essentially a closed system with no external sediment sources and only one permanent sink (the dredged channel). The following budget has been estimated by Christiansen et al. (2004):

- Cross-shore (offshore to onshore) sediment transport: 90,000m$^3$/year;
- Longshore sediment transport (net to the south): 641,000m$^3$/year;
- Deposition of sediment in lee of foredunes: 65,000m$^3$/year
- Erosion at the end of the barrier-spit: 96,000m$^3$/year

The budget suggests that the narrowing and shortening of the barrier-spit over time (as shown by its geomorphology) is due to substantial sediment losses by longshore transport (into the dredged tidal inlet channel).

*Edible crab at the sea bed*

# 6. WORST CASE SCENARIOS

The hydrography, sediment spill and water quality effects are predicted by comparing the existing environmental conditions with the worst case conditions created by the construction, operation and decommissioning of Horns Rev 3. Several numerical modelling tools and conceptual techniques have been used to support the assessment of existing conditions and the potential effects of the proposed wind farm and cables on hydrography, sediment spill and water quality.

The worst case characteristics of Horns Rev 3 in terms of its effects on hydrography, sediment spill and water quality are adopted. The concrete GBS represent the worst case foundations, in terms of physical blockage to waves and tidal currents. There is now a considerable evidence base across the offshore windfarm industry which indicates that the greatest potential effect is associated with conical gravity base structures (Forewind, 2013). This is because these structures occupy a significant proportion of the water column as a solid mass (as opposed to an open lattice of slender columns and cross-members, like for example jackets or tripods, or a single slender column like a monopile). They do, therefore, have the potential to affect wave propagation and near-surface tidal currents in a manner that other foundation types do not.

Hence, the conical GBS foundation has been incorporated in the numerical modelling of operational effects on these physical processes elements for Horns Rev 3. Should other foundation types ultimately be selected following the design optimisation of the development, then the effects on waves and tidal currents will be less than those presented for the worst case GBS.

Nine potential worst case gridded layouts for Horns Rev 3 have been considered to determine the worst case for hydrography, sediment spill and water quality. These are layouts across the eastern side of the pre-investigation area, the centre of the pre-investigation area and the western side of the pre-investigation area, either filled entirely with 3MW, 8MW or 10MW GBS foundations (Figures 1.3 to 1.5). The layouts composed entirely of 3MW GBS foundations represent the smallest foundation type with a relatively narrow spacing, whereas layouts composed entirely of 10MW foundations represent the largest foundation type with a relatively wide spacing.

For the purpose of predicting effects on waves, tidal currents and sediment transport, the worst case scenario is considered to be a layout composed on 3MW foundations across the western side of the pre-investigation area (Figure 1.3 left column). This provides the layout with the maximum potential for interaction of wave and tidal current processes because the spacing is the narrowest, inducing the largest potential blockade. Also, the water depths across the western half of Horns Rev 3 are the shallowest and the foundations will be subject to the highest reflection and scattering (diffraction) of incoming waves.

## 6.1. Modelling Approach to Determine the Worst Case Wave Blocking Effect of a GBS Foundation

When waves coincide with a wind turbine foundation, part of the energy is reflected and part of it is diffracted around the structure. This effect changes the wave climate in the vicinity of the structure and is referred to as the wave shadow effect. Other causes for the redistribution/loss of wave energy are wave-structure friction and flow separation behind the structures. The effects on the wave field from friction and flow separation are not as important as reflection and diffraction for large offshore structures, and so in this report, only the effects of reflection and diffraction are considered. The magnitude of these effects is gauged by using a wave reflection coefficient which is the equivalent of the reflection effects of a wind turbine foundation.

The effect of a 3MW GBS foundation on waves was quantified using the computer program DIFFRACT developed by the University of Oxford (Zang et al., 2006; Zang et al., 2009). DIFFRACT has been developed to calculate linear and second order wave diffraction from three-dimensional arbitrary-shaped fixed or floating structures. It is based on potential flow theory using the panel method. A wide range of benchmarking tests has been performed to validate the implemented solution algorithms and numerical code against published results. Very good agreement was obtained for all the test cases including bottom mounted circular cylinders, multiple columns and floating vessels. Details of the mathematical solutions for calculating wave reflection coefficients at a structure are provided in Box 6.1.

**Box 6.1**

**Calculation of wave reflection coefficient**

When considering the energy flow through the wind turbine foundations, an energy balance can be set up based on the figure below. The relationship between incoming energy $\hat{E}_{f,I}$, reflected energy $\hat{E}_{f,R}$ and transmitted energy $\hat{E}_{f,T}$ can be written as:

$$\hat{E}_{f,R} = \hat{E}_{f,I} - \hat{E}_{f,T} \quad (1)$$

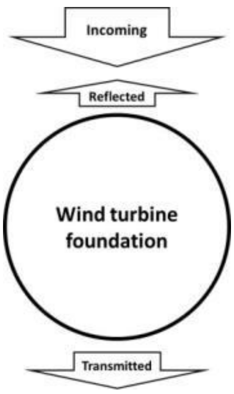


Redistribution of wave energy due to a wind turbine foundation

Under first-order assumptions, the wave energy flux for waves over a plane seabed can be expressed by:

$$E_f = \frac{1}{T}\int_0^T \int_{-h}^{\eta} p^+ u dz dt \quad (2)$$

Where *u* is the horizontal velocity of a water particle, $p^+$ is the excess pressure, *T* is wave period and *h* is water depth.

For undisturbed waves (incoming waves), the energy flux can be expressed as:

$$E_{f,I} = \frac{1}{16}\rho g H^2 c\left(1 + \frac{2kh}{\sinh(2kh)}\right) \quad (3)$$

where $\rho$ is mass density, *g* is gravitational acceleration, *H* is wave height, *c* is wave celerity and $c = \omega/k$ (here $\omega=2\pi/T$), *k* is the wave number and $k=2\pi/L$ (*L* is the wavelength)

The transmitted energy flux $\hat{E}_{f,T}$ can be calculated by integrating the wave energy flux from the foundation surface to infinity, perpendicular to the wave direction, which is:

$$\hat{E}_{f,T} = \int_{-\infty}^{\infty} E_{f,T} dy \quad (4)$$

Usually, wind turbine foundations are axisymmetric structures and only half the plane is needed in calculations. So the transmitted energy $\hat{E}_{f,T}$ can be obtained from the integration from CL(*y=0*) to infinity:

$$\hat{E}_{f,T} = 2\int_{CL}^{\infty} E_{f,T}dy = 2\int_{CL}^{\infty}\left[\frac{1}{T}\int_{0}^{T}\int_{-h}^{\eta} p^{+}udzdt\right]dy \quad (5)$$

The wave reflection coefficient can be defined as

$$C = \frac{\hat{E}_{f,I}-\hat{E}_{f,T}}{E_{f,I}} = 2\frac{\int_{CL}^{\infty}\left\{E_{f,I}-\left[\frac{1}{T}\int_{0}^{T}\int_{-h}^{\eta} p^{+}udzdt\right]\right\}dy}{E_{f,I}} \quad (6)$$

This wave reflection coefficient indicates the equivalent reflection effects of wind turbine foundation (in metres).

**Wave diffraction calculation**

Excess pressure $p^{+}$ and horizontal velocity *u* are needed for calculating the wave reflection coefficients. Under the first-order assumption using potential flow theory, the expressions for calculating excess pressure and horizontal velocity can be written as:

$$p^{+} = Re[\mathrm{i}\omega\rho\varphi e^{-\mathrm{i}\omega t}] \quad (7)$$
$$u = Re[\frac{\partial\varphi}{\partial x}e^{-\mathrm{i}\omega t}] \quad (8)$$

where $Re[\,]$ denotes the real parts of complex numbers, $\varphi$ is the first-order velocity potential in a fluid domain. In wave diffraction problems, velocity potential $\varphi$ can be decoupled into:

$$\varphi = \varphi_I + \varphi_D \quad (9)$$

where $\varphi_I$ is incident potential which has analytical expression and $\varphi_D$ is diffraction potential which can be obtained numerically by solving the boundary value problem of wave-structure interactions.

Across the Horns Rev 3 pre-investigation area, the bathymetry varies from -11m to -21m. Hence, the geometry of the foundations has been scaled in size to be appropriate for these depths. Diffraction calculations were completed on 3MW GBS foundations in water depths of 10m, 15m and 20m (Figures 6.1 to 6.3).

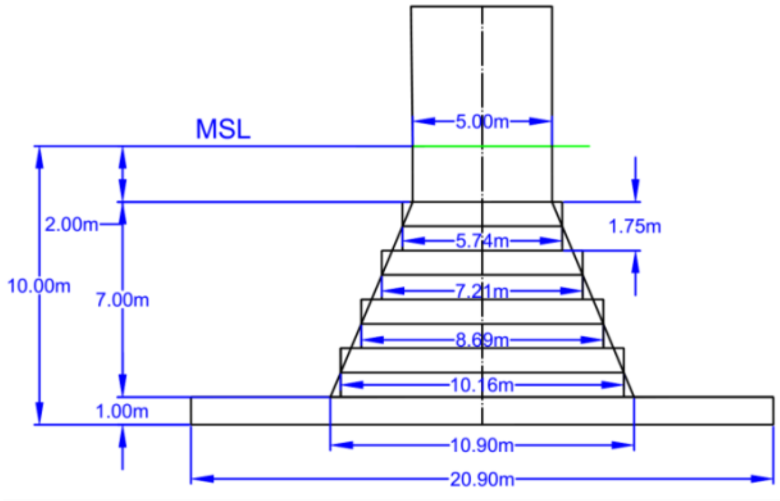


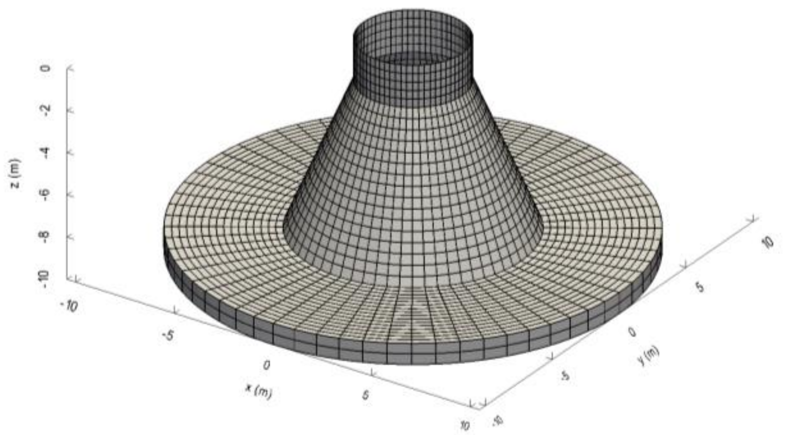


Figure 6.1. Cross-section (top) and numerical mesh (bottom) of a 3MW GBS foundation in a water depth of 10m.

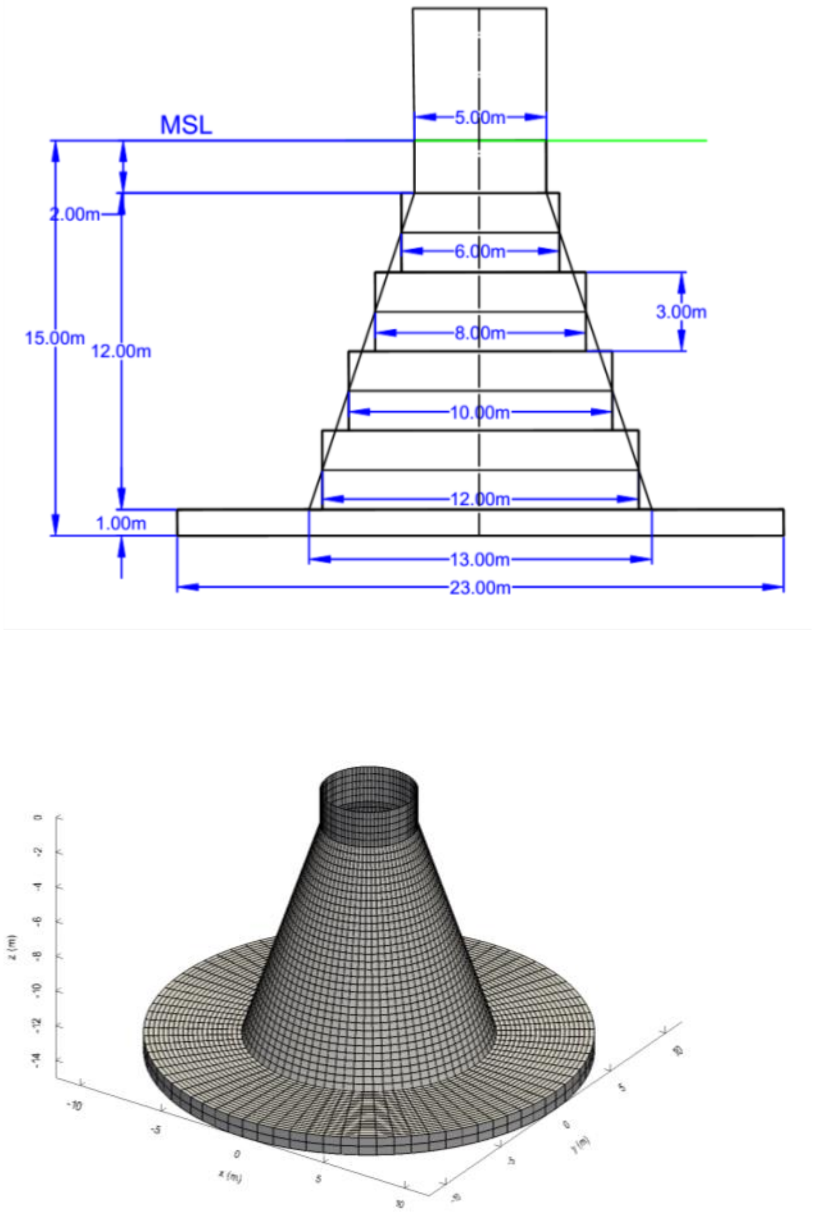


Figure 6.2. Cross-section (top) and numerical mesh (bottom) of a 3MW GBS foundation in a water depth of 15m.

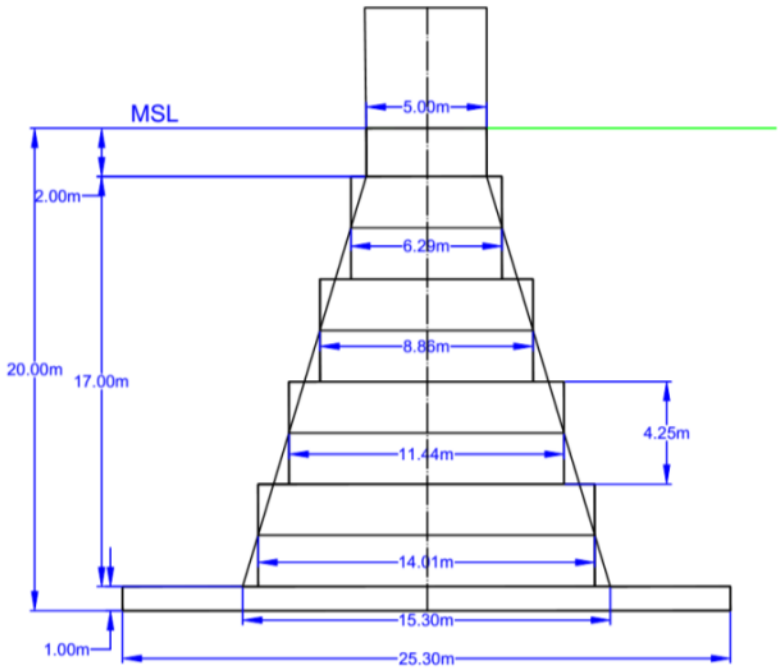


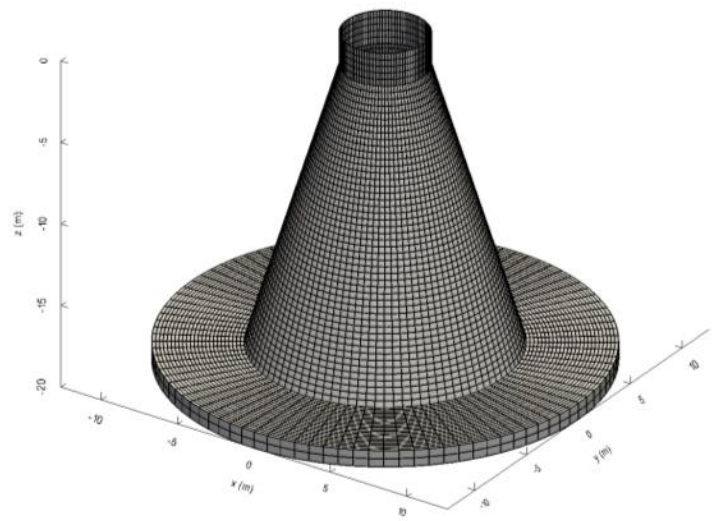


Figure 6.3. Cross-section (top) and numerical mesh (bottom) of a 3MW GBS foundation in a water depth of 20m.

The DIFFRACT computations were carried out using wave periods between 2 and 25 seconds in steps of one second. The output from DIFFRACT is a set of wave reflection coefficients as a function of wave period for each water depth (Table 6.1 and Figure 6.4). The results show that the worst case wave blocking effect occurs in the shallowest water (10m).

Table 6.1. Wave reflection coefficients (metres) of 3MW GBS foundations in 10m, 15m and 20m water depth.

| Wave Period (s) | Water Depth (m) | | |
|---|---|---|---|
| | 10 | 15 | 20 |
| 2.0 | 3.871 | 3.241 | 3.151 |
| 3.0 | 3.930 | 4.339 | 4.253 |
| 4.0 | 4.755 | 3.221 | 3.160 |
| 5.0 | 3.014 | 1.513 | 1.358 |
| 6.0 | 1.990 | 0.916 | 0.769 |
| 7.0 | 1.357 | 0.611 | 0.495 |
| 8.0 | 0.955 | 0.422 | 0.327 |
| 9.0 | 0.694 | 0.299 | 0.216 |
| 10.0 | 0.520 | 0.218 | 0.142 |
| 11.0 | 0.401 | 0.162 | 0.093 |
| 12.0 | 0.316 | 0.124 | 0.060 |
| 13.0 | 0.255 | 0.096 | 0.037 |
| 14.0 | 0.209 | 0.076 | 0.021 |
| 15.0 | 0.175 | 0.061 | 0.010 |
| 16.0 | 0.148 | 0.050 | 0.002 |
| 17.0 | 0.127 | 0.041 | 0.001 |
| 18.0 | 0.111 | 0.034 | 0.001 |
| 19.0 | 0.097 | 0.028 | 0.001 |
| 20.0 | 0.086 | 0.024 | 0.001 |
| 21.0 | 0.077 | 0.020 | 0.001 |
| 22.0 | 0.069 | 0.017 | 0.001 |
| 23.0 | 0.063 | 0.015 | 0.001 |
| 24.0 | 0.057 | 0.013 | 0.001 |
| 25.0 | 0.053 | 0.011 | 0.001 |

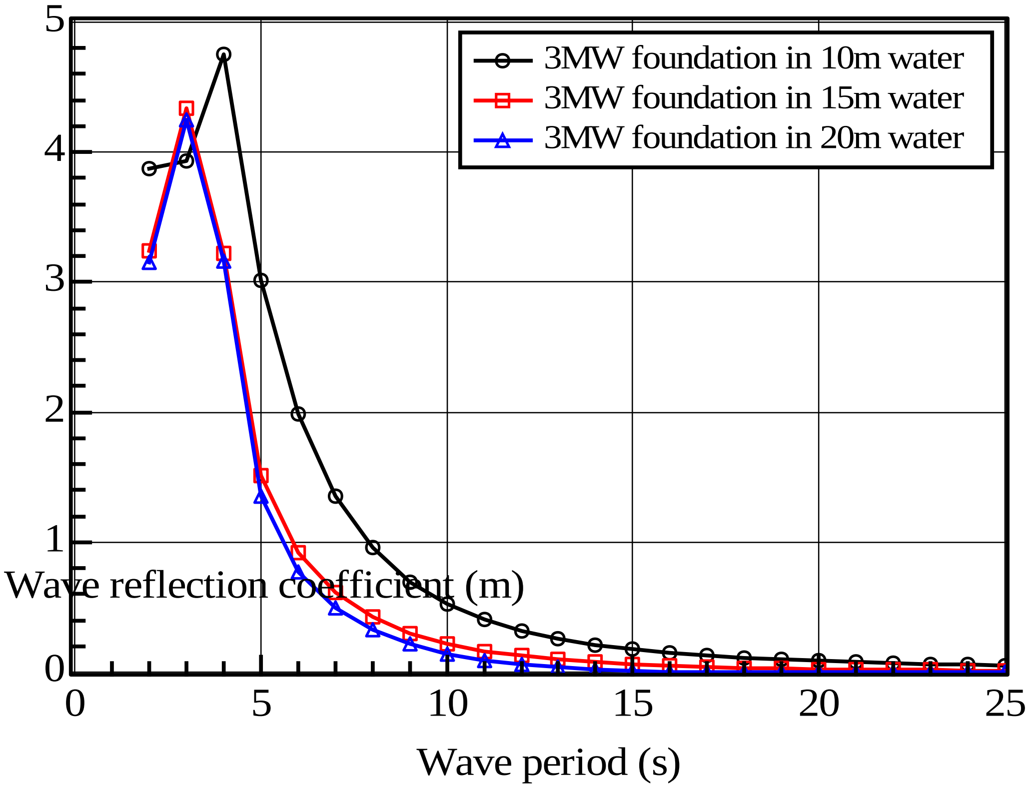


Figure 6.4. Wave reflection coefficients of 3MW GBS foundations in 10m, 15m and 20m water depth.

These wave reflection coefficients were used as input into the wave model to account for blocking effect of the GBS foundations. The wave reflection factors are effectively 'blocking widths', and so for example, the wave reflection coefficient peaked at 4.339 in 15m of water, which actually means an equivalent 4.339m of blocking by the foundation.

## 6.2. Worst Case Construction Process and Assumptions for Foundations and Inter-array Cables

Increases in suspended sediment concentration may result from disturbance arising from construction activities. In order to define the worst case scenario for foundation installation and inter-array cable laying a conservative approach was adopted. In this approach, four sets of nine conical GBS foundations distributed across the western side of the pre-investigation area and a set of inter-array cables connecting them (Figure 6.5), were installed over a 27-day period and simulated over a 30-day period. The locations of the four sets of foundations have been chosen to capture differences in tidal flows, and consequently potential differences in plume dispersion patterns, across the pre-investigation area. The plume extents from the four modelled simulations are then transposed across the entire pre-investigation to produce a boundary containing the indicative worst case 'outer extent' of increases in suspended sediment concentration.

The worst case scenario adopted here is a proportionate and practical approach, which is suitable to cover sediment dispersion from the entire site over the entire construction programme. This is because it is an intensive (i.e. very conservative) construction sequence and a less intense situation (i.e. longer term diffuse sediment dispersion) would be within those bounds. The construction of the entire site would mean that the location of the 'source' of sediment would move across the site as the installation progresses and from each source the dispersion patterns will take the sediment along a similar tidal stream, but to a different end destination. Hence, an interpretation / extrapolation of the results from the four sets of nine conical GBS foundations provide the intensive (i.e. worst case) basis for those assessments.

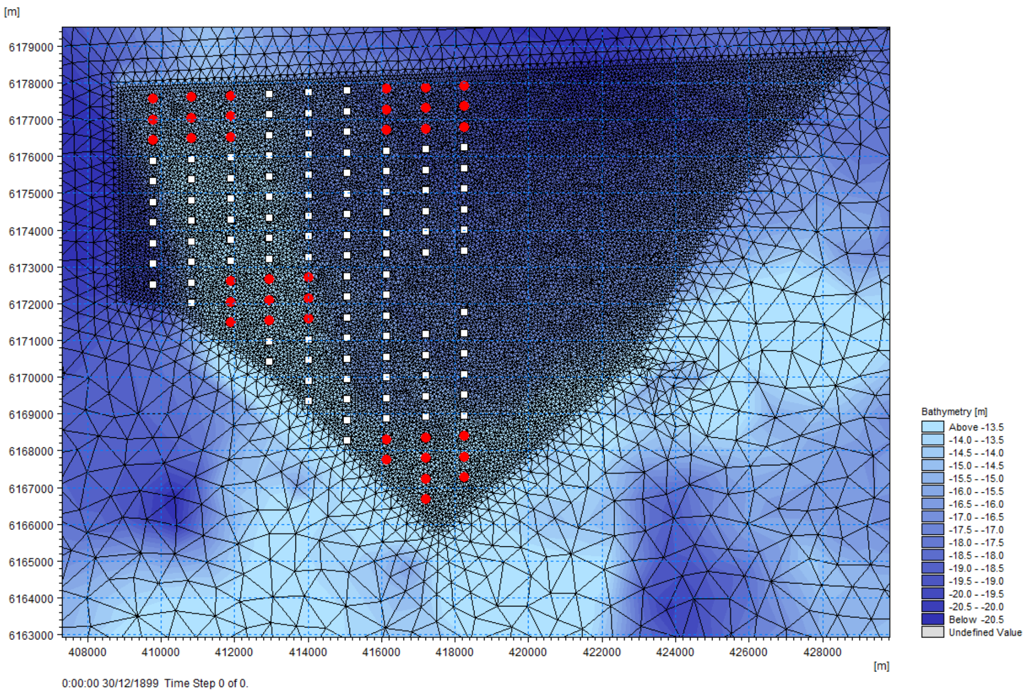


Figure 6.5. Location of foundations (in red) for worst case scenario construction.

## 6.2.1 Seabed Preparation for Foundations

Seabed preparation is potentially required for GBS foundations in order to provide them with a stable surface on which to sit. An assumption is made that seabed preparation will be carried out using a dredger or an excavator placed on a barge or other floating vessel. The seabed preparation at each foundation is expected to take three days (Energinet.dk, 2014) and will be continuous (i.e. 27 days for nine foundations). An assumption is made that four excavator vessels are operating simultaneously at the four sets of nine foundations. After the three day installation it is assumed that scour protection is applied immediately to the foundation and no scour takes place. As a worst case, each foundation will have 1,300m$^3$ of sediment excavated for seabed preparation over the three day period (Energinet.dk, 2013 suggested 900-1,300m$^3$ per foundation). Of this 1,300m$^3$ a conservative estimate of 5% (65m$^3$) is released into the water column for dispersion, equating to a release rate at each foundation of 0.00025m$^3$/sec. The remainder (95%) is secured on barges for disposal (Energinet.dk, 2014).

### 6.2.2 Jetting the Inter-array Cables

The worst case installation method for the inter-array cables is considered to be jetting. The volume of sediment affected during cable laying is 1.5m$^3$ per metre of jetting, assuming jetting to a worst case depth of 2m into the seabed, a triangular cross-section with a worst case top width of 1.5m (Figure 6.6). Using an excavation rate of 250m per hour (based on various estimates of jetting rates of between 150m and 450m per hour quoted by offshore developers), equates to a release rate of 0.1m$^3$/sec, which is 415 times higher than the sediment release rate of 0. 00025m$^3$/sec for GBS foundation seabed preparation. Cables will be installed from north to south along each line of foundations proceeding from east to west (six cables per block of nine foundations). At a rate of 250m per hour, each cable would be completed in just over two hours because they have lengths of 560m.

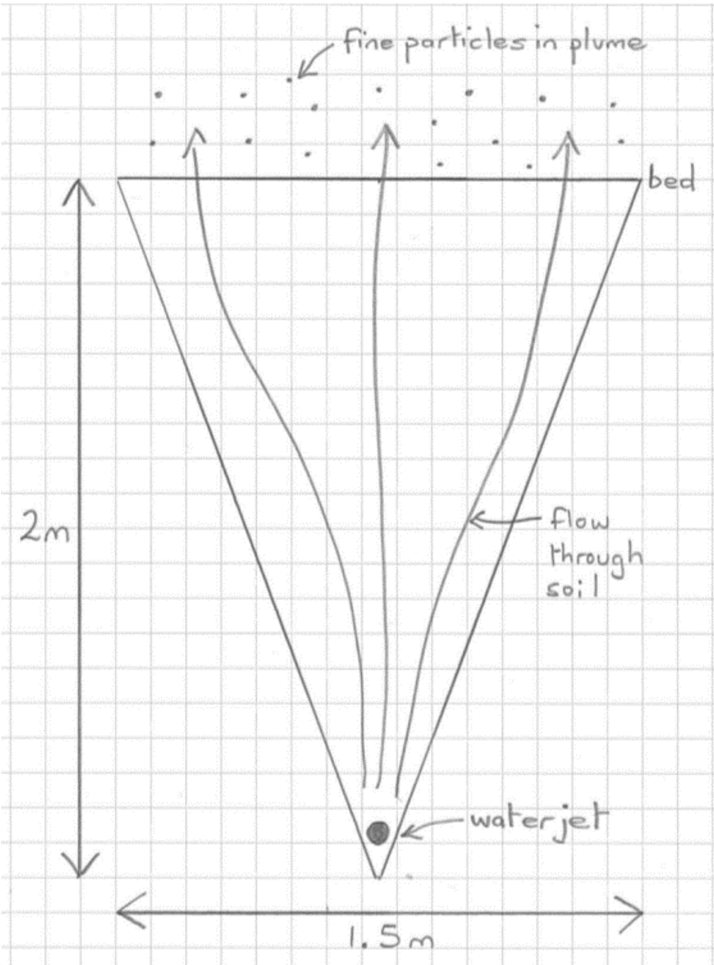


Figure 6.6. Process of jetting in cross-section.

### 6.2.3 Particle Size

Tables 5.1 and 5.2 summarise particle size distributions for surface sediment samples recovered across Horns Rev 3. A conservative particle size distribution for sediment released due to seabed preparation is based on an average of all these samples. Table 6.2 presents the average particle size distribution for Horns Rev 3 used as the worst case. Sand is consistent down to 2m (Ramboll, 2013a, b; GEO, 2013) which is assumed to be the average depth of seabed preparation across the site (and is deeper than the 1m depth for jetting the inter-array cables).

Table 6.2. Average particle size for seabed sediments across Horns Rev 3.

| Size Class | Sediment Size (mm) (Mid-Point of Class) | Quantity (%) |
|---|---|---|
| Gravel | 2 | 2.91 |
| Coarse sand | 1.3 | 16.03 |
| Medium sand | 0.41 | 51.99 |
| Fine sand | 0.125 | 27.97 |
| Silt and clay | 0.063 | 1.11 |
| **Total** | | **100** |

## 6.3. Worst Case Construction Process for the Export Cable and Substation

The Horns Rev 3 export cable corridor is approximately 34km long from its exit point at the substation within the pre-investigation area to the landfall at Houstrup Strand. A variety of techniques could be used to excavate a trench for the export cable, but the worst case method is considered to be jetting.

### 6.3.1 Jetting the Export Cable

Installation of a substation (three days) and a single cable in a trench over a 15-day simulation period was modelled as the worst case scenario. Given an excavation rate of 250m/hour, the trench would be completed in about 5.7 days. The volume of sediment released during cable laying is 1.5m$^3$ per metre of jetting equating to a release rate of 0.1m$^3$/sec (the same as for the inter-array cables, Figure 6.6).

### 6.3.2 Seabed Preparation for Substation

As a worst case, the substation will have 2,400m$^3$ of sediment excavated for seabed preparation (for a hybrid foundation; Energinet.dk, 2013) over the three day period. Of this 2,400m$^3$ a conservative estimate of 5% (120m$^3$) is released into the water column for dispersion (DHI, 2009).

### 6.3.3 Particle Size

A conservative particle size distribution for released sediment due to export cable jetting is based on an average of a small sub-set of the seabed samples that are located on or close to the cable corridor. Table 6.3 describes the average particle size distribution for the export cable used as the worst case. It is assumed that the sand is consistent to 1m sub-bottom.

Table 6.3. Average particle size for seabed sediments along the export cable.

| Size Class | Sediment Size (mm) (Mid-Point of Class) | Quantity (%) |
|---|---|---|
| Gravel | 2 | 0.21 |
| Coarse sand | 1.3 | 5.63 |
| Medium sand | 0.41 | 36.05 |
| Fine sand | 0.125 | 56.55 |
| Silt and clay | 0.063 | 1.56 |
| **Total** | | **100** |

## 6.4. Worst Case Landfall Construction

The key components of the construction methodology with the potential to affect coastal processes are:

- the connection of the landfall to the onshore portion of the cables;
- the connection of the landfall to the offshore export cables;
- the placement of structures on the shore to achieve the connections; and
- the sequencing of activities.

The landfall at Houstrup Strand (Figure 1.2) is where the offshore export cable and the onshore cable will be connected at the Blåbjerg substation, situated in Blåbjerg Klitplantage. The submarine cable will be pulled to shore and then placed in a trench cut to a depth of maximum 3-5m into the beach. Excavated sand will be side-cast on the adjacent beach and backfilled once the cable has been placed in the trench. Each trench would be excavated and backfilled with a mechanical digger. During the backfilling process the beach will be re-profiled, with the re-instatement of beach levels. The landfall construction is anticipated to take approximately two weeks.

## 6.5. Worst Case in Relation to Water Quality

The worst case impact on water quality relates to the scenario which gives rise to the most sediment being re-suspended because this will impact on transparency and potential contamination of the water column via desorption of chemical contaminants from sediment particles. There will also be materials used both during the construction and operational phase of the turbines such as grout and ballast material, depending on the type of foundation installed. In addition, oil may be used during maintenance for transformer cooling which could lead to water quality impacts if discharged to the marine environment. There could also be spills of lubricants and substances during decommissioning as these are removed. For each of the phases the potential discharges of material can be summarised as follows:

During construction:

- use of ballast material in the concrete GBS foundation, which is likely to be infill sands from an offshore source or heavy ballast material (Olivine or Norit). Installation will occur by pumping or use of excavators into the ballast chambers;
- grout (cement based product) used in most foundation options; and,
- corrosion protection for all turbine types using protective paint coating and installation of sacrificial anodes on the subsea surface.

During operation:

- various fluids will be required such as oils and lubricants to ensure the turbines function correctly.

During decommissioning:

- removal of all fluids such as oils and lubricants.


*Foundations ta Horns Rev 2 Offshore Wind Farm*

# 7. TIDAL CURRENT MODEL SET-UP AND BASELINE CONDITIONS

The hydrodynamic regime is defined as the behaviour of bulk water movements driven by the action of tides. In order to investigate tidal current flows across the eastern North Sea and provide a baseline for prediction of changes due to Horns Rev 3, a hydrodynamic model was run for a 30-day simulation period.

Tidal current simulations were completed using Royal HaskoningDHV's established European Continental Shelf Regional Tidal Model built in MIKE21 software. MIKE21 is a widely used, state of the art integrated modelling package for application in coastal and port areas and was developed for simulation of non-steady water flow and transport of dissolved matter (DHI, 2011). The MIKE21 hydrodynamic (HD) module solves the three-dimensional shallow-water equations for arbitrary boundary conditions using a finite volume method on a rectangular or a triangular grid. In this assessment, MIKE21-HD is used in the one layer mode, in which the tidal current velocities predicted by the model are depth-averaged.

## 7.1. Model Boundaries

The modelling was based on integration and downscaling from a large scale (regional model) to a small scale (local model) of tidal currents. The regional model covers the North Sea, Baltic Sea, English Channel, Norwegian Sea, and extends into the North Atlantic Ocean (Figure 7.1). It was developed to simulate large-scale circulation patterns and provided the boundary conditions input into the more detailed local model. The local model was nested within the regional model and covers the coastal area between Norway, Denmark and The Netherlands (Figure 7.2) and is run to simulate the tidal current patterns.

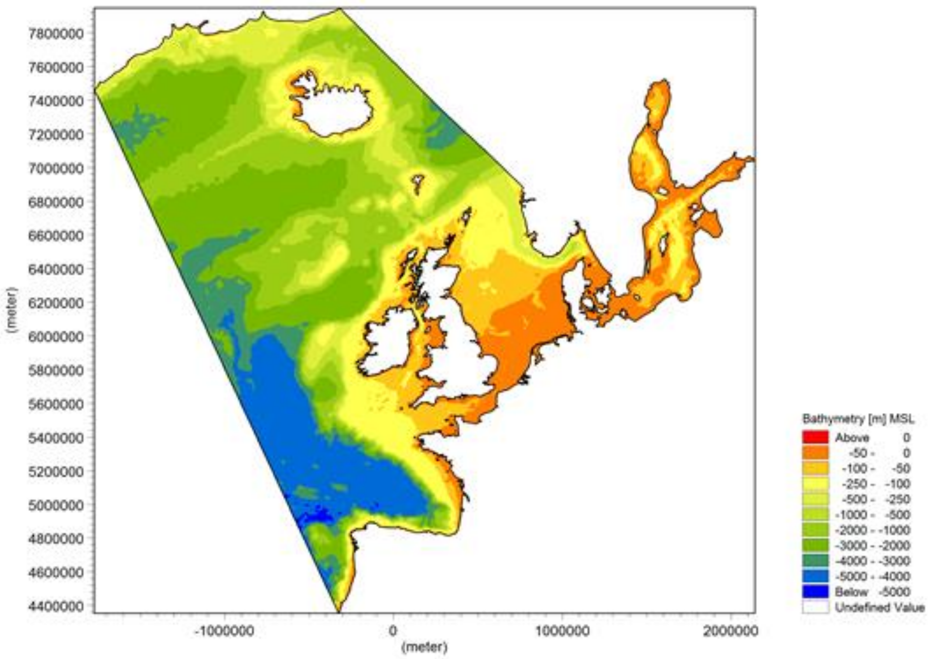


Figure 7.1.Boundaries of the regional model.

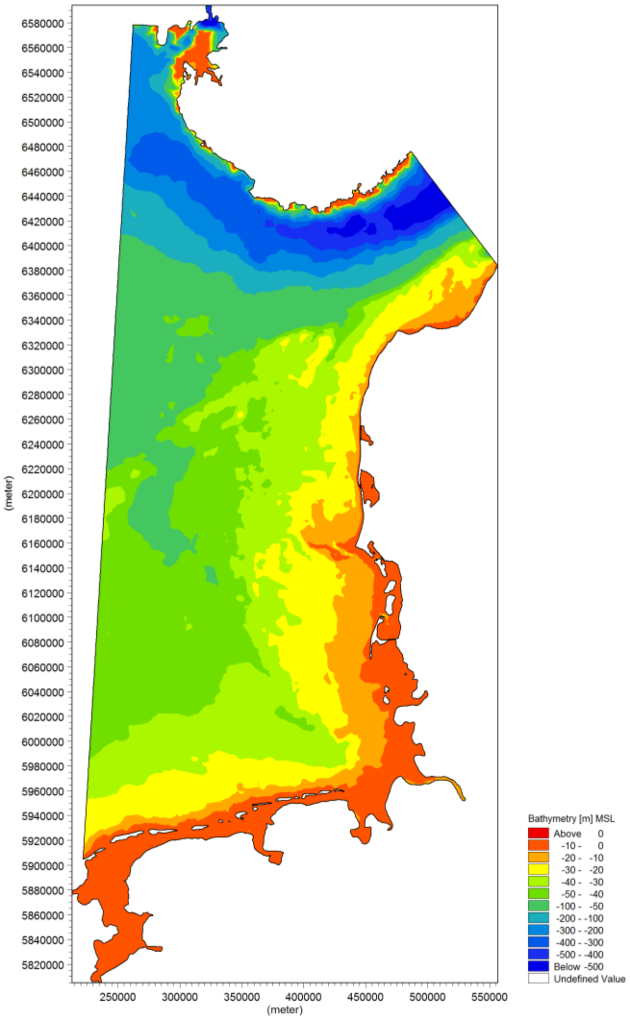


Figure 7.2. Boundaries of the local model.

## 7.2. Model Bathymetry

The bathymetric data for the model domains was obtained from three sources; detailed surveys of the Danish and United Kingdom coasts with C-Map data coverage elsewhere (Figure 7.3). The Danish coastal data includes the bathymetric survey conducted for Horns Rev 3. The United Kingdom bathymetry was collected by Royal HaskoningDHV from previous studies. The model domain covered by C-map data includes the North Sea in more detail extending in less detail into the North Atlantic.

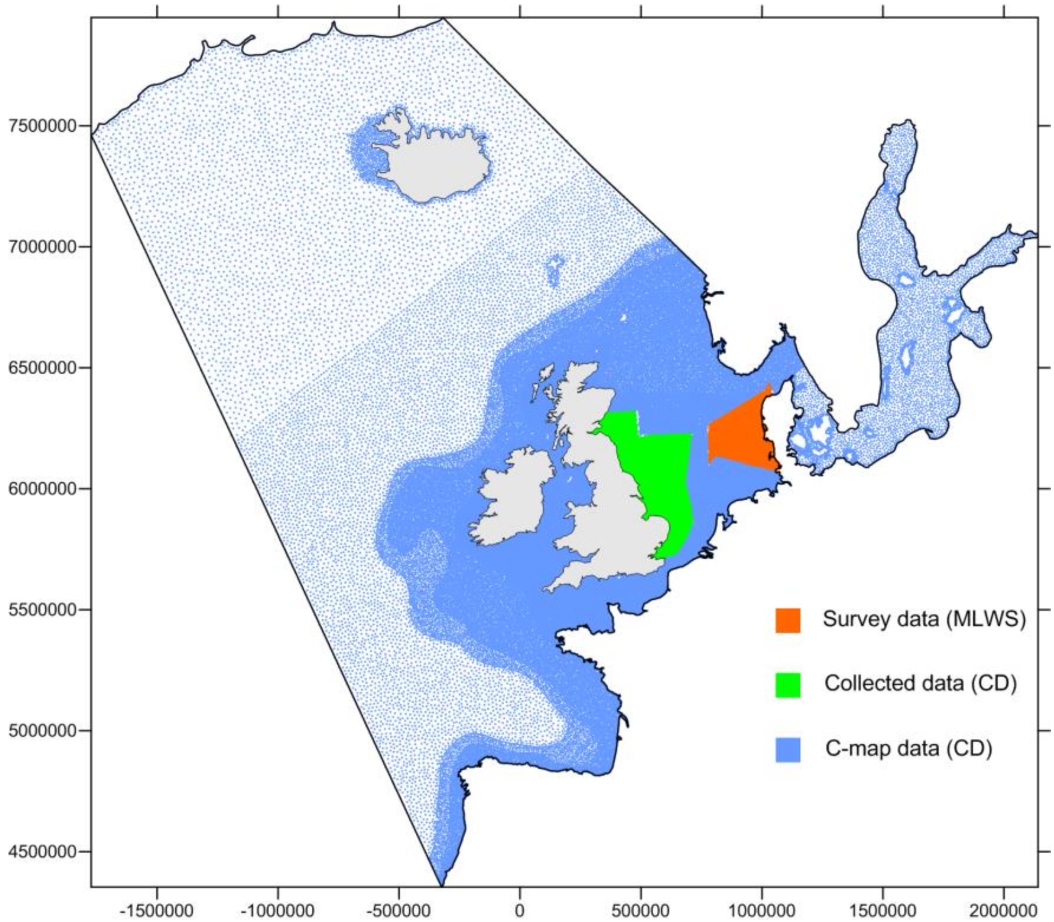


Figure 7.3. Sources of bathymetry data used in the model.

## 7.3. Model Grid

Computational grids were created in order to model the tidal current patterns for the existing and worst case conditions (Figure 7.4). The grids describe the bathymetry in the model with enough detail to produce sufficiently accurate model results within acceptable simulation times. The size of the computational grids varies over the model domain, and has been refined in and around the pre-investigation area in order to provide a detailed representation of the hydrodynamics locally. The grid has a resolution of approximately 100m across the pre-investigation area (Figure 7.4).

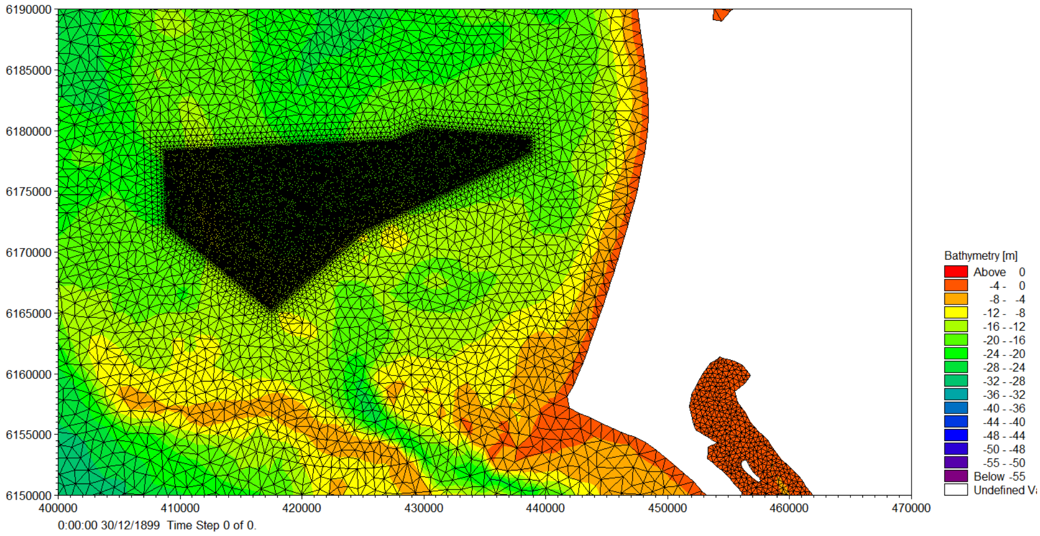


Figure 7.4. Bathymetry and computational grid in and adjacent to Horns Rev 3.

## 7.4. Model Calibration

In order to accurately simulate tidal currents, the regional and local models were re-calibrated. Calibration is the process of defining the optimum model parameters, so the model results are as close as possible to the measured data (tidal current velocities and water levels). The calibration process primarily included the adjustment of the size and resolution of the computational grid and the bed resistance (Manning coefficient) until good agreement was obtained between the simulated outputs and the measured data.

Calibration was performed based on the measured data of current and water levels (Section 3) extracted from the International Hydrographic Organization (IHO). The re-calibration of the regional model is focused on the water level from numerous IHO tidal stations along the coastlines of United Kingdom, France, Germany, Belgium, Spain, The Netherlands and Denmark.

The calibration of the detailed local model focused on tidal levels and current data more local to Horns Rev 3. Reliable current measurements were available at FINO3 and tidal levels at Hvide Sande (Figure 1.8). The models were calibrated over a period of one month between 1$^{st}$ August 2011 and 30$^{th}$ August 2011. During the selected period, the highest and lowest water levels at FINO3 were approximately 0.63m MSL on 31$^{st}$ August 2011 at 13.15 and -0.56m MSL on 2$^{nd}$ August 2011 at 15.00, respectively. These water levels are very close to the estimated HAT/LAT values of 0.66m MSL (3$^{rd}$ March 2006) and -0.58m MSL (1$^{st}$ February 2006), and therefore, it is expected that the tidal flow conditions during the selected period are similar to those most governing the tidal conditions across the pre-investigation area.

### 7.4.1 Regional Model Calibration Results

The simulated water levels were plotted against the measurements at the IHO tidal stations. Overall, the regional model shows good agreement between the measured water levels and model results for most of the stations particularly those along the east coast of the United Kingdom and along the coastline of France and The Netherlands, which are relatively close to Horns Rev. Overall, the good calibration results demonstrate that the regional model is suitable to derive the water level boundary conditions for local model. The calibration statistics are presented in Box 7.1 and Appendix A.

**Box 7.1**

**Statistical parameters**

**R squared**

The correlation between measured data ($x_i$) and predicted data ($y_i$) is quantified by the correlation coefficient R squared, expressed as:

$$R^2 = 1 - \frac{SSE}{TSS}$$

in which SSE is the error sum of squares and TSS is the total sum of squares. The error sum of squares is expressed as:

$$SSE = \sum_i (x_i - y_i)^2$$

in which $x_i$ and $y_i$ are the measured value and the predicted value. The total sum of square is expressed as:

$$TSS = \sum_i (x_i - \bar{x})^2$$

where $\bar{x}$ is the mean value of the measured data.

**Bias**

The bias is the difference between the mean of the measured and the predicted values. The closer the bias is to zero, the better both time series correspond:

$$Bias = \bar{y} - \bar{x}$$

where $\bar{x}$ and $\bar{y}$ is is the mean value of the measured data and predicted data, respectively. These are expressed as:

$$\bar{x} = \frac{1}{N}\sum_{i=1}^{N} x_i, \ \bar{y} = \frac{1}{N}\sum_{i=1}^{N} y_i$$

where N is the number of observations/predictions.

**Root mean square error (RMSE)**

The root mean square error (RMSE) is defined mathematically as:

$$RMSE = \sqrt{\frac{\sum_{i=1}^{N}(x_i - y_i)^2}{N}}$$

RMSE is a measure of the "average" error, weighted according to the square of the error.

A value closer to 0 indicates that the model has a smaller random error component, and that the fit will be more useful for prediction.

### 7.4.2 Local Model Calibration Results

Figure 7.5 presents the comparison between the simulated and recorded tidal levels at Hvide Sande for the model calibration period. The results show that there are certain deviations (less than 0.1m) between the troughs and crests of the simulated tidal levels and recorded data. The simulated water levels at high tide (crests) match better with the measured data than at low tide (troughs).

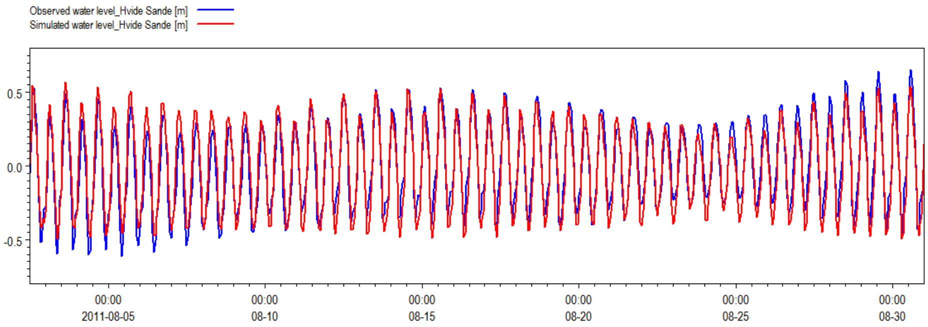


Figure 7.5. Time series comparison between simulated (red) and recorded (blue) tidal levels at Hvide Sande.

The computed current velocities and directions provide a good fit to the measured calibration data at FINO3 (Figure 7.6). Minor differences of less than 0.05m/s occur during ebb tides. Overall, the root mean square error for current velocity was less than 0.04m/s (Figure 7.7), which indicates a high level of agreement between the simulated and measured results for the calibration period. This analysis indicates that the local model is reliable to be used for the baseline and assessment of effects runs.

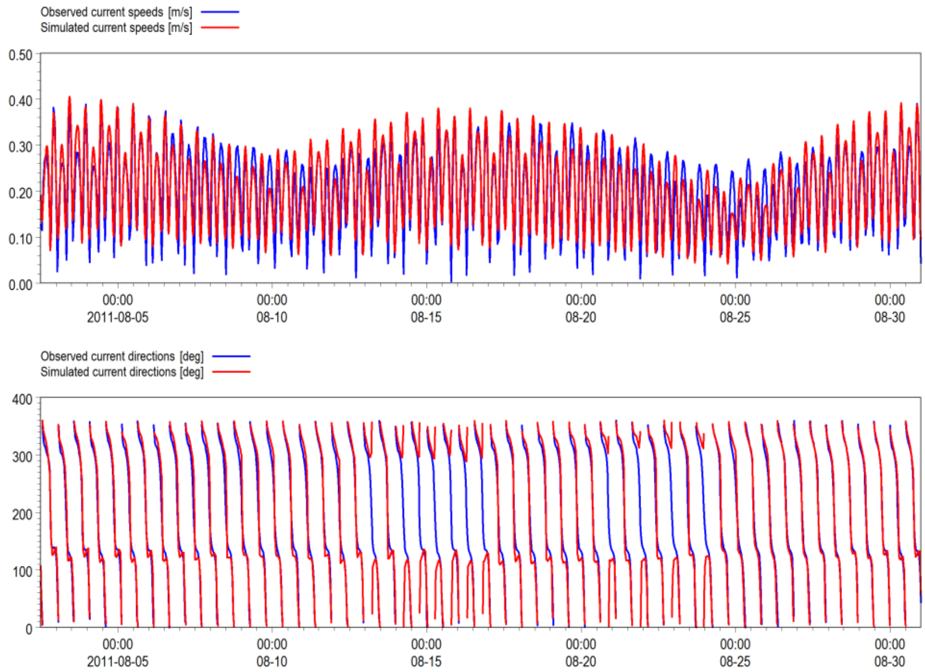


Figure 7.6. Time series comparison between simulated (red) and measured (blue) tidal current velocities (top panel) and directions (bottom panel).

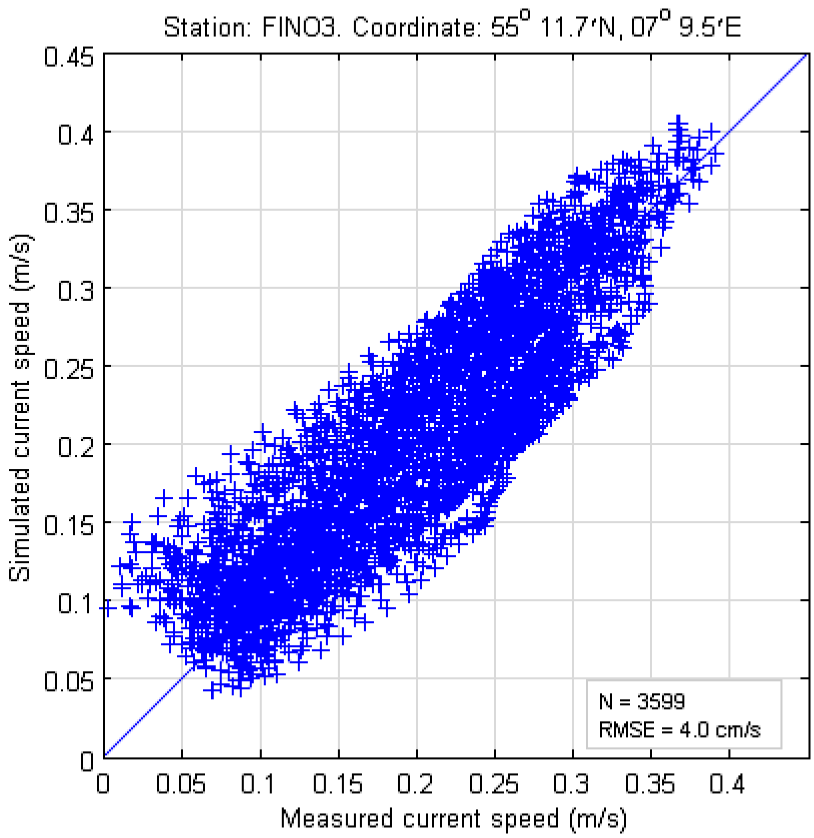

Figure 7.7. Scatter plot of tidal current velocities comparing observations from FINO3 with matching simulated data.

## 7.5. Modelled Baseline Tidal Current Velocities

A series of model production runs were completed to determine the baseline (existing) tidal current velocities and current direction in the vicinity of Horns Rev 3. Current flows across the central North Sea vary temporally, as a function of the tide and tidal range, and spatially as they interact with bathymetry such as shoals and channels. Hence, for each spring-neap tidal period, three time steps corresponding to ebb tide, slack tide and flood tide have been selected (Figures 7.8 and 7.9). Tidal currents have been simulated for a spring-neap tidal cycle from 26th February 2006 to 11th March 2006. This period includes the extreme event of highest astronomical tide on 3rd March 2006 at 2am. The model outputs are recorded every ten minutes.

Astronomical tides have a 30-day cycle of spring and neap tides. However, not every spring-to-neap tide has the same tidal range because of the 18.6 year nodal cycle. The spring (astronomical) tide peaked on 3rd March 2006 (i.e. it is highest astronomical tide) which means that selection of the 30-day period containing this tide would produce extreme tidal currents.

Figures 7.8 and 7.9 clearly show the variation in current velocity corresponding with the different tidal stages. The maximum current velocities occur during flood and ebb tide, with average values of 0.5m/s during a spring tide and 0.23m/s during a neap tide. When the low stand of slack water is reached, the current velocities reduce by over a half for both spring and neap tides. The tidal currents flow south on the flood tide and flow north on the ebb tide.

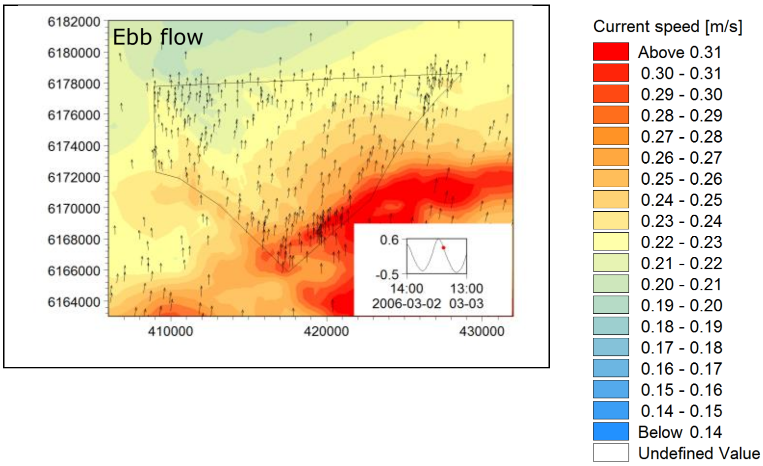

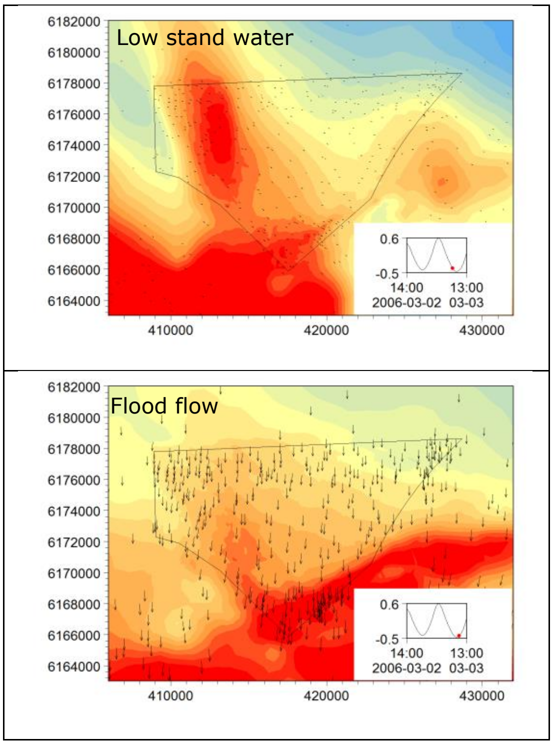


Figure 7.8. Simulated tidal currents for the baseline condition for a spring tide.

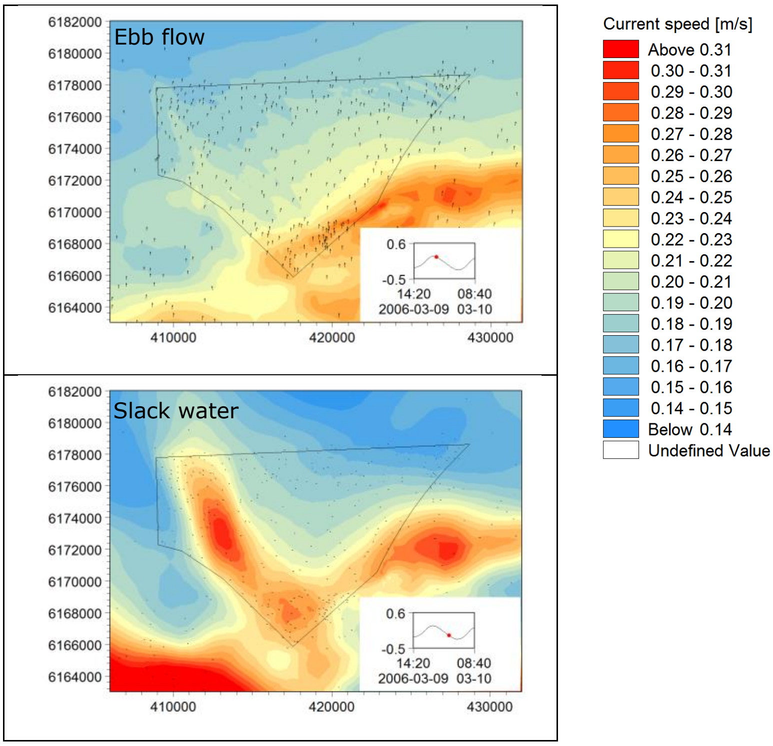

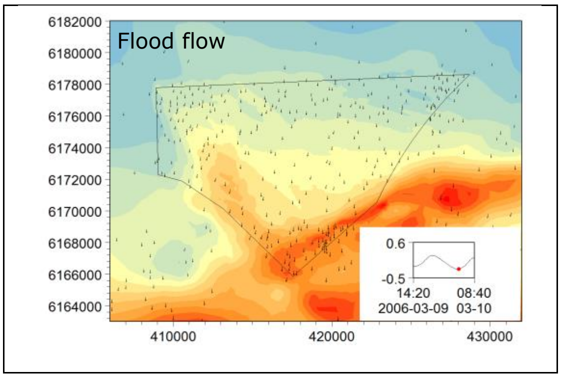


Figure 7.9. Simulated tidal currents for the baseline condition for a neap tide.

An understandable representation of the tidal stage current is maximum depth-averaged velocity at any time over the 30-day simulation period (1st August 2011 to 30th August 2011). The spatial variation in current velocity is broadly related to changes in bathymetry. The highest velocities occur across the ridge in the west and south of the pre-investigation area where the water is shallower (10-12m). The maximum current velocities over the simulation period are shown in Figure 7.10 and range from 0.4m/s to 0.62m/s.

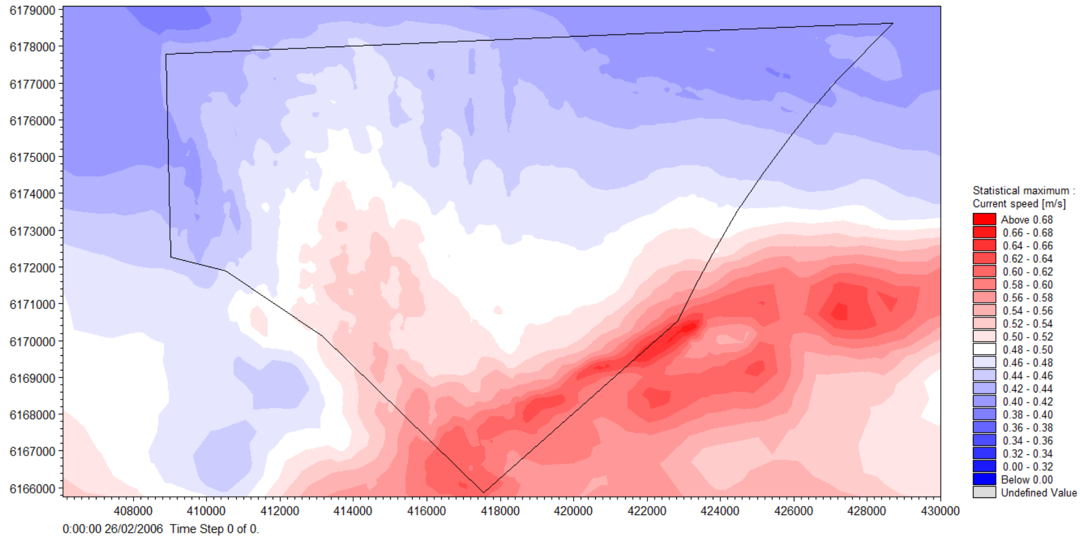


Figure 7.10. Simulated maximum tidal current velocities over the simulation period for the baseline condition.

## 7.6. Sediment Plume Dispersion Model

Over the construction period, there is potential that the seabed and coastline will be disturbed. Installation of foundations and cables will generate additional suspended sediment into the water column, which may result in the formation of sediment plumes. The mobilised sediment may then be transported away from the disturbance by waves and tidal currents. The magnitude of the plume will be a function of seabed type, the installation method and the hydrodynamic conditions in which dispersion takes place.

Mobilisation of sediment on the seabed occurs when the wave and tidal current forces exert a shear stress that exceeds a threshold relevant to the sediment type. When shear stress drops below this threshold, the sediment begins to fall out of suspension and is re-deposited on the seabed. If the shear stress is then increased above the threshold again, the sediment will be re-suspended. It is, therefore, possible for sediment to be continually re-deposited and re-suspended, as tidal and wave conditions change. Typically, finer sediments are suspended at lower shear stresses compared to coarser sediments, and will remain in the water column for longer periods of time. Coarser sediments are more likely to be transported as bedloads.

The simulation of the release and spreading of fine sediments as a result of foundation and cable installation activities have been modelled using the 3D model MIKE21-FM Mud Transport (MT) (DHI, 2011). MIKE21-FM MT is integrated with MIKE21-FM HD, which has been used to predict tidal current velocity changes, and takes into account:

- the actual release of sediments as a function of time, location and sediment characteristics;
- advection and dispersion of the suspended sediment in the water column as a function of the 3D flow field predicted by MIKE21-FM HD;
- settling and deposition of the dispersed sediment; and
- re-suspension of the deposited sediment, predominantly by bed shear stresses from surface waves.

### 7.6.1 Model Parameterization

The available sediment from seabed preparation has been released evenly over the thickness of the water column. Of the sediment released into the water (either by seabed preparation or jetting), an average of 98.89% is sand and gravel, which is assumed to settle out quickly near the foundations. An average of 1.11% of the sediment is less than 0.063mm (silt and clay), which is the fraction dispersed in the plume. The release of sediment results in dispersion that has been estimated as suspended sediment concentration in excess of zero sediment concentration.

The size fraction simulated by the model is defined by its settling velocity and its critical shear stress. The applied settling velocity and critical shear stress used in the model for the less than 0.063mm fraction are 2.28mm/sec and 0.12N/m$^{-2}$, respectively. A sediment density of 1,590kg/m$^3$ has been used to represent the undisturbed seabed sediments, assuming a porosity of 0.4 and a density of dry sediment of 2,650kg/m$^3$.

The modelling of sediment dispersion for foundation seabed preparation and inter-array cable jetting was carried out over a 30-day simulation period using the baseline 30-day hydrodynamic simulation described in Section 7.5. The dispersion from the shorter installation of the export cable was modelled over a 15-day period. The sediment along the Horns Rev 3 inter-array and export cables was released continuously for dispersion as the excavation progresses.

# 8. WAVE MODEL SET-UP AND BASELINE CONDITIONS

The wave model MIKE21-SW was used to transform offshore waves to the nearshore. MIKE21-SW is a state of the art third generation spectral wave model developed at the Danish Hydraulic Institute (DHI) and takes into account all relevant nearshore and deep water wave processes (DHI, 2011). The MIKE21-SW modules takes into account diffraction, refraction, shoaling, bottom friction, depth induced breaking, white-capping, wind growth and non-linear interactions that affect waves propagating from offshore to nearshore.

## 8.1. Model Boundaries

There are three types of boundary for the wave model including a water level boundary in the west, a closed boundary in the northeast and land boundaries elsewhere. The boundary conditions used for the nearshore wave modelling are based on forecasted data (wave height, direction and peak period of combined sea and swell waves) extracted at Gorm (Figure 1.8). The wave model covers the nearshore area around Horns Rev 3 and the area of available offshore data points.

## 8.2. Model Bathymetry and Computational Grid

The model domain shown in Figure 8.1 was set up using the bathymetry of the local model (Figure 7.4) (same as hydrodynamic model). The following have been taken into account when designing the grid:

- the wave conditions can be defined at the boundary of the grid. In practice, this means they can be considered uniform or that their variation must be known;
- the boundaries where the wave condition cannot be defined will have no influence in the area of interest;
- the grid resolution is sufficiently high to reproduce the spatial depth variations that influence the wave conditions; and
- the overall area should be sufficiently small to be able to consider the situation quasi-stationary.

The optimum computational grid is a compromise between these parameters and the geographic limits of the model. A local refinement of the computational grid has been made for the pre-investigation area. The model grid has a resolution that ranges between a node distance of 100m in the pre-investigation area to a node distance of several tens of kilometres in the offshore area.

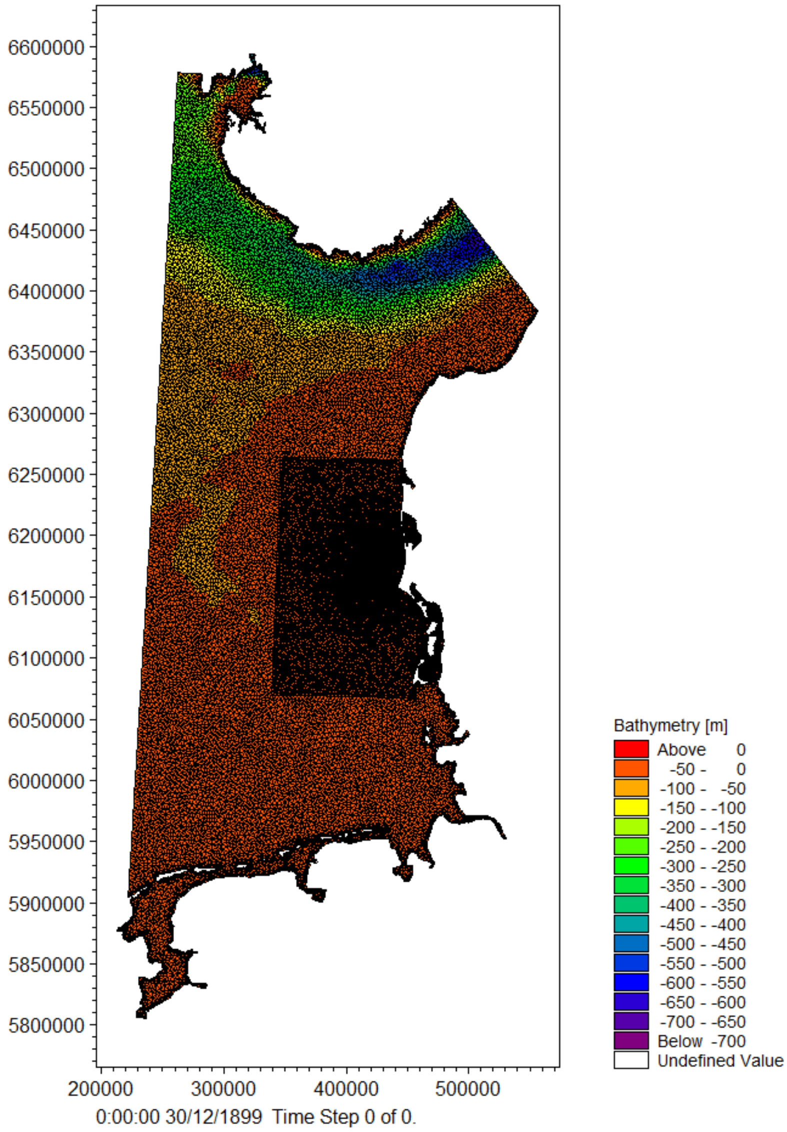


Figure 8.1. Extent of the MIKE21-SW wave model.

## 8.3. Model Calibration

Wave data measured nearshore from 1st January 2007 to 26th December 2012 at Nymindegab are used for the calibration. The forecasted waves at Gorm, about 200km from the Danish coastline, from the same period were also used, providing wave input at the offshore boundary.

The 12 largest storms over the last six years at Gorm are summarised in Table 8.1. Three of these events corresponding to three relevant directions for Horns Rev (northwest, west and southwest) as recorded at Nymindegab were selected to calibrate the wave model (Table 8.2). These three events were chosen because they represent the largest storms from their respective directions. Each storm lasted for two or three days.

Table 8.1. Wave 'events' that occurred at Gorm between 2007 and 2012.

| No | Start | End | Wave Direction |
|---|---|---|---|
| **1** | **20/01/2007 0:00** | **22/01/2007 0:00** | **West** |
| 2 | 08/11/2007 0:00 | 10/11/2007 0:00 | Northwest |
| 3 | 30/01/2008 12:00 | 02/02/2008 0:00 | Southwest |
| 4 | 29/02/2008 0:00 | 03/03/2008 0:00 | Northwest |
| 5 | 02/10/2009 0:00 | 05/10/2009 0:00 | Northwest |
| 6 | 02/01/2012 0:00 | 04/01/2012 0:00 | West |
| 7 | 08/11/2008 0:00 | 10/11/2008 0:00 | Southwest to South |
| 8 | 10/11/2010 0:00 | 12/11/2010 0:00 | Southwest to South |
| 9 | 09/12/2011 0:00 | 11/12/2011 0:00 | West |
| **10** | **18/03/2007 0:00** | **20/03/2007 0:00** | **Northwest** |
| 11 | 25/11/2011 12:00 | 27/11/2011 12:00 | West to Northwest |
| **12** | **11/01/2007 0:00** | **13/01/2007 0:00** | **Southwest** |

Table 8.2. Three extreme wave events measured at Nymindegab from the northwest, west and southwest sectors used to calibrate the wave model.

| Event | Start | End | Hs (m) | Tp (s) | Wave Direction | Calibration Point |
|---|---|---|---|---|---|---|
| 1 | 20/01/2007 00:00 | 22/01/2007 00: 00 | 7.6 | 12 | West | Nymindegab |
| 2 | 18/03/2007 00:00 | 20/03/2007 00:00 | 8.6 | 10 | Northwest | Nymindegab |
| 3 | 11/01/2007 00:00 | 13/01/2007 00:00 | 7.8 | 8.2 | Southwest | Nymindegab |

### 8.3.1 Calibration Results

Figures 8.2 to 8.4 show the comparisons of simulated and measured time series of the wave height, peak wave period and wave directions at Nymindegab.

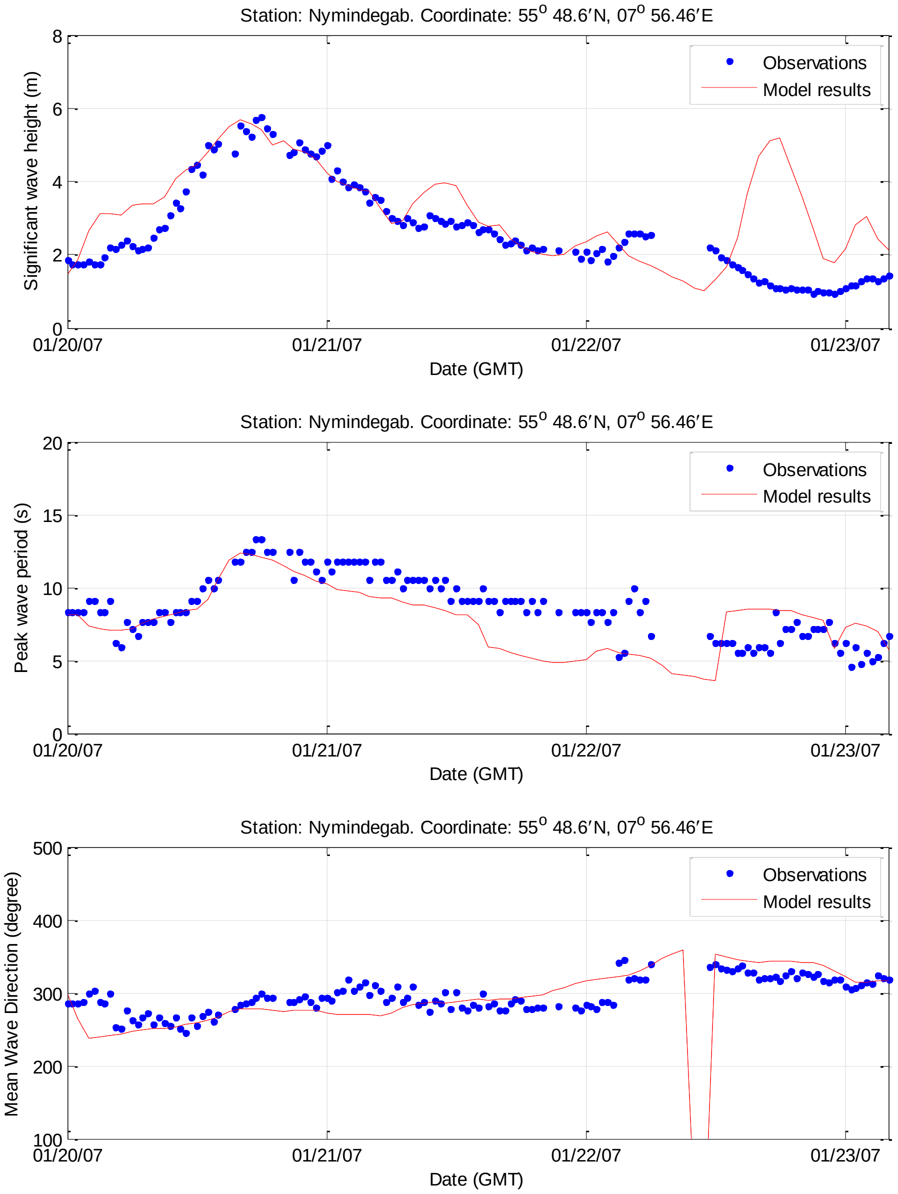


Figure 8.2. Calibration results of extreme wave event 1 – waves from the northwest.

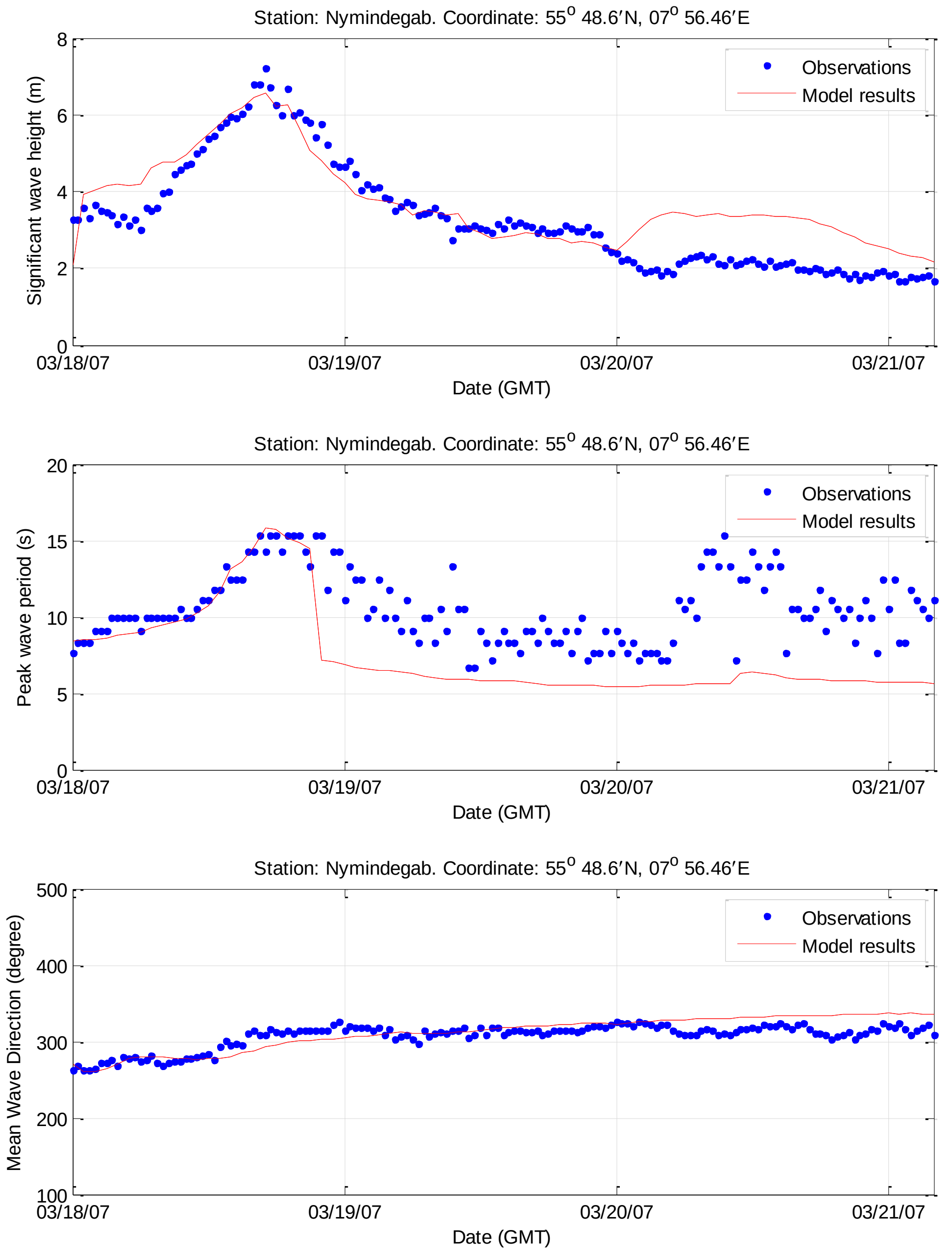


Figure 8.3. Calibration results of extreme wave event 2 – waves from the west.

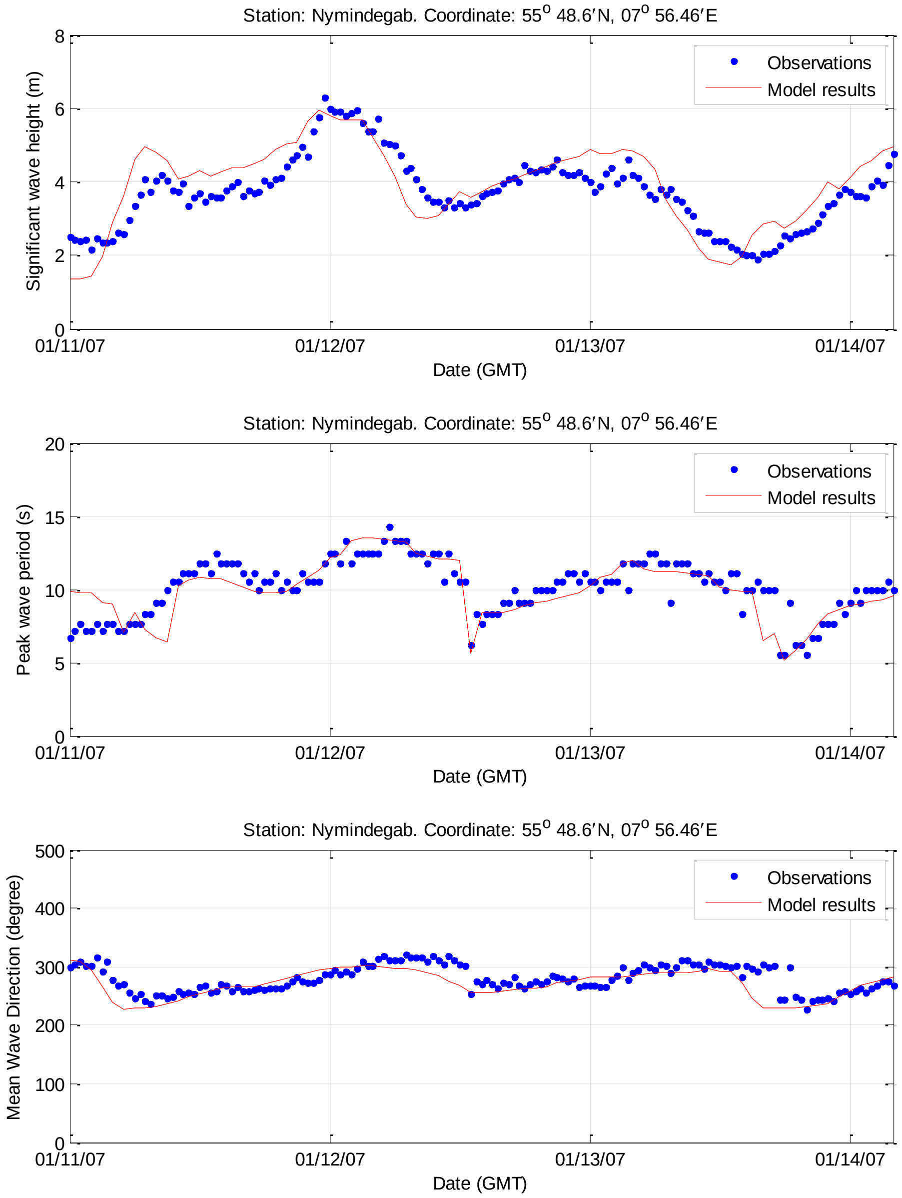


Figure 8.4. Calibration results of extreme wave event 3 – waves from the southwest.

The model results for wave event 1 (northwest) show a reasonably good match between the measured and simulated significant wave heights, although for the first six hours the model overestimates the wave height (Figure 8.2). The simulated peak wave periods are also in good agreement with the measured data for the first 1.5 days, after which they underestimate.

For wave event 2 (Figure 8.3), the simulated significant wave heights are in good agreement with the measured data for the first two days. During the last day of the storm, the simulated wave height is overestimated. The simulated peak wave period is in good agreement with the measured data for the first day, then drops to around six seconds for the rest of the storm, hence underestimating compared to the measured data.

For wave event 3, a fairly good calibration was achieved for waves approaching from the southwest (Figure 8.4). Both the modelled wave height and peak wave period are comparable to the measured data. The model appears to perform much better for this event than the events from the northwest and west. The following can be concluded from the calibration process:

Overall, there is good agreement between predicted and measured waves for the three selected wave events, particularly for wave event 3 (waves from southwest). Due to the effects of wave systems, there are some mismatches of the significant wave heights and peak wave periods in the calibrations for wave events 1 and 2. The accuracy of MIKE21-SW is closely related to the accuracy of the wind field specification. The wind data applied in this calibration is forecasted at Gorm and the overestimation of the wave height during some extreme events is likely to be due to the possible inaccuracy of the wind/wave conditions at the offshore boundary.

## 8.4. Modelled Baseline Wave Heights

The MIKE21-SW model has been used to simulate baseline significant wave heights, using one-year and 50-year wave conditions, from northwest, west and southwest directions. These directional sectors were chosen because offshore waves from these directions (particularly the northwest) are larger and more frequent compared to other directions. Figures 8.5 to 8.10 show the simulated one-year and 50-year return frequency wave heights for the baseline condition. The results show that the wave conditions at the pre-investigation area are depth–limited. This means that wave heights at Horns Rev 3 are independent of the offshore wave heights, and so offshore wave and wind conditions have limited impact on the waves at Horns Rev 3. Hence, the one-year and 50-year baseline conditions for each wave direction are similar. Wave heights range from 5m to 7.5m across the site for every direction and the spatial variation is strongly related to the bathymetry. The smallest wave heights correspond with areas of shallow bathymetry and higher waves occur in deeper water.

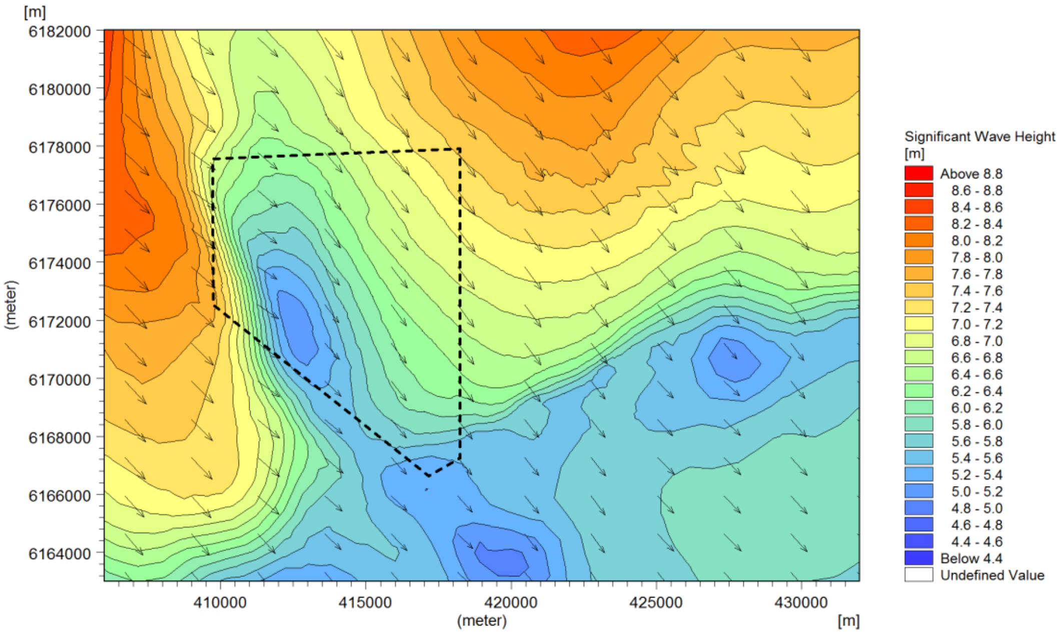


Figure 8.5. Baseline significant wave height for one-year return period waves from the northwest. Dashed line represents the limit of the western layout of 3MW foundations.

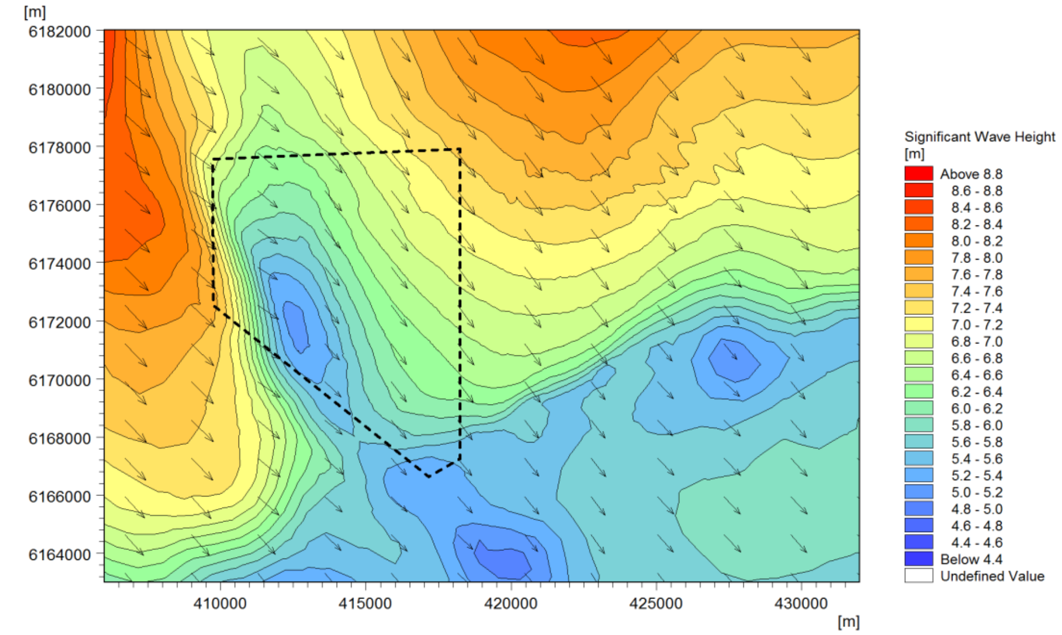


Figure 8.6. Baseline significant wave height for 50-year return period waves from the northwest. Dashed line represents the limit of the western layout of 3MW foundations.

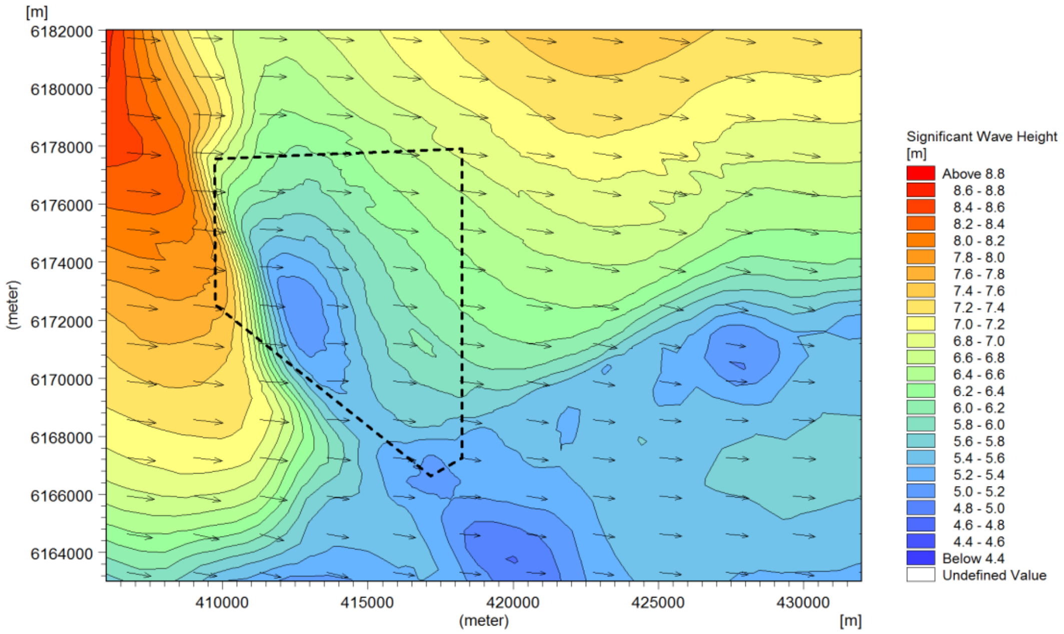


Figure 8.7. Baseline significant wave height for one-year return period waves from the west. Dashed line represents the limit of the western layout of 3MW foundations.

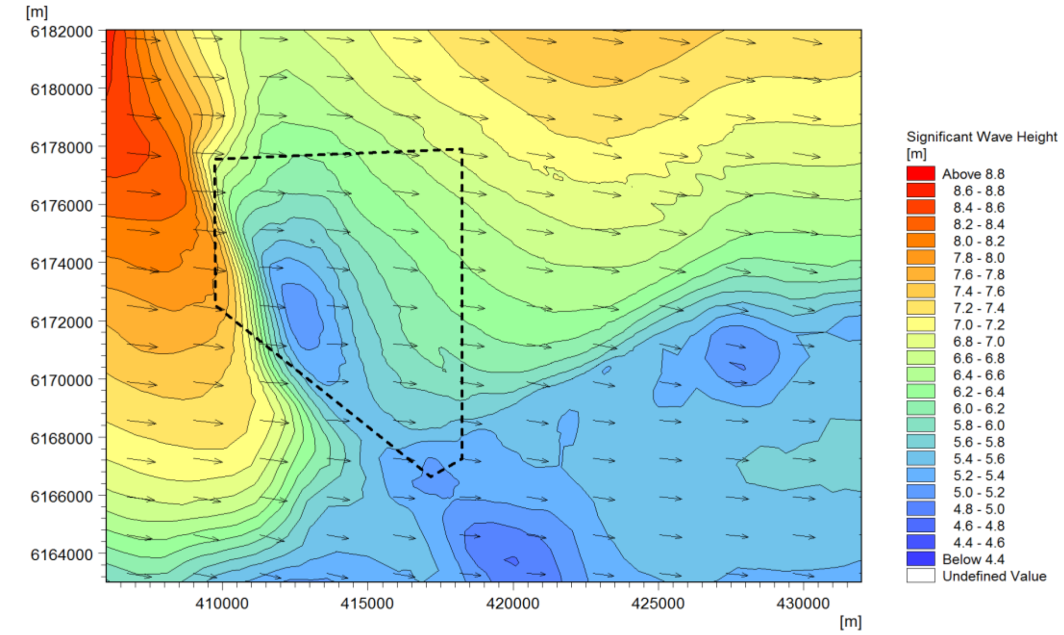


Figure 8.8. Baseline significant wave height for 50-year return period waves from the west. Dashed line represents the limit of the western layout of 3MW foundations.

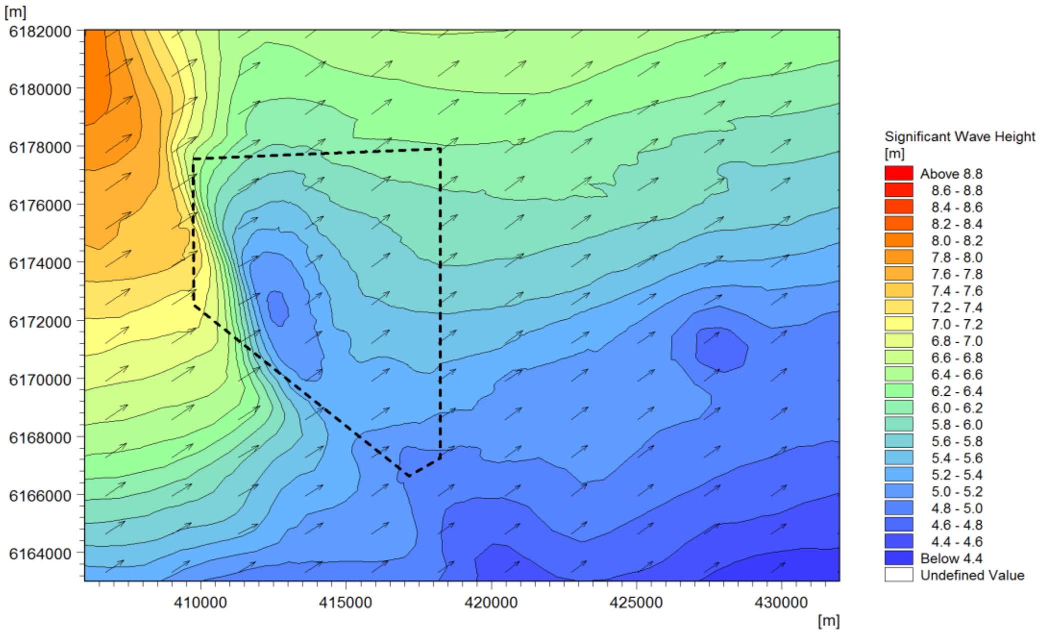


Figure 8.9. Baseline significant wave height for one-year return period waves from the southwest. Dashed line represents the limit of the western layout of 3MW foundations.

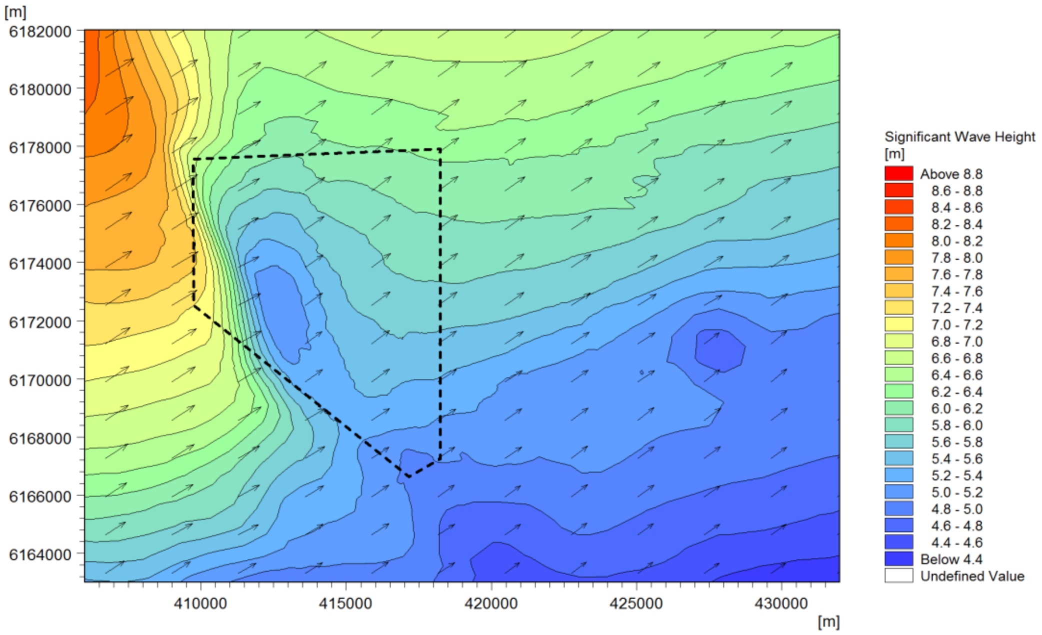


Figure 8.10. Baseline significant wave height for 50-year return period waves from the southwest. Dashed line represents the limit of the western layout of 3MW foundations.

## 9. POTENTIAL PRESSURES DURING CONSTRUCTION

The construction phase of Horns Rev 3 has the potential to affect hydrography, sediment spill and water quality both locally and further afield. Offshore construction activities include installation of the foundations and laying of inter-array and export cables, all of which may affect the tidal current regime, wave climate, water quality and sediment transport processes.

At the landfall site, activities to install the cables (including the potential for open trenching across the beach) can affect coastal processes. Changes to the bedload sediment transport processes near Houstrup Strand may result in disturbances to the sediment supply to other parts of the coast and construction activities may increase turbidity in the water column.

The results of the sediment plume dispersion modelling are presented as a series of maps showing depth-averaged suspended sediment concentration and sediment deposition on the seabed from the plume, using the following statistical measures over the simulation period:

- the maximum values of depth-averaged suspended sediment concentration;
- the time over which suspended sediment concentration exceeds 10mg/l; and
- the maximum thicknesses of deposited sediment.

The threshold of 10mg/l was adopted because many marine organisms are sensitive to concentrations around 10mg/l. This is an indicative value used by many marine biologists for pelagic fish (Orbicon, 2014).

### 9.1. Increase in Suspended Sediment Concentrations as a Result of Foundation and Inter-array Cable Installation

Figure 9.1 shows the maximum depth-averaged suspended sediment concentration predicted by the model at any time over the 30-day simulation period for foundation seabed preparation only. Predicted suspended sediment concentrations are increased locally at each of the foundation locations by up to 1.5mg/l and there is no interaction between any of the plumes.

Figure 9.2 shows predicted suspended sediment concentration for seabed preparation and inter-array cable installation combined. When the effect of inter-array cable jetting is added, the predicted maximum suspended sediment concentrations increase significantly to greater than 200mg/l. However, these highest values are very restricted in geographical extent and the majority of the plume has maximum suspended sediment concentrations of less than 100mg/l. The predicted suspended sediment concentrations reduce to zero within 500m of the foundations and cable transects in all directions and do not extend to the coast or designated Natura 2000 areas (Figure 9.2).

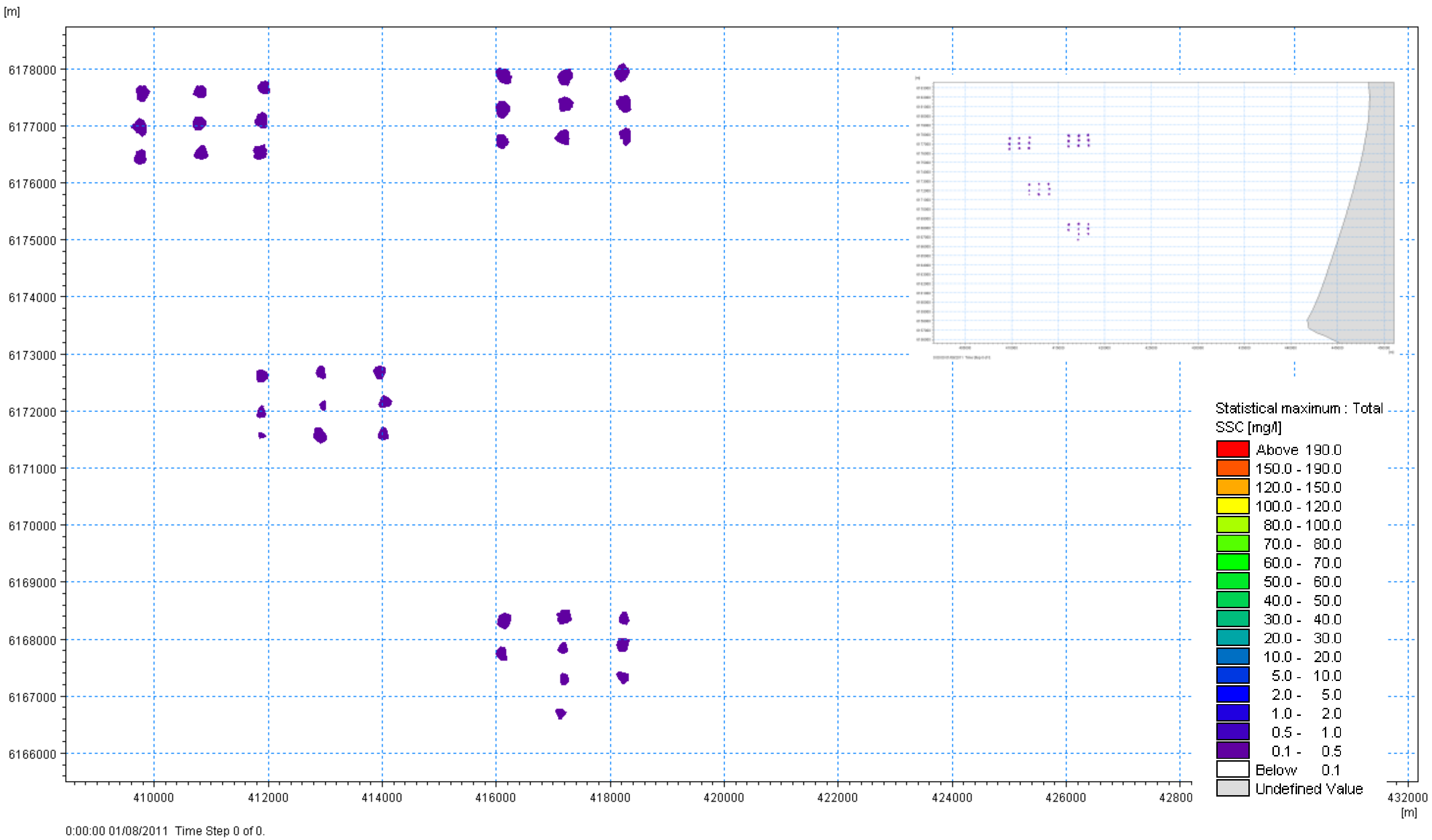


Figure 9.1. Maximum suspended sediment concentration (mg/l) predicted over the simulation period for the construction phase for GBS foundations, including the coast (top) and zoomed in (bottom).

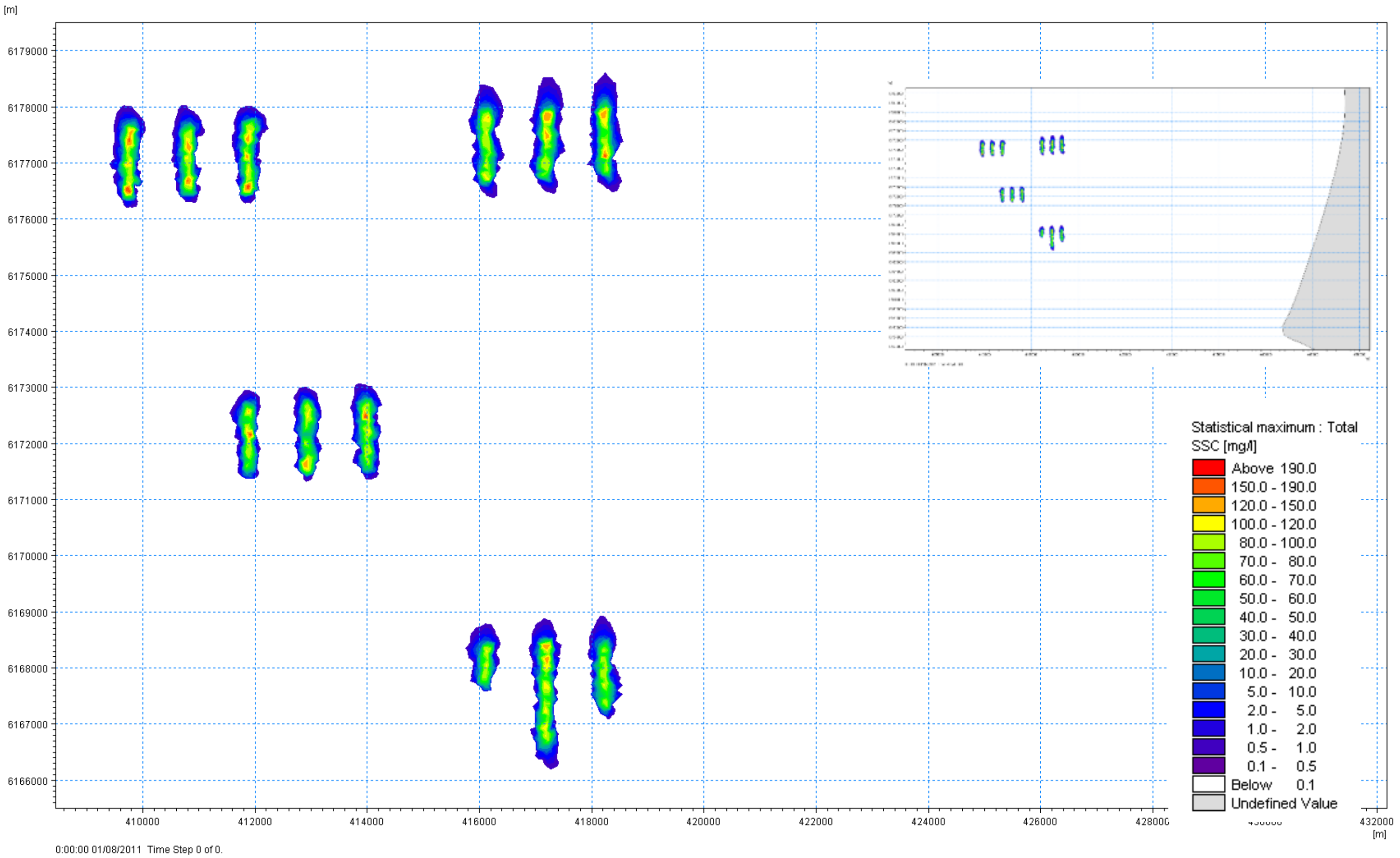


Figure 9.2. Maximum suspended sediment concentration (mg/l) predicted over the simulation period for the construction phase for GBS foundations and inter-array cable installation combined, including the coast (top) and zoomed in (bottom).

The model predictions using the four blocks of foundations show that increases in suspended sediment concentrations are limited to areas adjacent to the foundations. To expand this analysis to include installation of all foundations, the results from the four blocks can be transposed across the entire pre-investigation area to create a boundary containing the indicative worst case ‘outer extent’ of the sediment plume. Consequently, the overall sediment plume would be contained within the pre-investigation area. The extent of plumes from each foundation would be at the same scale or less than those modelled, thus of very modest magnitude.

Given that the baseline suspended sediment concentrations can be very high during storm conditions indicates that concentrations due to jetting are within the scale of natural processes (Bio/consult, 2000). Hence, the Magnitude of Pressure of additional suspended sediment in the water column caused by construction of foundations and installation of inter-array cables is considered to be low.

Figures 9.3 and 9.4 present the percentage of time of the entire simulation period (30 days) when the predicted suspended sediment concentrations exceed 10mg/l. For the GBS foundations alone, seabed preparation is predicted to never induce suspended sediment concentrations above 10 mg/l. For seabed preparation and cable jetting combined, 10mg/l is predicted to be exceeded less than 0.5% of the 30-day simulation period.

*Jelly fish*

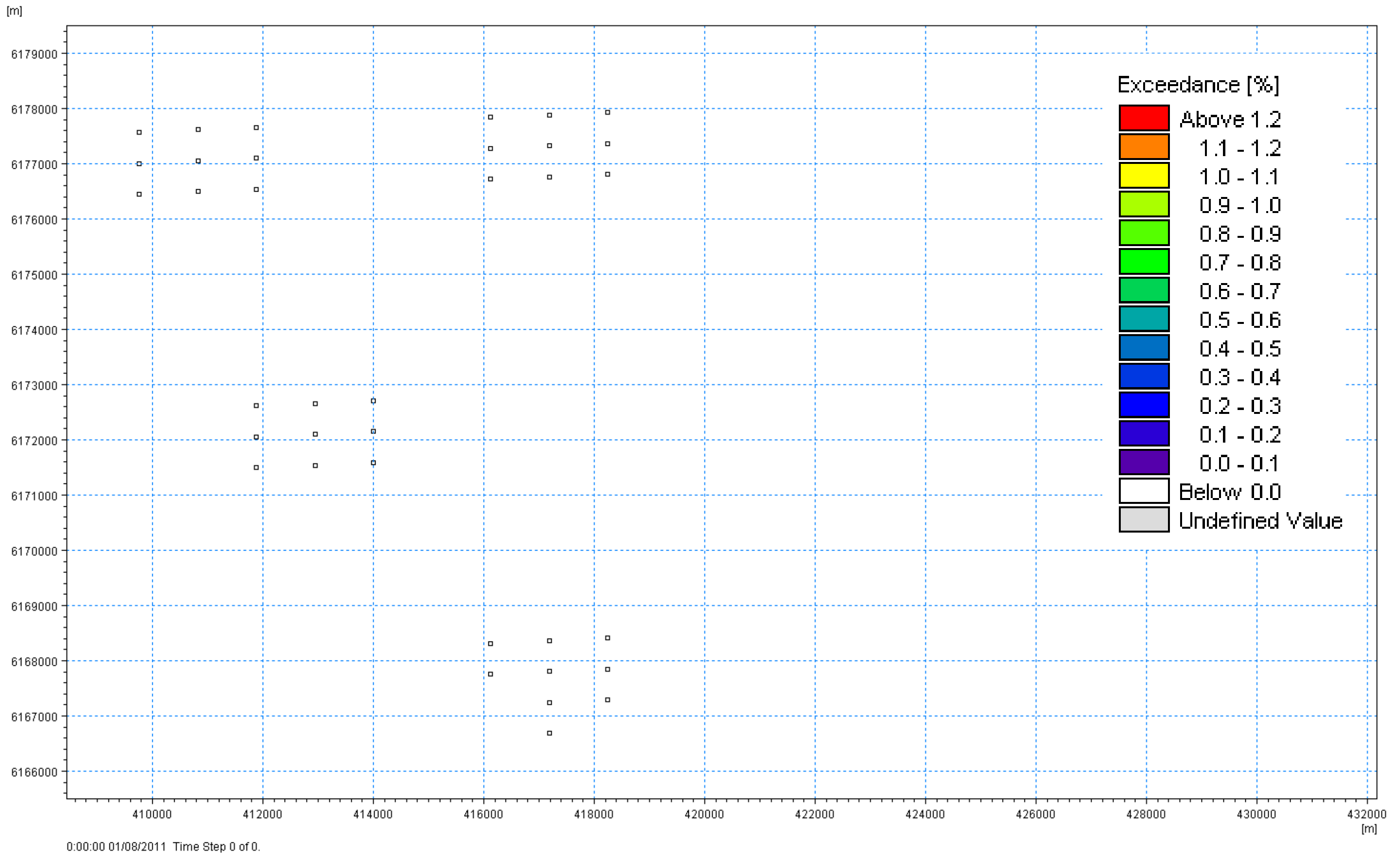


Figure 9.3. Simulated percentage of time during construction of GBS foundations when suspended sediment concentrations exceed 10mg/l.

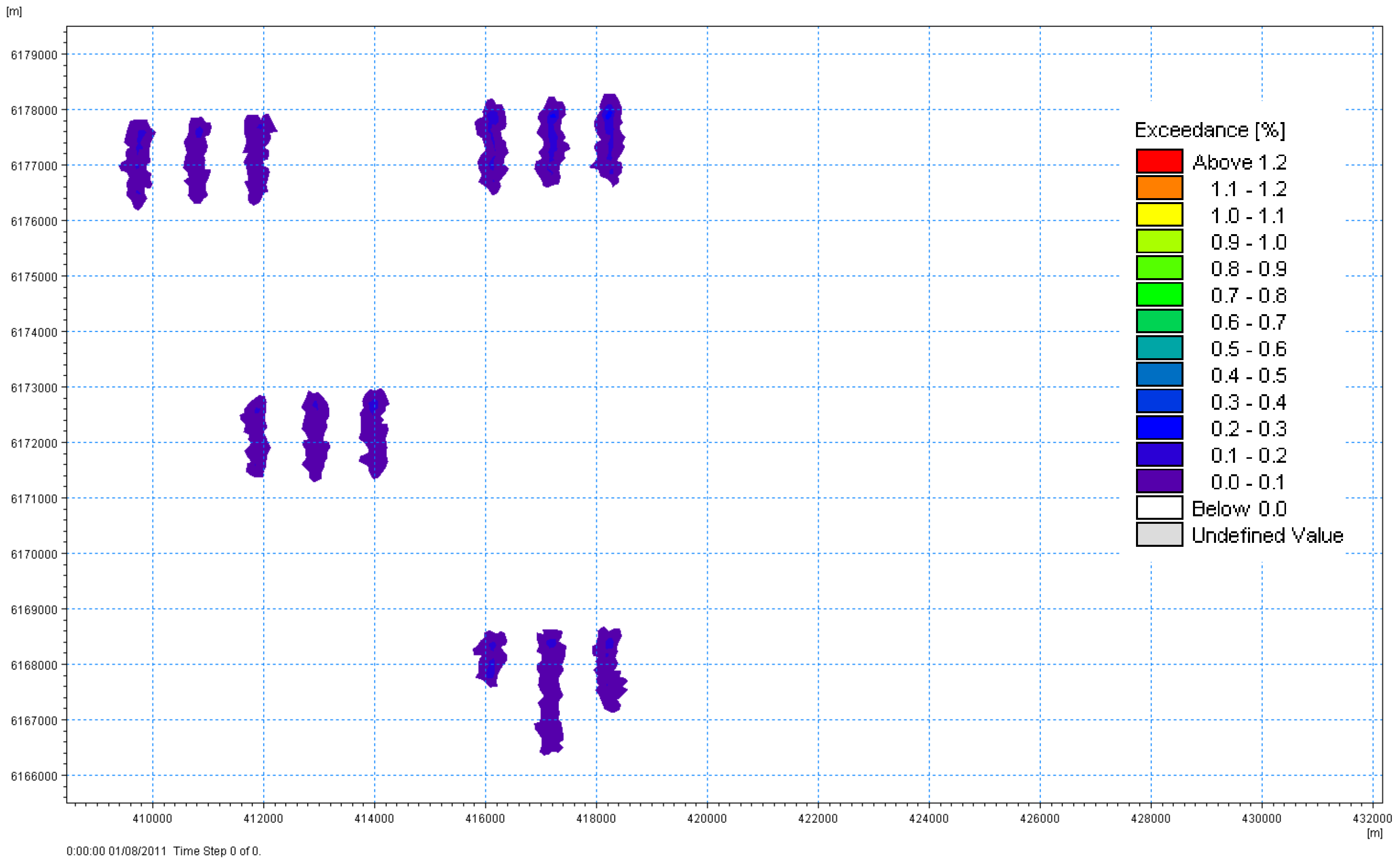


Figure 9.4. Simulated percentage of time during construction of GBS foundations and inter-array cable installation combined when suspended sediment concentrations exceed 10mg/l.

Figures 9.5 and 9.6 show the maximum change in deposition predicted at any time over the 30-day simulation period. The largest predicted change for seabed preparation only is less than 8mm in very small patches close to a few foundations. The majority of deposition is 2-4mm. For seabed preparation and cable installation combined, the largest predicted deposition increases to approximately 50mm, but limited to locations close to the foundations. Additional deposition, the majority of which is between 10mm and 15mm, is limited to within approximately 200m of the foundations and does not extend to the coast (Figure 9.6).

Transposing the individual deposition areas across the entire pre-investigation area shows that deposition would be contained within the pre-investigation area. The magnitude of deposition from each foundation would be at the same scale or less than those modelled. Given the dynamic and sandy nature of the substrate at Horns Rev 3, deposition of 50mm of sediment is likely to be very small compared to the natural variation of bed level changes across the area. Hence, the Magnitude of Pressure of additional deposition of sediment on the seabed caused by construction of foundations and installation of inter-array cables is considered to be low.


Cabling

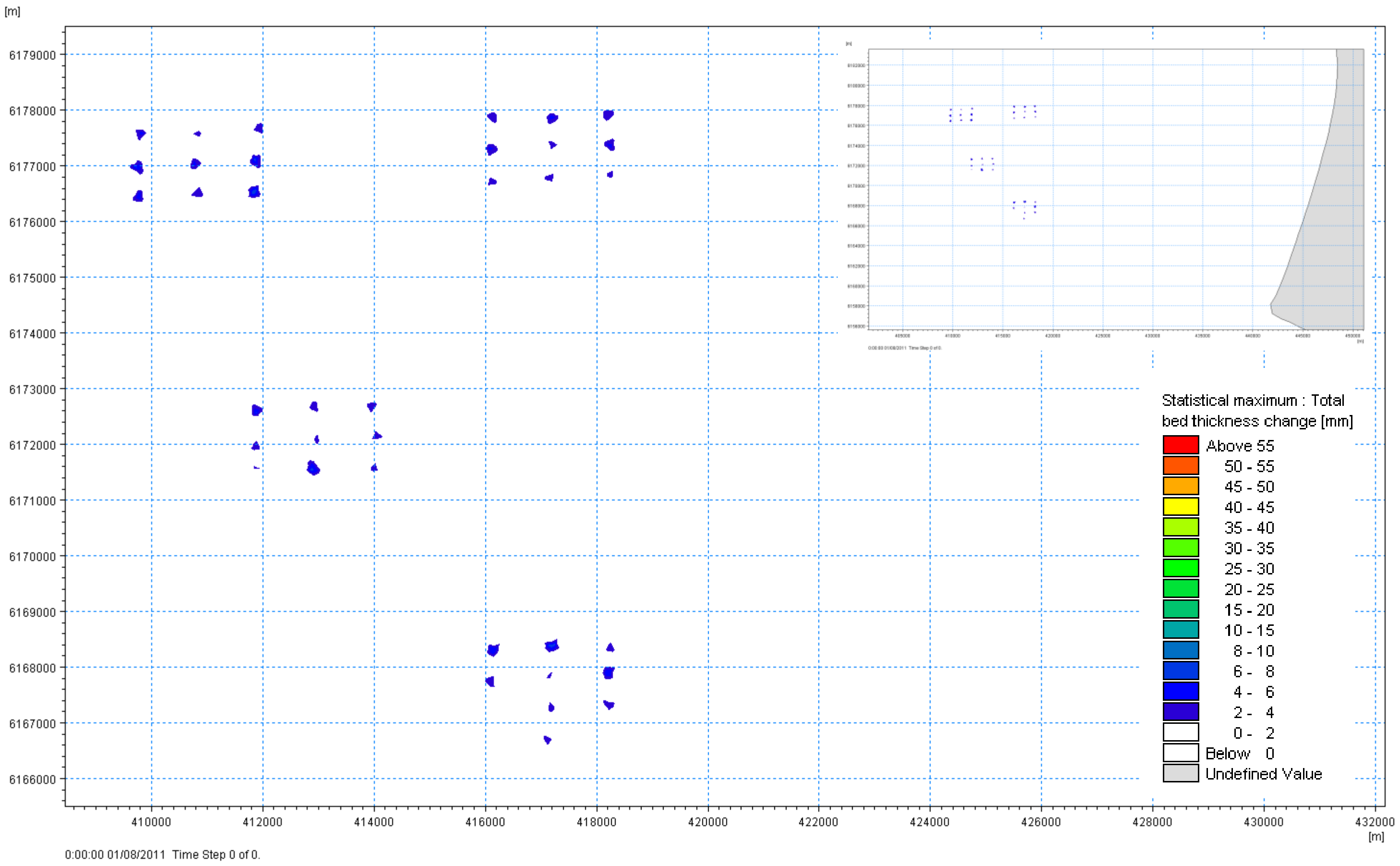


Figure 9.5. Deposition (mm) from plume for the construction phase for GBS foundations, including the coast (top) and zoomed in (bottom).

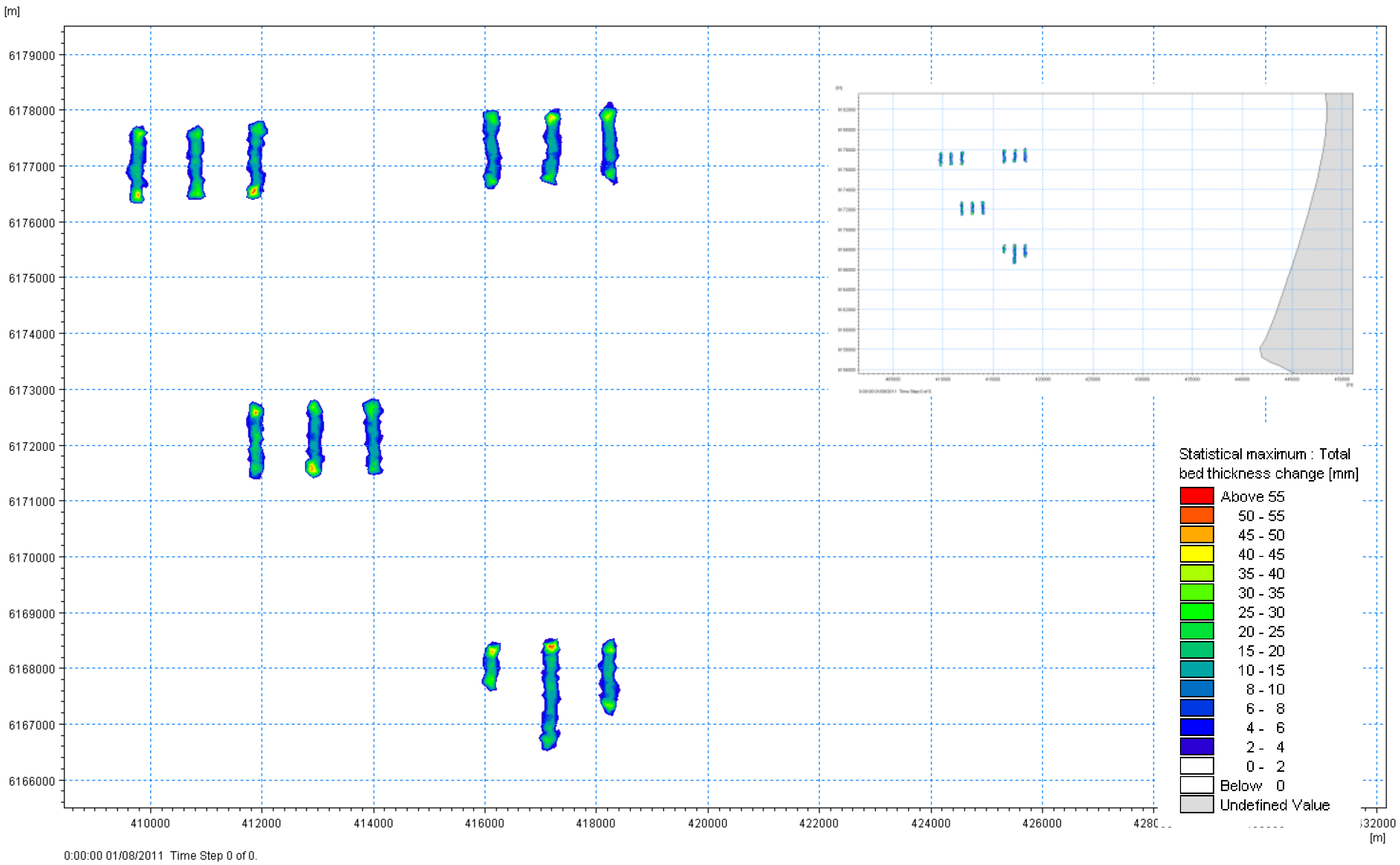


Figure 9.6. Maximum deposition (mm) from plume for the construction phase for GBS foundations and inter-array cable installation combined, including the coast (top) and zoomed in (bottom).

## 9.2. Increase in Suspended Sediment Concentrations as a Result of Export Cable and Substation Installation

Figure 9.7 shows the maximum suspended sediment concentration predicted by the model at any time over the 15-day simulation period for jetting the export cable and preparing the seabed for substation installation. Predicted suspended sediment concentrations are increased along the line of the cable by over 200mg/l decreasing with distance away from the cable. The 'sinusoidal' pattern of dispersion relates to the change in tidal current direction as the cable is continuously jetted over the period of the simulation. The predicted suspended sediment concentrations reduce to zero up to 2km north or south of the cable (depending on the current direction and velocity). Given that the naturally induced suspended sediment concentrations can be several hundred mg/l during storm conditions (Bio/consult, 2000) indicates that concentrations due to jetting are within the scale of natural processes. Hence, the Magnitude of Pressure of additional suspended sediment in the water column caused by installation of export cable and construction of the substation is considered to be low.

Figure 9.8 presents the percentage of time of the entire simulation period (15 days) when the predicted suspended sediment concentrations exceed 10mg/l. The map shows that 10mg/l is predicted to be exceeded less than 1.5% of the 15-day simulation period along the cable, reducing to 0% a short distance (less than 500m) to the north and south.

Figure 9.9 shows the maximum change in deposition predicted at any time over the 15-day simulation period. The largest predicted change is predominantly less than 15mm local to the route of the cable. Deposition increases to a maximum of 30mm closer to the coast. Predicted deposition from the plume reduces rapidly away from the cable extending for no more than 200m to the north or south. Given the dynamic and sandy nature of the substrate along the export cable route, deposition of 30mm of sediment is within the natural variation of bed level changes. Hence, the Magnitude of Pressure of additional deposition of sediment on the seabed caused by installation of the export cable and construction of the substation is considered to be low.

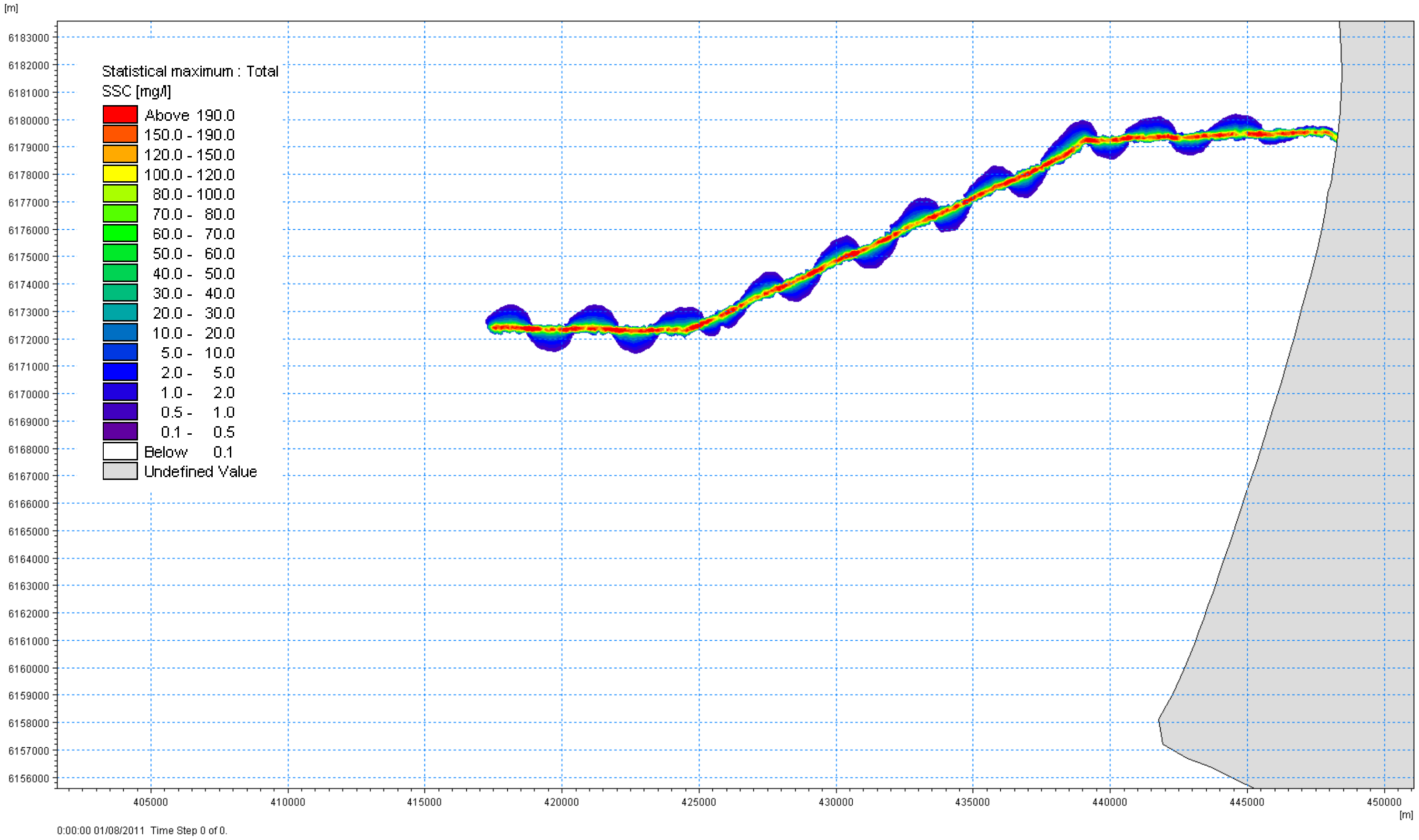


Figure 9.7. Maximum suspended sediment concentration (mg/l) predicted over the simulation period for the construction phase of the export cable corridor and substation.

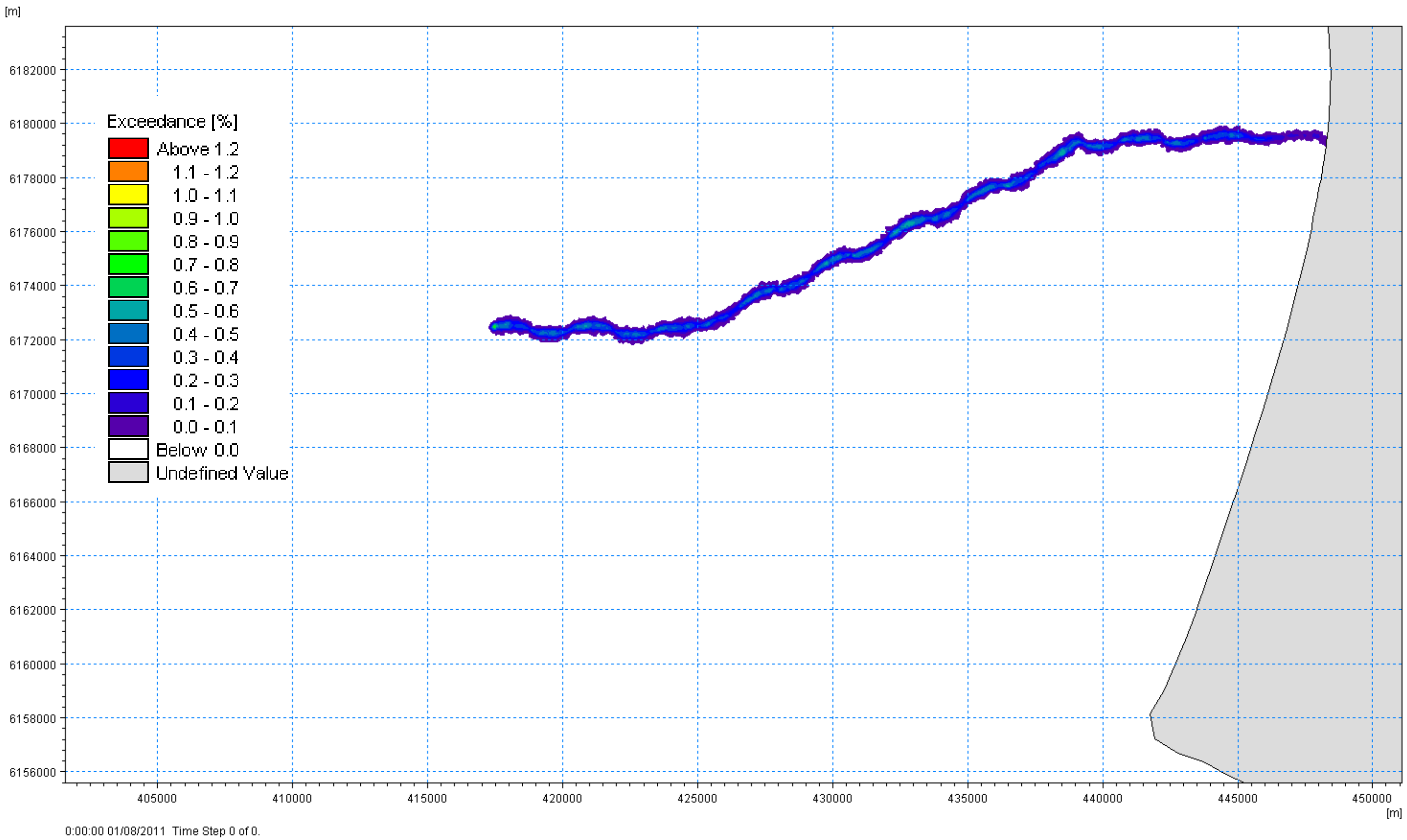


Figure 9.8. Simulated percentage of time during the construction phase of the export cable corridor and substation when suspended sediment concentrations exceed 10mg/l.

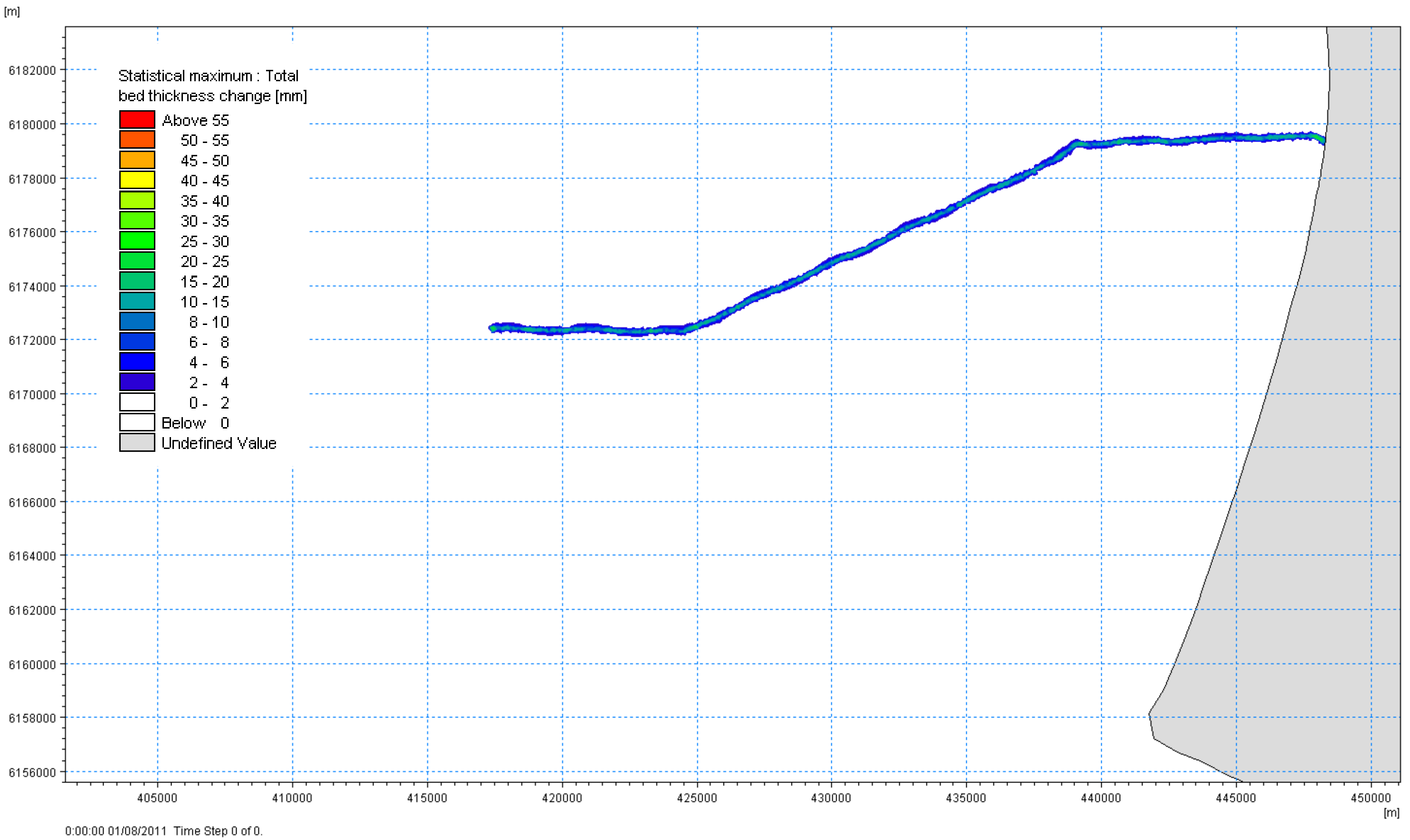


Figure 9.9. Maximum deposition (mm) from plume for the construction phase of the export cable corridor and substation.

## 9.3. Interruption of Sediment Transport as a Result of Landfall Construction Activities

The consideration of the assessment of effects at the landfall site uses the baseline understanding of coastal processes and geomorphology against which the potential effects and sensitivities of sediment transport to changes in the system are determined. Sediment transport across the intertidal zone has the potential to be affected by open trenching and installation of the cable in the trench.

Net sediment transport at Houstrup Strand is to the south, driven by waves approaching predominantly from the northwest. The trench may comprise a cross-shore obstruction to this sediment transport stretching from the dune face seaward. This would potentially, over time, result in a depletion of sediment on the 'downdrift' (south) side of the trench. As the dominant net transport is south, no effects are anticipated to features north of the landfall due to this process.

The short-term nature of the construction period means that the change will be temporary and the presence of the trench will not have a longer term effect on natural coastal processes. Also, not all of the longshore transport of sediment occurs in the intertidal zone. Sediment transport occurs throughout what is termed the 'active' beach profile, which extends offshore to a nearshore point below low water, which is determined by the 'closure depth' of the beach profile (a parameter defined by the wave height and period in the nearshore zone). This could be described as the water depth offshore from which sediment is not disturbed during fair weather (wave) conditions. Whilst the predominant transport is from north to south, onshore to offshore movement occurs during storms.

Given the short duration of the effect and its local range, the Magnitude of Pressure of construction activities at the landfall related to sediment transport is considered to be low.

## 9.4. Pressures on Water Quality associated with Re-suspension of Contaminated Sediments

The suspension of sediments through seabed preparation and inter-array cable jetting may release chemical contaminants bound to the particles. However, existing levels of contamination are very low in the sand (Table 4.3) that is likely to be disturbed across the pre-investigation area. Since concentrations of contaminants are very low within the offshore sediments and large dilution is available, the Magnitude of Pressure on water quality related to re-suspension of contaminated sediments through foundation construction and inter-array cable jetting is considered to be low.

The installation of the export cable may pose more risk to the environment as concentrations of contaminants are likely to be greater near the coastline, due to river and estuary inputs. However, whilst there is additional risk associated with possible increases in contaminant levels closer to the coast, installation is a relatively quick process whereby the jetting equipment moves relatively rapidly through the environment (up to 250m per hour). As a result, the plume and any contaminants contained within it will be very short lived and quickly diluted within the open environment. Given that the effect will be very short term and baseline conditions will be returned quickly following cessation of the activities means that the Magnitude of Pressure on water quality related to re-suspension of contaminated sediments through export cable jetting is considered to be low.

## 9.5. Pressures on Water Quality associated with Re-suspension of Nutrients

There are two potential activities that could re-suspend sediments into the water column thus releasing any nutrients bound to the particles:

- seabed preparation or disturbance to the seabed during foundation and ancillary installation; and
- cable installation (both inter-array and export cable).

The sediment samples collected across the pre-investigation site to determine the baseline conditions did not contain high nutrient concentrations and most samples recorded levels below the limit of detection. As a result, little change to water quality in terms of nutrient concentrations is anticipated and the Magnitude of Pressure is considered to be low.

In terms of the export cable and inter-array cable installation, it is considered that the export cable installation poses more risk to the environment as concentrations of nutrients are likely to be greater around the coastline. (Sediment samples were collected during the C-POD surveys. Due to bad weather conditions during the survey, no samples were collected in shallow waters close to the coast). This is due to river and estuary inputs. Whilst there is additional risk associated with possible increases in nutrient concentrations closer to the coast, installation is a relatively quick process whereby the jetting equipment moves relatively quickly through the environment (up to 250m per hour). As a result, the plume is likely to be very short lived and quickly diluted within the open environment. Given that the effect will be very short term and baseline conditions will be returned quickly following cessation of the activities means that the Magnitude of Pressure on water quality related to re-suspension of nutrients through export cable jetting is considered to be low.

## 9.6. Pressures on Water Quality associated with use of Materials/Fluids

There are a number of materials which if released into the marine environment could impact on water quality (Sections 4.5 and 4.6). Oils and fluids are used within each turbine to ensure that they function correctly. Varying quantities of these materials may be used depending on which size turbine is eventually installed. However, all turbines are designed to capture a lubricant spill from all components which could potentially leak into the marine environment. All ballast options potentially available will use non-toxic material either from an uncontaminated offshore source or Olivine or Norit, which are both non-toxic (Energinet.dk, 2014). As a result, if any spillage should occur during filling of the foundation bases then impacts on water quality will not occur.

Grouting is a cement-based substance which if released into the water can have an effect on its pH. However, it is used extensively in the offshore environment and any grout used in construction will conform to relevant environmental standards. In addition, the grout will be mixed in large tanks on a jack-up barge, crane vessel or mixed onshore before being pumped through grout tubes so that it is introduced directly to the area in which it is required. This reduces risk of the grout being introduced to the marine environment. Overall, the Magnitude of Pressure on water quality related to use of materials/fluids is considered to be low on the basis that the likely size of a spill will be very small both in duration and range.

## 9.7. Pressures on Natura 2000 Sites of Construction Activities

Due to the considerable distance from the proposed wind farm area and the limited, local and temporary magnitude of change of hydrography and sediment transport and associated contaminants caused by construction of the wind farm and export cable, the Magnitude of Pressure is considered to be low.

*Construction of offshore wind farm – Horns Rev 1*

# 10. POTENTIAL PRESSURES DURING OPERATION

The operational phase of the proposed Horns Rev 3 equates, at a minimum, to the duration of the lease (nominally 25 years). During this time, the hydrography, sediment spill and water quality effects of the development are likely to be evident through persistent and direct changes, resulting from wave and tidal current interactions with the foundation structures.

There are anticipated to be no hydrography, sediment spill and water quality effects during the operation of the inter-array cables or export cables, where they are buried beneath the seabed, or during the operation of the landfall site, because the cables will be buried beneath the beach.

## 10.1. Effect of Foundation Structures on Tidal Current Velocities

The regional effects on tidal currents of the foundation layout have been examined as changes to depth-averaged current velocity relative to the baseline. The worst case foundation layout used in the simulation is shown in Figure 1.3 (top panel) and comprises 3MW foundations across the western side of the pre-investigation area.

The results of the hydrodynamic modelling are presented as a series of maps showing changes to depth-averaged current velocity relative to the baseline at different states of the tide (high spring, high neap, slack spring and slack neap) and as maximum changes in tidal current velocity over the 30-day simulation period.

Figures 10.1 and 10.2 describe the effect of the foundation layout on tidal current velocities at high spring tide and high neap tide respectively. A maximum change of only 0.008m/s is predicted on a spring tide, reducing to 0.003m/s on a neap tide. The changes on the spring tide are limited to within the layout and to a maximum of 2km outside the layout boundary. The changes do not approach the coast.

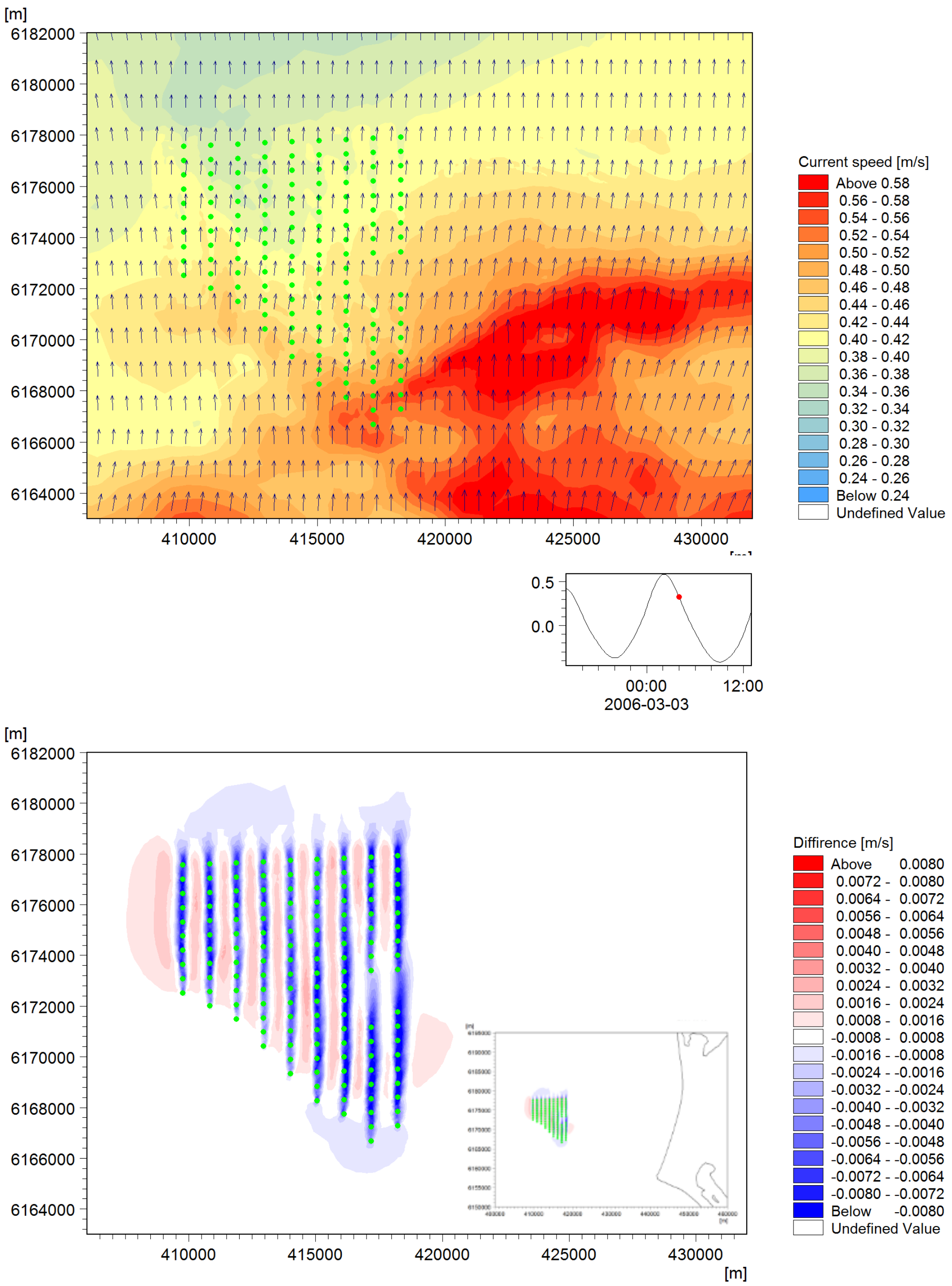


Figure 10.1. Simulated tidal current velocities (m/s) during a spring ebb tide (top panel) and the change in tidal current velocities (m/s) due to the foundation layout (bottom panel).

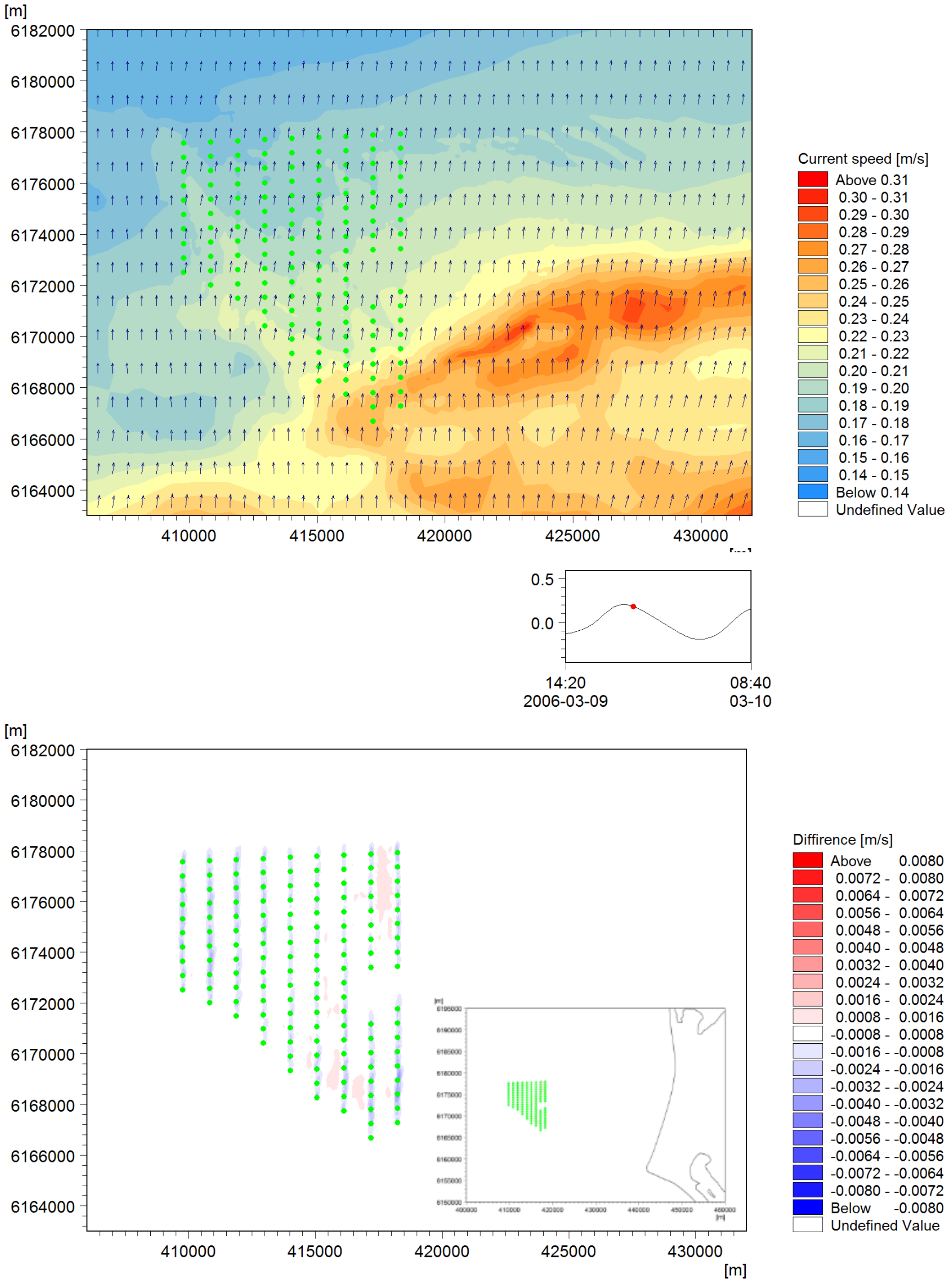


Figure 10.2. Simulated tidal current velocities (m/s) during a neap ebb tide (top panel) and the change in tidal current velocities (m/s) due to the foundation layout (bottom panel).

Figures 10.3 and 10.4 present the predicted effect of the layout at slack spring tide and slack neap tide respectively.  They describe maximum changes of 0.003m/s on a spring tide and approximately 0.002m/s on a neap tide. Although the slack spring tide changes are very small, they can extend greater 4km outside the boundary of the layout. The changes do not approach the coast.

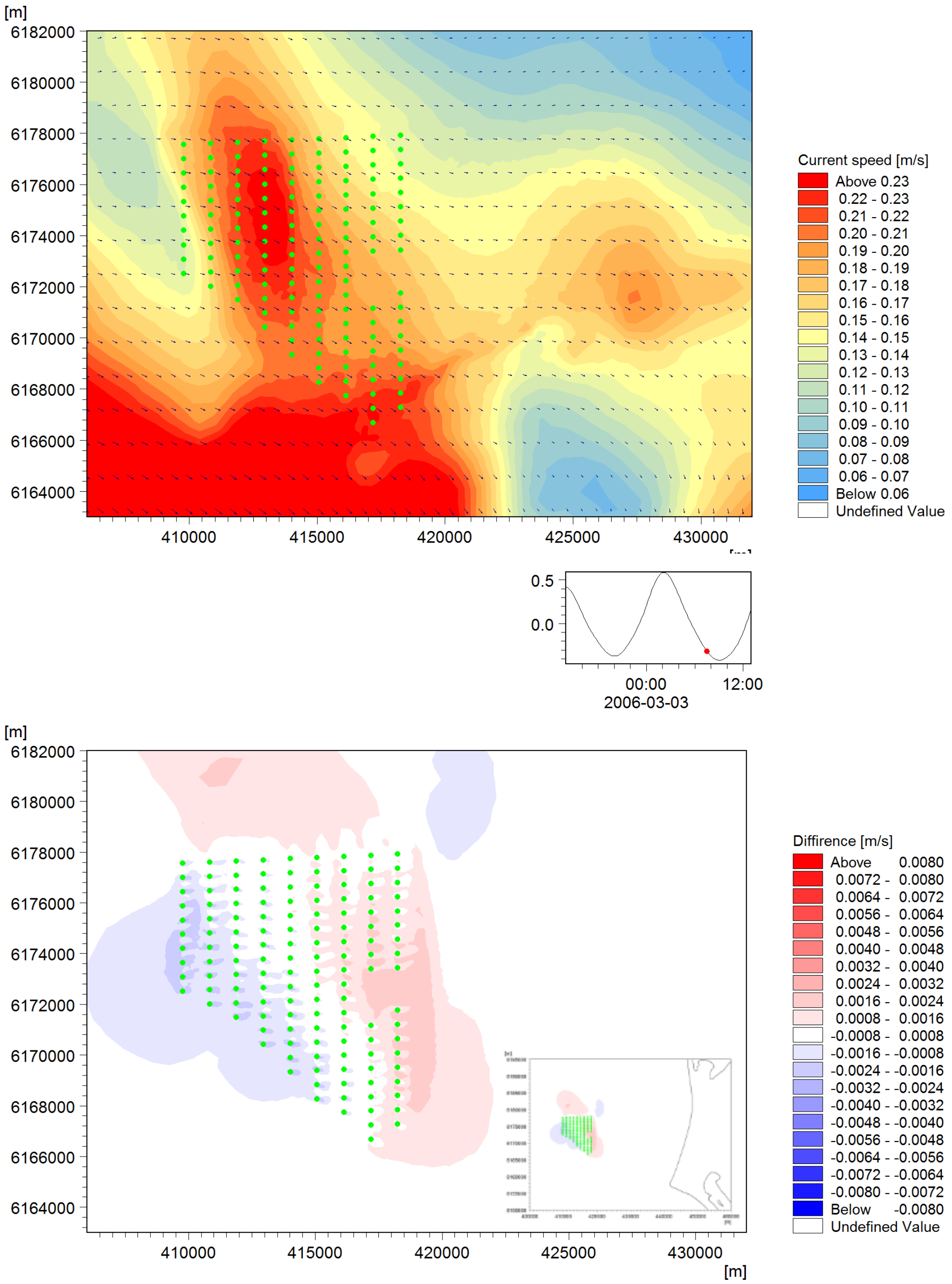


Figure 10.3. Simulated tidal current velocities (m/s) during a slack spring tide (top panel) and the change in tidal current velocities (m/s) due to the foundation layout (bottom panel).

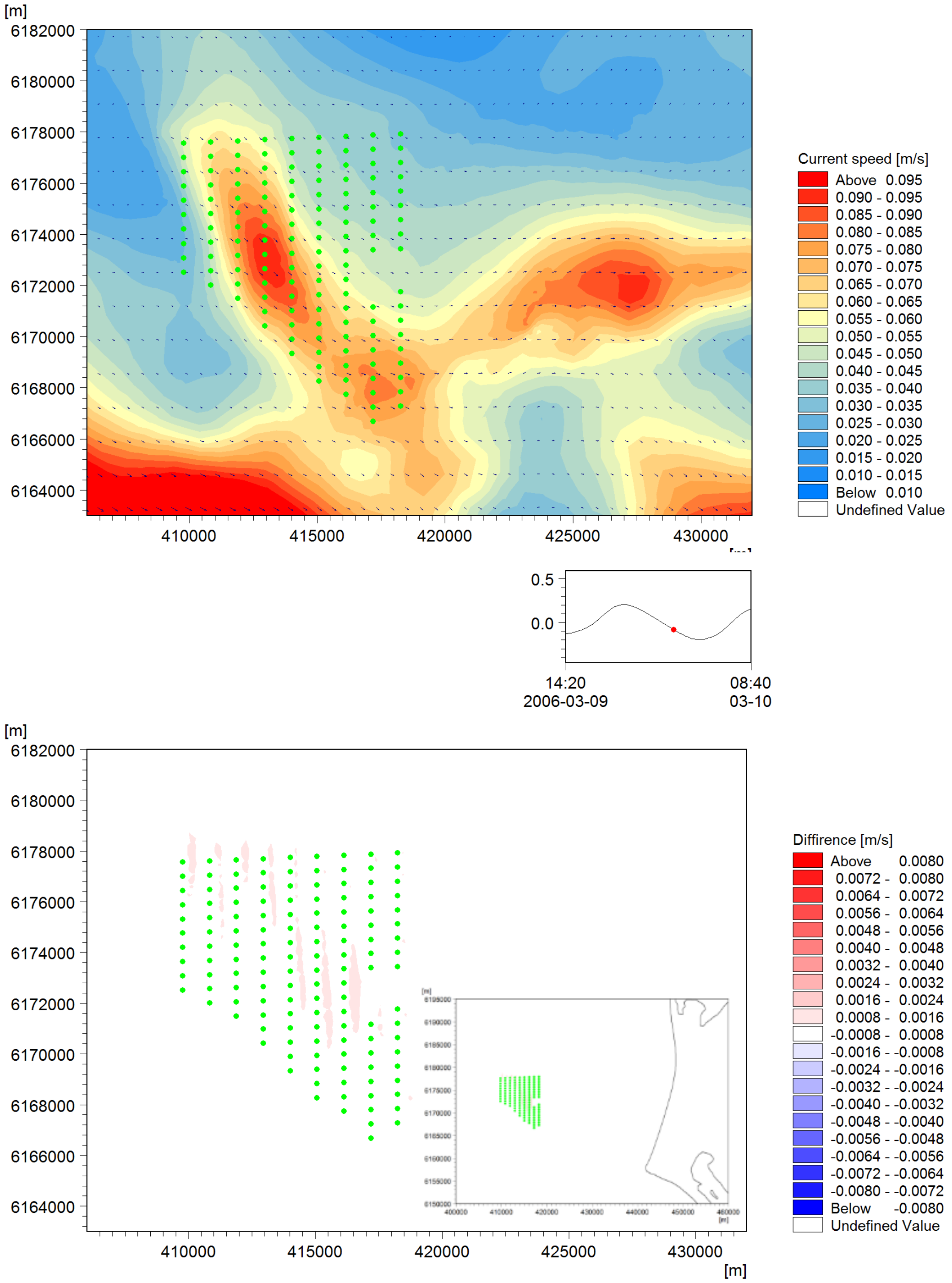


Figure 10.4. Simulated tidal current velocities (m/s) during a slack neap tide (top panel) and the change in tidal current velocities (m/s) due to the foundation layout (bottom panel).

Figure 10.5 shows that the maximum tidal current velocities over the 30-day simulation period with the layout in place are about 0.5-0.6m/s across the south of the layout with 0.4m/s across the remainder. The maximum difference in current velocity is less than 0.008m/s, demonstrating an overall inconsequential effect on tidal current patterns across

Horns Rev 3 and regionally (there is no effect at the coast). Hence, the Magnitude of Pressure of changes to tidal currents caused by operation of Horns Rev 3 is considered to be low.

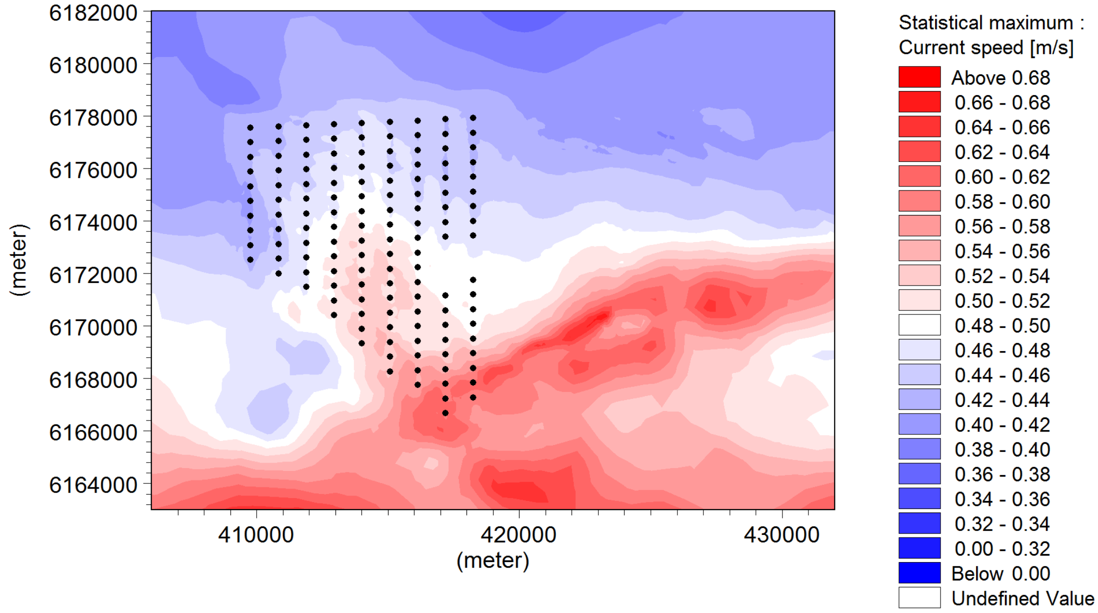


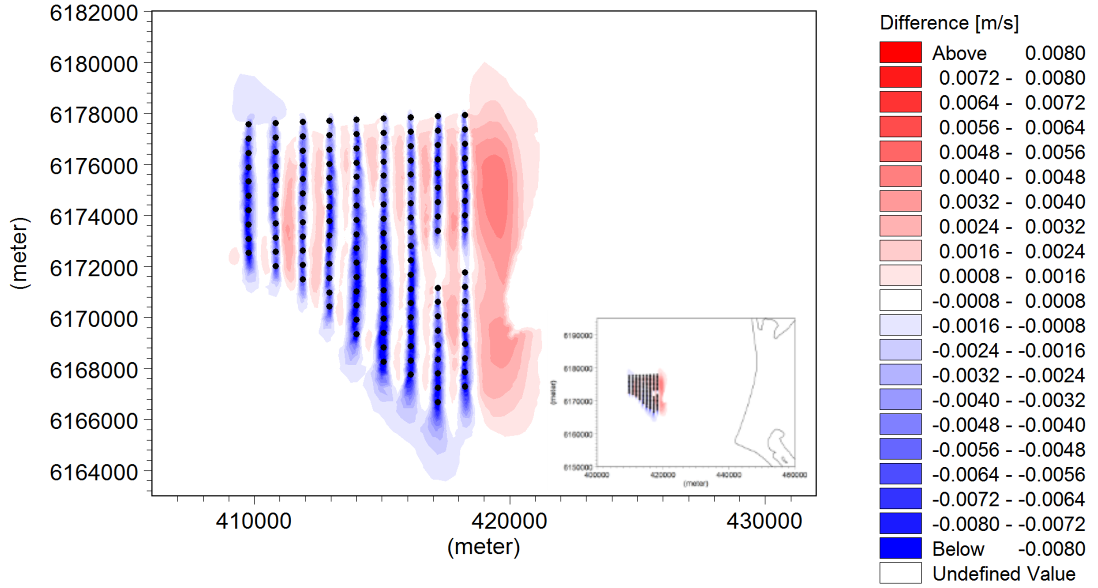


Figure 10.5. Simulated maximum tidal current velocities (m/s) (top panel) and the maximum change in tidal current velocities (m/s) due to the foundation layout (bottom panel).

## 10.2. Effect of Foundation Structures on Wave Heights

Six different wave conditions were modelled, combining the three commonest directions of approach across Horns Rev 3 and two return periods:

- one-year return period waves approaching from the northwest;
- one-year return period waves approaching from the west;
- one-year return period waves approaching from the southwest;
- 50-year return period waves approaching from the northwest;
- 50-year return period waves approaching from the west; and
- 50-year return period waves approaching from the southwest.

The wind, wave and water level conditions input as the model boundary conditions are shown in Table 10.2.

Table 10.2. Wind and wave input into the wave model.

| Return Period | Wind Speed* (m/s) | Wave Height (m) | Wave Period (s) | Wave Direction |
|---|---|---|---|---|
| One-year | 29.6 | 12.2 | 16.7 | Northwest |
| | 32.6 | 11.5 | 16.3 | West |
| | 29.6 | 9.6 | 14.9 | Southwest |
| 50-year | 38.5 | 16.6 | 19.5 | Northwest |
| | 38.7 | 14.0 | 17.9 | West |
| | 39.9 | 13.5 | 17.6 | Southwest |

*wind direction was assumed to be in the same direction as offshore waves, which is considered to be worst case

Figures 10.6 to 10.11 describe the effect of the foundation layout on wave heights for both one-year and 50-year return period waves approaching from the northwest, west and southwest. Given the depth–limited nature of the waves across the pre-investigation area means that the one-year and 50-year effects for each wave direction are similar. The effect of the foundation layout on significant wave height is very small in all cases with a maximum change of less than 0.007m (7mm). Waves increase slightly on the ‘up-wave’ sides of each structure and decrease on their lee sides. In all scenarios there is no interaction with the coast.

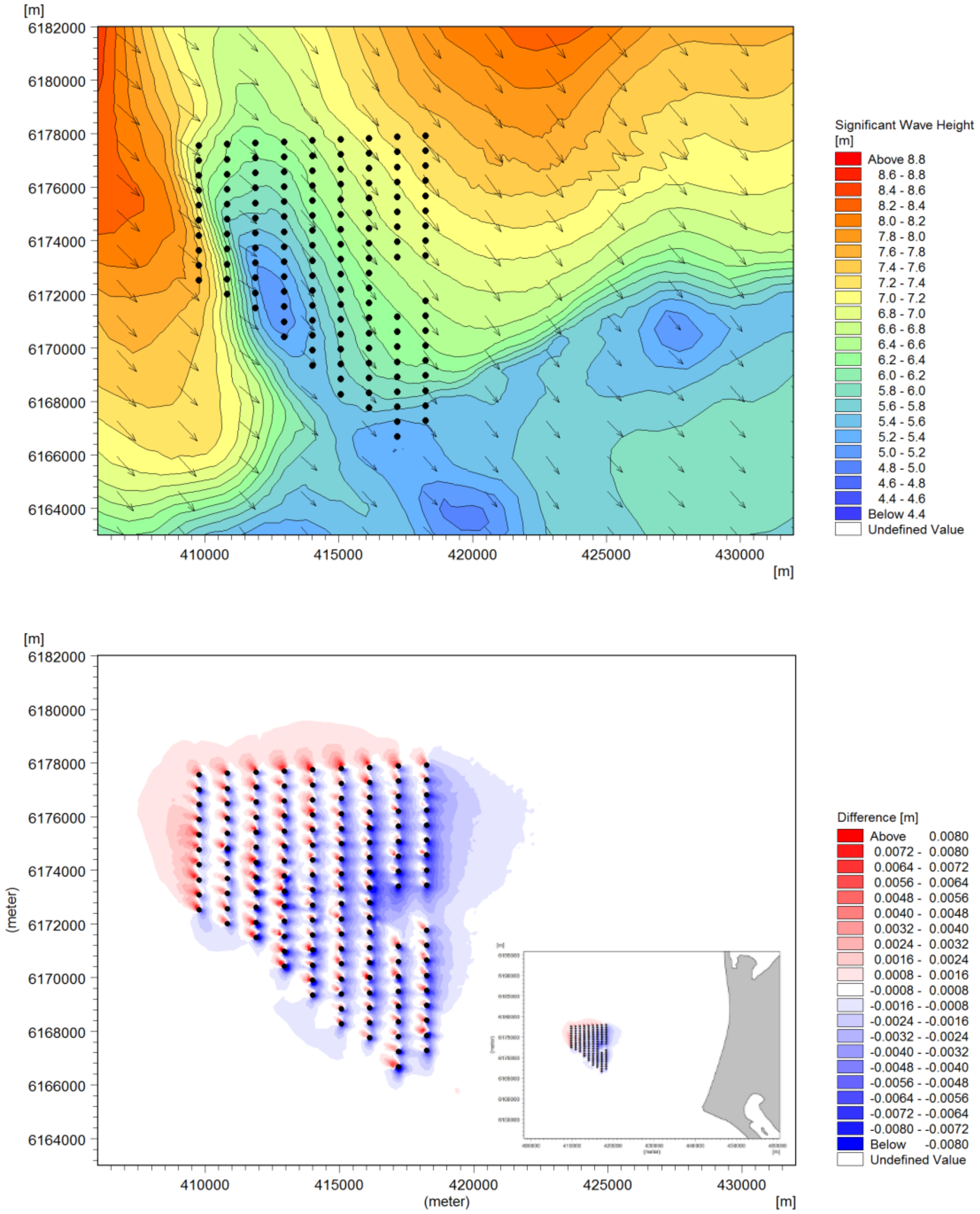


Figure 10.6. Simulated one-year return period significant wave heights (m) approaching from the northwest (top panel) and the change in significant wave heights (m) due to the foundation layout (bottom panel) (inset: with coast).

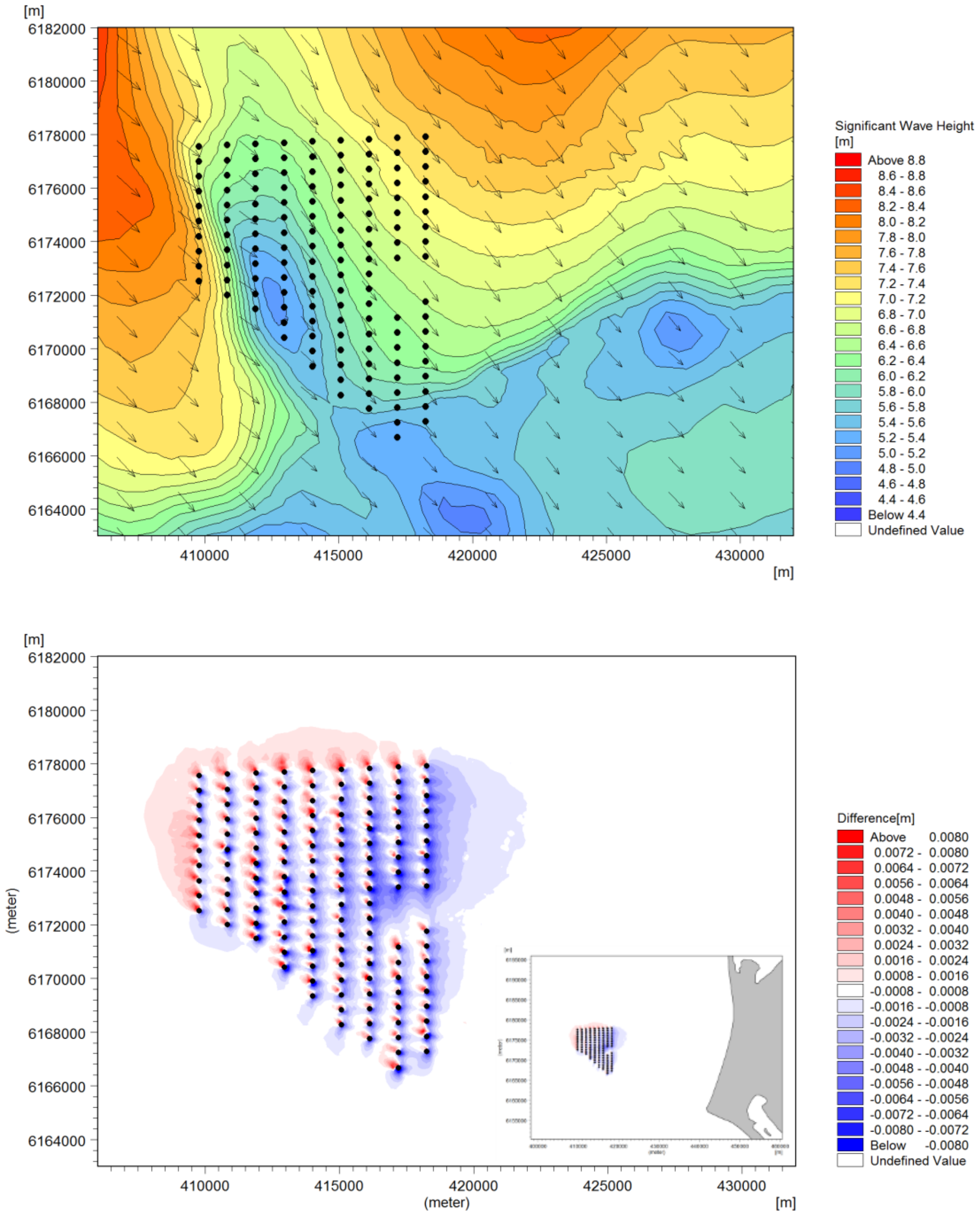


Figure 10.7. Simulated 50-year return period significant wave heights (m) approaching from the northwest (top panel) and the change in significant wave heights (m) due to the foundation layout (bottom panel) (inset: with coast).

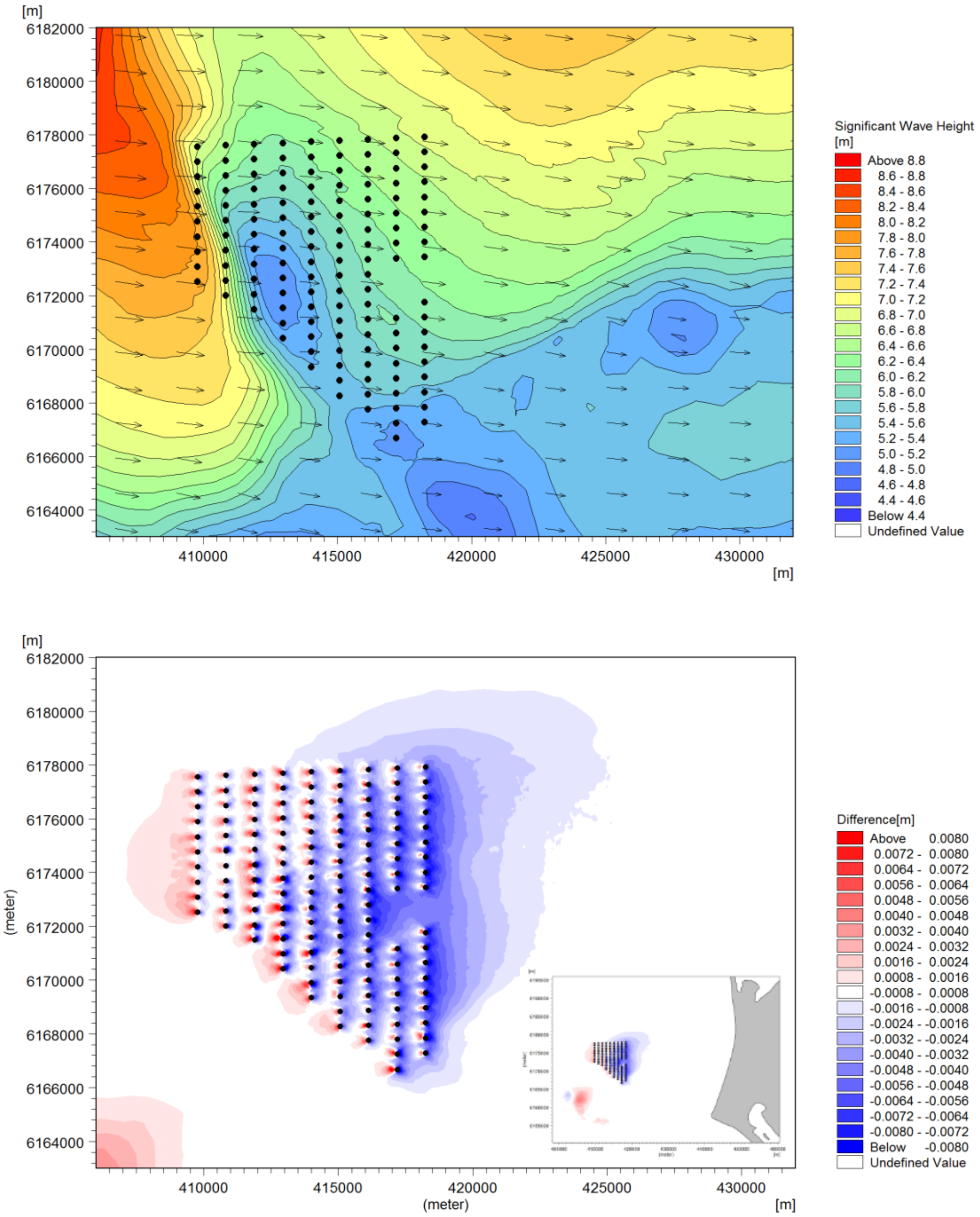


Figure 10.8. Simulated one-year return period significant wave heights (m) approaching from the west (top panel) and the change in significant wave heights (m) due to the foundation layout (bottom panel) (inset: with coast).

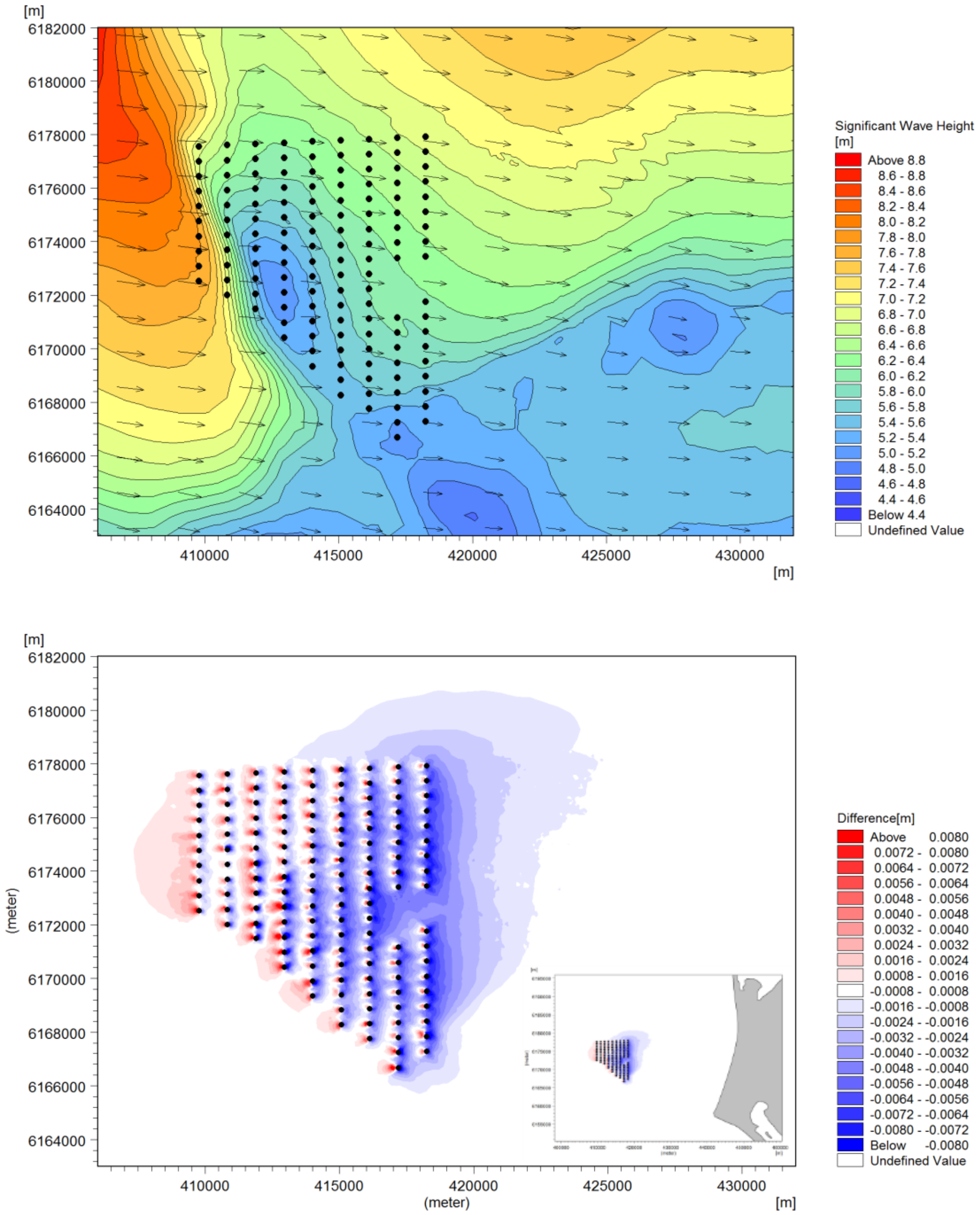


Figure 10.9. Simulated 50-year return period significant wave heights (m) approaching from the west (top panel) and the change in significant wave heights (m) due to the foundation layout (bottom panel) (inset: with coast).

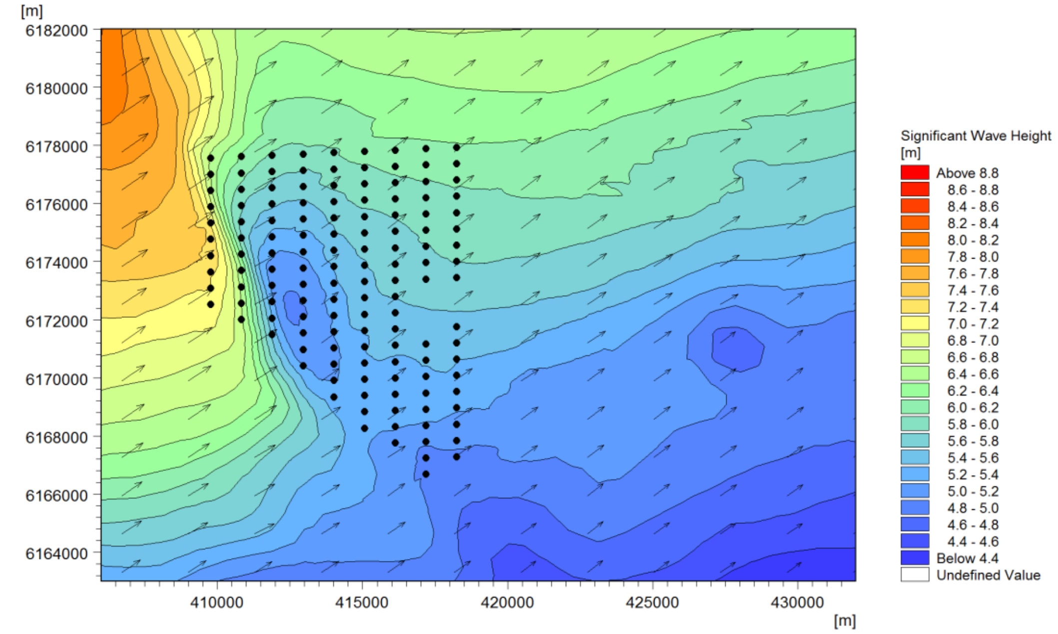


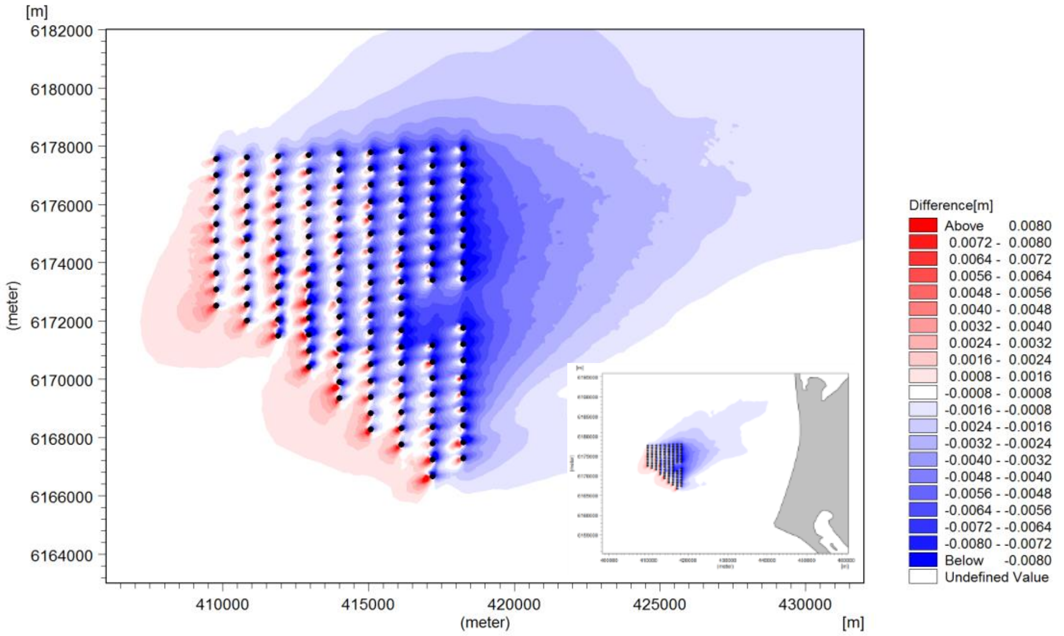


Figure 10.10. Simulated one-year return period significant wave heights (m) approaching from the southwest (top panel) and the change in significant wave heights (m) due to the foundation layout (bottom panel) (inset: with coast).

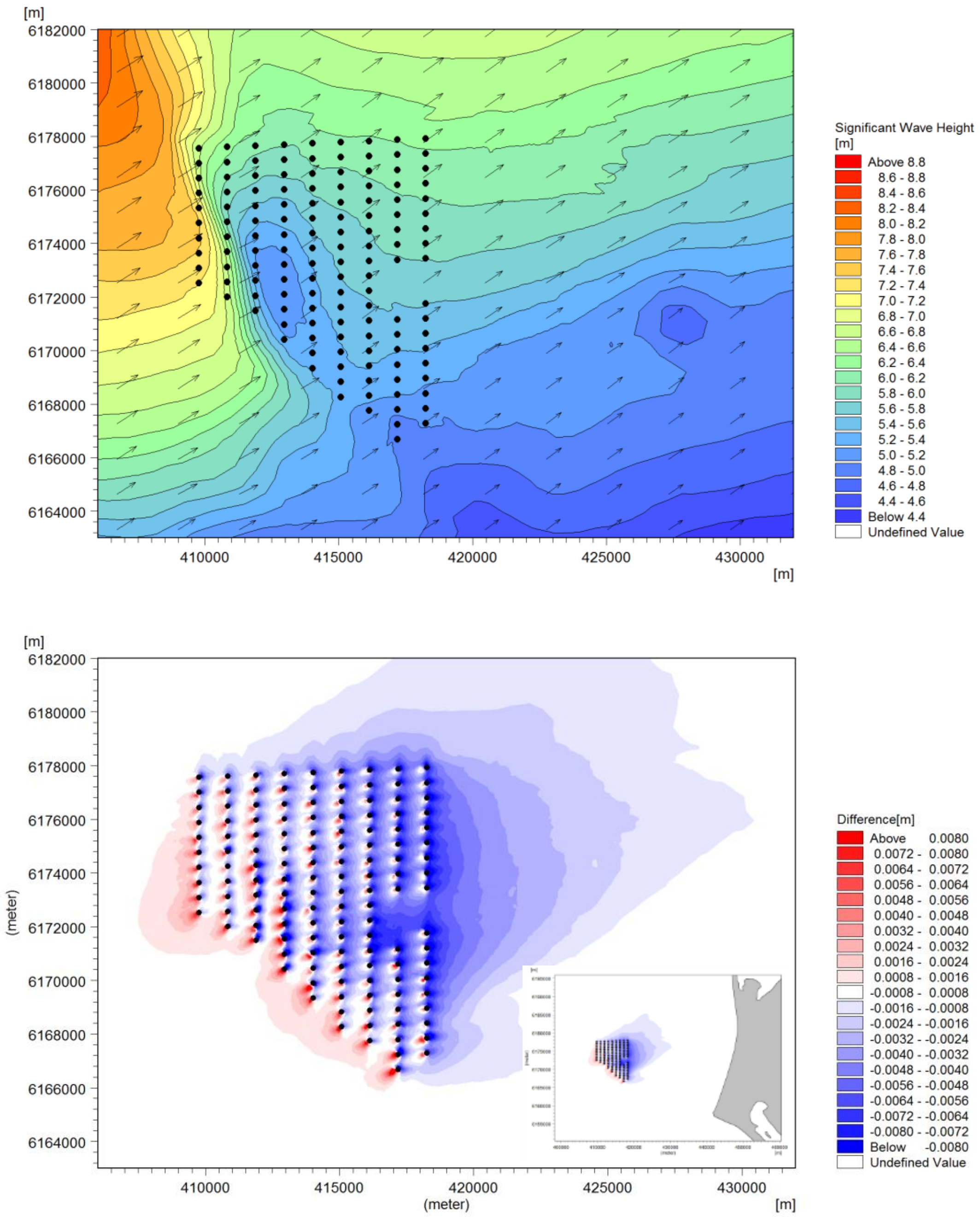


Figure 10.11. Simulated 50-year return period significant wave heights (m) approaching from the southwest (top panel) and the change in significant wave heights (m) due to the foundation layout (bottom panel) (inset: with coast).

## 10.2.1 Impact of Wind Reduction Caused by the Wind Turbines

The most relevant information with respect to the effect of wind speed reduction by wind turbines is Frandsen et al. (2009). Using experiments, they determined wind speed decay at hub height (70m above sea surface) through the 80-turbine Horns Rev 1 offshore wind farm. For a wind speed of 8-9m/s, they found that the mean wind speed was reduced by up to 19%, and recovery was approximately 6km down-wind from the last turbine. Based on the results of Frandsen et al. (2009), the impact of wind reduction on the wave field in the lee of Horns Rev 3 has been investigated using the wind speed reduction curve presented in Table 10.1 and Figure 10.12.

Table 10.1. Wind speed reduction in the lee of Horns Rev 3.

| Distance from Wind Turbines (m) | Wind Reduction Factor (%) |
|---|---|
| 0 | 16% |
| 500 | 17% |
| 1000 | 18% |
| 1500 | 13% |
| 2250 | 19% |
| 2750 | 19% |
| 3250 | 19% |
| 3900 | 19% |
| 4500 | 19% |
| 5000 | 19% |
| 7000 | 14% |
| 11000 | 7% |
| 15000 | 0% |

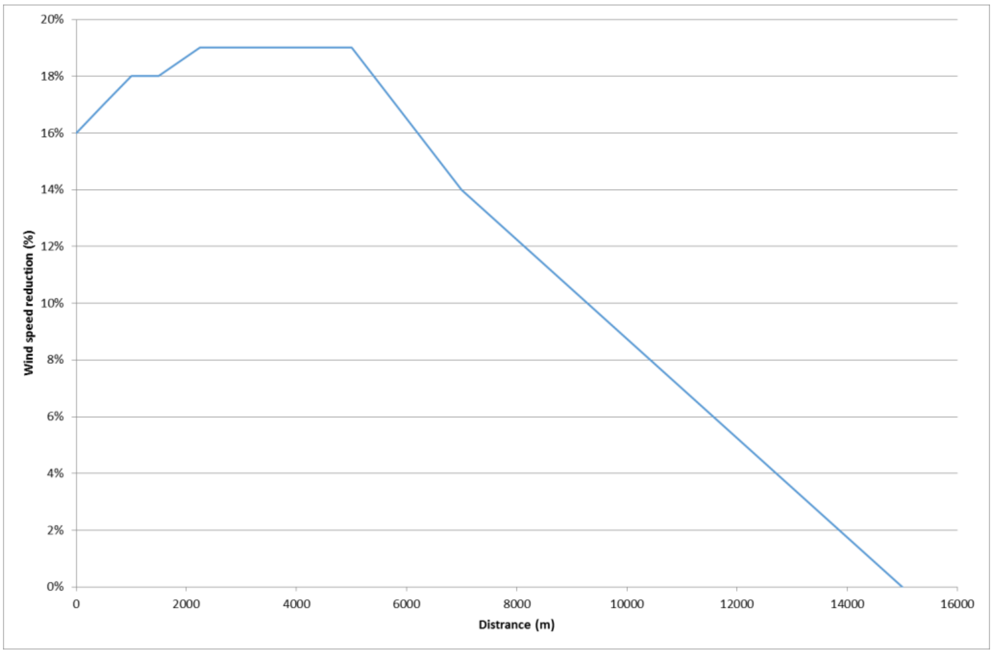


Figure 10.12. Wind speed reduction in the lee of Horns Rev 3.

A one-year westerly wind was chosen because it is the worst case return period and direction with respect to both wave height and distance to the shore from the proposed Horns Rev 3 development. Figure 10.13 shows the predicted difference (using the MIKE21-SW model) between wave heights using a uniform wind speed of 32.6m/s (Table 10.2) and a wind speed reduction in the lee of the wind turbines. In both model runs, the proposed wind turbines were included so the difference is purely due to wind speed reduction.

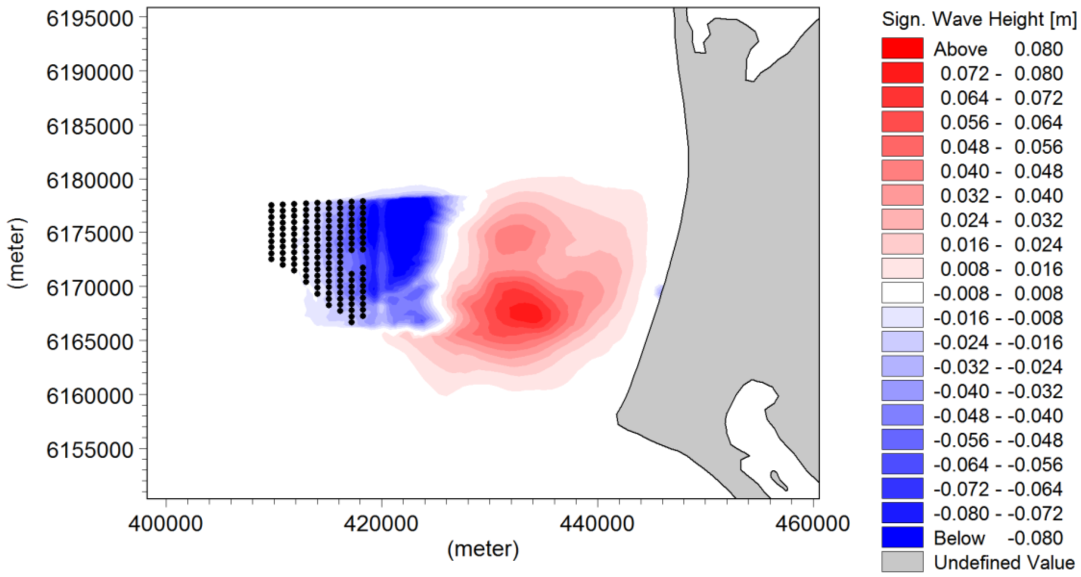


Figure 10.13. Change of wave height by wind speed reduction in the lee of Horns Rev 3 (positive means wave height is increased).

It is not surprising that wave height is predicted to reduce in the immediate lee of the wind turbines. However, the model results show that from a distance of approximately 6km from the most easterly turbine row, the wave height is predicted to increase. This unexpected increase may be explained by the effect of wind speed reduction on wave direction. Figure 10.14 presents the predicted change to wave direction. The model demonstrates that wave energy to the north and south of the wind farm will be ‘diverted’ into the lee area causing the wave height to increase in their zone of convergence. Nevertheless, the decreases and increases of wave height by wind speed reduction are relatively small and limited to offshore area (Figure 10.13).

The Magnitude of Pressure of changes to waves caused by operation of Horns Rev 3, both from direct changes due to the foundations themselves and changes to the wind field induced by the turbine towers is considered to be low.

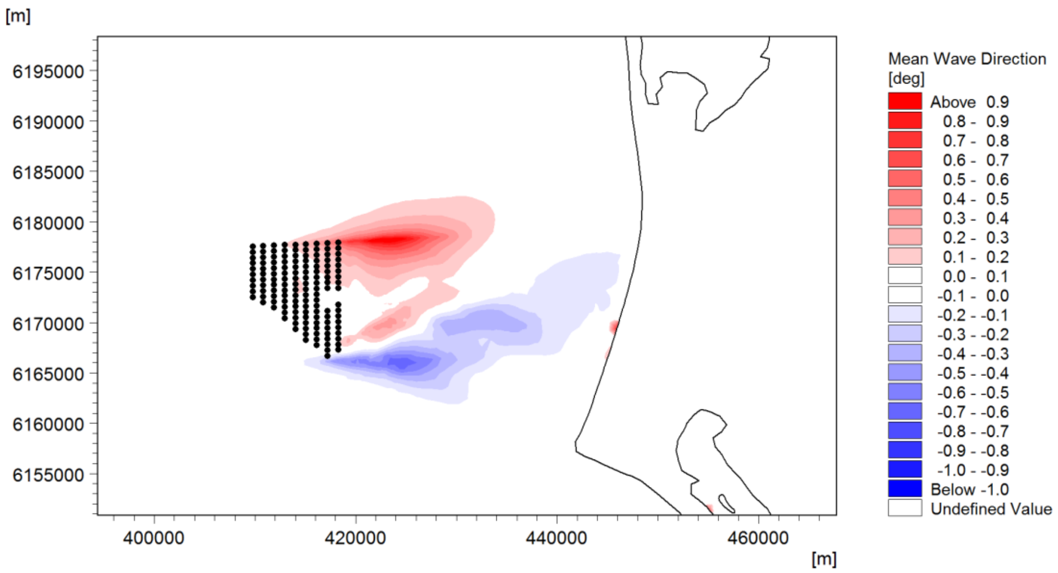


Figure 10.14. Change of wave direction by wind reduction in the lee of Horns Rev 3 (positive means wave height is increased).

## 10.3. Pressures of the Operational Phase on Water Quality

During normal operation of Horns Rev 3, no emissions into the water are anticipated as control measures will be in place to capture any accidental leaks or discharges from the turbines or ancillary structures. The turbines will be serviced and maintained throughout their life from a local port in the vicinity. Following commissioning, it is expected that the servicing interval for the turbines will be approximately six months. Periodic overhauls will include analysis of oil samples, lubrication and oil changes on gear boxes or hydraulic systems (Energinet.dk, 2014).

During these processes, control measures will be put in place in order to ensure accidental spillages do not occur. As a result, the Magnitude of Pressure on water quality related to operation of the wind farm is considered to be low although filtration of phytoplankton from mussels attached on the turbine foundations may locally have a small positive impact on water quality (Andersen, 2006).

## 10.4. Pressures on Natura 2000 Sites of the Operational Phase

Due to the considerable distance from the proposed wind farm area and the limited, local and temporary magnitude of change of hydrography and sediment transport caused by operation of the wind farm and export cable, the Magnitude of Pressure is considered to be low.

# 11. POTENTIAL PRESSURES DURING DECOMMISSIONING

The lifetime of the wind farm is expected to be around 25 years. Prior to expiry of the production time a decommissioning plan should be submitted. Currently, the decommissioning approach has not been defined, and therefore this assessment of potential pressures uses a worst case scenario of full removal of foundations, cables, turbine components and ancillary structures.

## 11.1. Foundations and Cables

The effects are likely to include short-term increases in suspended sediment concentration and sediment deposition from the plume caused by foundation cutting or dredging and seabed disturbance caused by removal of cables and cable protection. Limited impacts on water quality are anticipated as the sediments are not contaminated. Although there is no evidence base on these potential effects, the effects during decommissioning of the foundations, inter-array cables and export cables are considered to be less than those described during the construction phase. This is because there will be no need for seabed preparation and there is a possibility that cables are left *in situ* with no consequential increase in suspended sediment concentration or changes to water quality. As a result, the Magnitude of Pressure of changes to hydrography, sediment spill and water quality caused by decommissioning of Horns Rev 3 is considered to be low.

## 11.2. Removal of Turbine Components and Ancillary Structures

During decommissioning of both the turbine components and ancillary structures, all fluids and substances will need to be removed. The effects during decommissioning are considered to be similar to those described during the construction phase; hence, the Magnitude of Pressure is considered to be low.

## 11.3. Landfall

A plan for decommissioning the cable at the landfall has yet to be defined although at the end of its field life it may be dismantled and re-used or decommissioned and left *in situ*, depending on foreseeable dune erosion. During any decommissioning process, sections of buried cable under the dune may be removed if there is a potential for exposure due to dune erosion. This could have local effects on the stability of the dunes. If the cable is left *in situ*, there will be no effects on coastal processes. If the cable is removed from the beach and intertidal zone, there will be temporary local effects of a type and duration likely to be similar to the construction phase activities. Hence, the Magnitude of Pressure of decommissioning the landfall is considered to be low.

# 12. CUMULATIVE PRESSURES

The assessment of cumulative effects evaluates the extent of the environmental effects of Horns Rev 3 in terms of intensity and geographic extent compared with other projects in the area. The assessment of the cumulative conditions includes activities associated with existing utilised and un-utilised permits or approved plans for projects. When projects within the same region affect the same environmental conditions simultaneously, they are defined to have cumulative impacts. Cumulative effects can potentially occur on a local scale, such as within the Horns Rev 3 wind farm area, and on a regional scale covering the entire Horns Rev / Blåvands Huk area. A project is relevant to include, if it meets one or more of the following requirements:

- the project and its impacts are within the same geographical area as Horns Rev 3;
- the project affects some of the same or related environmental conditions as Horns Rev 3; and
- the project has permanent impacts in its operational phase interfering with impacts from Horns Rev 3.

Specific plans, projects and activities screened in to the assessment of cumulative effects include the offshore wind farm developments of Horns Rev 1 and Horns Rev 2.

## 12.1. Cumulative Pressures with Horns Rev 1 and Horns Rev 2

The northern perimeter of Horns Rev 1 is located approximately 20km south-southeast of the southern boundary of Horns Rev 3 (Figure 1.1). Horn Rev 1 covers an area of 21km$^2$ and generates 160MW of electricity. The northern perimeter of Horns Rev 2 is located about 3km southwest of the southwestern boundary of Horns Rev 3 (Figure 1.1). Horn Rev 2 covers an area of 33km$^2$ and generates 209MW of electricity.

The sediment transport (and therefore water quality) effects of construction of the Horns Rev 3 foundations and cable do not extend beyond 500m from the structures and will not interact with either Horns Rev 1 or Horns Rev 2. The operational effects of Horns Rev 3 on tidal currents are small (less than 0.008m/s) and restricted to within and immediately adjacent to the pre-investigation perimeter. The effects on waves are more widespread, but the changes are distributed to the east and northeast, away from Horns Rev 1 and Horns Rev 2.

# 13. IMPACT ASSESSMENT SUMMARY

## 13.1. Impacts on Water Quality

The suspension of sediments through seabed preparation, inter-array and export cable jetting during the construction phase may release chemical contaminants and nutrients bound to the particles. The existing levels of contamination and nutrients are very low in the sand that is likely to be disturbed across the pre-investigation area and along the export cable. As a result, little change to water quality is anticipated and therefore the degree of impact is predicted to be low.

In order to determine the severity of impact, the importance of water quality has to be considered. Based on the descriptions provided in Section 1.6, an importance level of high is defined for chemical contamination, since European legislation protects water quality in relation this parameter. An importance level of medium is defined for nutrients, since their levels in the water are important for local ecosystem functioning. The resulting severity of impact is therefore low. Overall, no impact on water quality (contaminants and nutrients) is predicted for the construction phase (Table 13.1) for the following reasons:

- concentrations of contaminants and nutrients are very low within the offshore sediments and large dilution is available,
- installation is a relatively quick process whereby the jetting equipment moves relatively rapidly through the environment (up to 250m per hour), so any release of contaminants and/or nutrients is predicted to be very short lived and quickly diluted within the open environment.

Accidental spillage of materials and fluids into the marine environment could also impact on water quality during construction (Sections 4.5 and 4.6). However, the likelihood of such a spill is very small and therefore the degree of impact is predicted to be low. Based on the descriptions provided in Section 1.6, an importance level of medium has been defined since pH changes in the water column are important for local ecosystem functioning. The resulting severity of impact is predicted to be low. Overall, an impact of negligible negative significance is predicted on the basis that it is difficult to determine the likely size of a spill and, therefore, a precautionary approach has been adopted (Table 13.1).

Table 13.1. Summary of impact assessment for water quality from re-suspending sediments and accidental spillage for the foundations, substation, inter-array and export cables.

| Parameter | Construction | | | Operation | Decommissioning | |
|---|---|---|---|---|---|---|
| | Re-suspension | | Accidental Spillage | | | |
| | Contaminated sediments | Nutrients | Construction Materials | Maintenance Materials | Foundations / Cables | Turbines / Ancillary Structures |
| Magnitude of Pressure | Low | Low | Low | Low | Low | Low |
| Sensitivity | Medium | Medium | Medium | Medium | Medium | Medium |
| Degree of Impact | Low | Low | Low | Low | Low | Low |
| Importance | High | Medium | Medium | Medium | Medium | Medium |
| Severity of Impact | Low | Low | Low | Low | Low | Low |
| Overall Impact Significance | No Impact | No Impact | Negligible Negative | Negligible Negative | Negligible Negative | Negligible Negative |

During operation, control measures will be put in place in order to ensure accidental spillages of maintenance materials do not occur. As a result, the degree of impact is predicted to be low (Table 13.1). In order to determine the severity of impact, the importance of the receptor has to be considered. Based on the descriptions provided in Section 1.6, an importance level of medium has been defined since water quality changes are important for local ecosystem functioning. The resulting severity of the impact is low. Overall, the impact is considered to be of negligible negative significance as it is difficult to predict the likely scale of a spill and, therefore, a precautionary approach has been adopted (Table 13.1).

During decommissioning of the various pieces of infrastructure, limited impacts on water quality are anticipated as the sediments are not contaminated. As a result, the degree of impact is considered to be low. The importance of the receptor is defined as medium due to the importance of water quality for local ecosystem functioning. The resulting severity of the impact is low. Overall, an impact of negligible negative significance is predicted (Table 13.1).

## 13.2. Impacts on Natura 2000 Sites

Due to the considerable distance from the proposed wind farm area and the limited, local and temporary magnitude of change to hydrography, sediment spill and water quality caused by construction, operation and decommissioning of the wind farm, the degree of impact is predicted to be low. Due to the designated status of the potential receptor, the importance is assessed as very high and so the resulting severity of the impact is predicted to be low. Overall, due to the distance of the development from the designated sites and the relatively small effects in terms of scale, no impact is predicted (Table 13.2).

Table 13.2. Summary of impact assessment for water quality related to Natura 2000 sites.

| Parameter | Construction | Operation | Decommissioning |
|---|---|---|---|
| Magnitude of Pressure | Low | Low | Low |
| Sensitivity | Medium | Medium | Medium |
| Degree of Impact | Low | Low | Low |
| Importance | Very High | Very High | Very High |
| Severity of Impact | Low | Low | Low |
| Overall Impact Significance | No Impact | No Impact | No Impact |

## 13.3. Impacts on Suspended Sediment Concentrations and Deposition

The degree of impact is predicted to be low for both suspended sediment in the water column and sediment deposition from the plume for both the construction and decommissioning of the wind farm. In order to determine the severity of impact, the importance of the receptor has to be considered. Based on the descriptions provided in Section 1.6, an importance level of medium has been defined, since changes to suspended sediment concentrations in the water column and variations in sediment deposition rates are important for local ecosystem functioning. The resulting severity of the impact is therefore low. Overall, the significance of the impact is considered to be negligible negative since the impacts are localised, short term and will revert to baseline conditions following cessation of the activities (Table 13.3).

Table 13.3. Summary of impact assessment for suspended sediment concentrations and deposition for the foundations, substation, inter-array and export cables..

| Parameter | Construction | Decommissioning |
|---|---|---|
| Magnitude of Pressure | Low | Low |
| Sensitivity | Medium | Medium |
| Degree of Impact | Low | Low |
| Importance | Medium | Medium |
| Severity of Impact | Low | Low |
| Overall Impact Significance | Negligible Negative | Negligible Negative |

## 13.4. Impacts on Tidal Currents and Waves

The degree of impact is predicted to be low for both tidal currents and waves during operation of the wind farm. In order to determine the severity of impact, the importance of the receptor has to be considered. Based on the descriptions provided in Section 1.6, an importance level of medium has been defined, since changes to tidal current velocities and wave heights may result in changes to sediment transport patterns both offshore and at the coast. The resulting severity of the impact is therefore low. Since the very small changes to tidal current velocities and wave heights caused by the foundations will not affect sediment transport over and above the natural baseline processes, no impact is predicted (Table 13.4).

Table 13.4. Summary of impact assessment for tidal current velocities and wave heights during operation of the foundations.

| Parameter | Operation | |
|---|---|---|
| | Tidal Currents | Waves |
| Magnitude of Pressure | Low | Low |
| Sensitivity | Low | Low |
| Degree of Impact | Low | Low |
| Importance | Medium | Medium |
| Severity of Impact | Low | Low |
| Overall Impact Significance | No Impact | No Impact |

## 13.5. Impacts at the Landfall

At the coastal landfall site, longshore sediment transport has the potential to be affected by the temporary construction of a trench. The results of expert judgement show that the short-term and temporary nature of the construction mean that the trench will have no impact on natural coastal processes. In addition, a large proportion of the sediment moving along the coast at Houstrup Strand will be able to bypass the trench on its seaward side.

*Construction works at Houstrup Strand*

## 14. REFERENCES


Aagaard, T., Nielsen, N., & Nielsen, J. (1995). Skallingen – origin and evolution of a barrier spit. Medd. F. Skallinglab, 35, 85pp.

Aagaard, T., Nielsen, J., Jensen, S.G., & Friderichsen, J. (2004). Longshore sediment transport and coastal erosion at Skallingen, Denmark. *Danish Journal of Geography*, 104, 5-14.

Aagaard, T., & Sørensen, P. (2013). Sea level rise and the sediment budget of an eroding barrier on the Danish North Sea coast. In: Conley, D.C., Masselink, G., Russell, P.E. and O'Hare, T.J. (eds): Proceedings of the 12th International Coastal Symposium (Plymouth, England), *Journal of Coastal Research, Special Issue*, 65, 434-439.

Andersen, P. (2006). *EIA Report. Water Quality. Horns Rev 2 Offshore Wind Farm*. Report to DONG Energy.

Anthony, D., & Leth, J.O. (2002). Large-scale bedforms, sediment distribution and sand mobility in the eastern North Sea off the Danish west coast. *Marine Geology*, 182, 247–263.

Bartholdy, J., & Madsen, P.F. (1985). Accumulation of fine grained material in a Danish tidal area. *Marine Geology*, 67, 121-137.

Bartholdy, J., Christiansen, C., & Kunzendorf, H. (2004). Long term variations in backbarrier salt marsh deposition on the Skallingen peninsula - the Danish Wadden Sea. *Marine Geology*, 203, 1-21.

Bio/consult. (1999). *Forundersøgelse for Havmøllepark på Horns Rev. Miljøbiologiske forhold. Kortlægning af bundforhold 1999*. Datarapport, August 1999.

Bio/consult. (2000). *Horns Rev Offshore Wind Power Farm Environmental Impact Assessment on Water Quality*. Report to I/S ELSAM, May 2000.

Bio/consult. (2006). *EIA Report Water Quality. Horns Rev 2 Offshore Wind Farm*. Report to ENERGI E2, July 2006.

Cefas. (2001). *Contaminant Status of the North Sea*. Technical Report Produced for Strategic Environmental Assessment. August 2001.

Christiansen, C., Aagaard, T., Bartholdy, J., Christiansen, M., Nielsen, J., Nielsen,N., Pedersen, J.B.T., & Vinther, N. (2004). Total sediment budget of a transgressive barrier-spit, Skallingen, SW Denmark: A review. *Danish Journal of Geography*, 104, 107-126.

Clemmensen, L.B., Pedersen, K., Murray, A., & Heinemeier, J. (2006). A 7000-year record of coastal evolution, Vejers, SW Jutland, Denmark. *Bulletin of the Geological Society of Denmark*, 53, 1-22.

DHI (Danish Hydraulic Institute). (2006). *Horns Rev 2 Offshore Wind Farm Coastal Impact Assessment*. Report to Energi E2 A/S, May 2006.

DHI (Danish Hydraulic Institute. (2009). *Anholt Offshore Wind Farm Hydrography, Sediment Spill, Water Quality, Geomorphology and Coastal Morphology*. Report to Energinet.dk, October 2009.

DHI (Danish Hydraulic Institute). (2011). *MIKE 21 & MIKE 3 Flow Model FM Hydrodynamic and Transport Module Scientific Documentation*.

Energinet.dk. (2014). *Technical Project Description for the Large-scale Offshore Wind Farm (400 MW) at Horns Rev 3*.

Forewind. (2013). *Dogger Bank Creyke Beck Offshore Wind Farm Environmental Statement*. Chapter 9 Marine Physical Processes.

Frandsen, S.T., Jørgensen, H.J., Barthelmie, R.B., Rathman, O., Badger, J., Hansen, K., Ott, S., Rethore, P.-E., & Larsen, S.E. (2009). The making of a second-generation wind farm efficiency model complex. *Wind Energy*, 12, 445–458.

Fruergaard, M., Andersen, T.J., Johannessen, P.N., Nielsen, L.H., & Pejrup, M. (2013). Major coastal impact induced by 1000-year storm event. *Nature Scientific Reports*, 3, 1-17.

GEO (Danish Geotechnical Institute). (2013). *Horns Rev 3 Offshore Wind Farm Geo Investigations 2013. Factual Report – Seabed CPTs and Geotechnical Boreholes*. Report to Energinet.dk, November 2013.

Horowitz, J.A. (1991). A Primer on Sediment-Trace Element Chemistry, 2nd Edition. United States Geographical Survey. Open File Report 91-76.

Houmark-Nielsen, M. (2003). The Pleistocene of Denmark: a review of stratigraphy and glaciation history. In: Ehlers, J. and Gibbard, P. (eds): Quaternary Glaciation-extent and chronology, Volume 1, Europe. Elsevier (Amsterdam), 321-336.

IPCC (Intergovernmental Panel on Climate Change). (2013). *Climate Change 2013: The Physical Science Basis. Working Group I Contribution to the IPCC Fifth Assessment Report*. Summary for Policymakers, September 2013, 36pp.

Knudsen, S.B., Sørensen, C., & Sørensen, P. (2008). *Mean Sea Levels in the Danish Wadden Sea*. Danish Coastal Authority, 38pp (in Danish with English summary).

Larsen, B. (2003). Blåvands Huk – Horns Rev området – et nyt Skagen? Geologi nyt fra GEUS. Temanummer, Issue 4.

Larsen, B., & Andersen, L.T. (2005). Late Quaternary stratigraphy and morphogenesis in the Danish eastern North Sea and its relation to onshore geology. *Netherlands Journal of Geosciences - Geologie en Mijnbouw*, 84, 113-128.

Leth, J.O., Larsen, B., & Anthony, D. (2004). Sediment distribution and transport in the shallow coastal waters along the west coast of Denmark. *Bulletin of the Geological Survey of Denmark and Greenland*, 4, 41-44.

Nielsen, S.T., Clemmensen, L.B., & Andreasen, F. (1995). The middle and late Holocene barrier spit system at Vejers, Denmark: structure and development. *Bulletin of the Geological Society of Denmark*, 42, 105-119.

Orbicon. (2013). *Horns Reef 3 Offshore Wind Farm. Method for EIA*. Report to Energinet.dk, July 2013 (draft).

Orbicon. (2014). Horns Rev 3 Offshore Wind Farm. Fish Ecology. Technical report no. 5. Report to Energinet.dk.

OSPAR (Oslo/Paris Convention). (2008). *Overview of Contracting Parties' National Action Levels for Dredged Material (2008 update)*.

OSPAR (Oslo/Paris Convention). (2010). *OSPAR Commission Quality Status Report 2010*. Available at http://qsr2010.ospar.org/en/ch01_02.html

Praem-Larsen, F., & Kofoed, C. (2013). *Extremes at Horns Rev III*. Internal note, 2013 [key words: mean wind speed, significant wave height, extremes, return periods].

Ramboll. (2013a). *Horns Rev 3 OWF Geophysical Survey Results*. Report to Energinet.dk, July 2013.

Ramboll. (2013b). *Horns Rev 3 OWF Interpretive Survey Report*. Report to Energinet.dk, July 2013.

Sørensen, C., Madsen, H.T., & Knudsen, S.B. (2013). *Højvandsstatistikker 2012*. Kystdirektoratet. 160pp.

Zang, J., Gibson, R., Taylor, P. H., Eatock Taylor, R., & Swan, C. (2006). Second order wave diffraction around a fixed ship-shaped body in unidirectional steep waves. *Journal of Offshore Mechanics and Arctic Engineering*, 128, 89-99.

Zang, J., Liu, S., Eatock Taylor, R., & Taylor, P. H. (2009). Wave run-up and response spectrum for wave scattering from a cylinder. *International Journal of Offshore and Polar Engineering*, 19, 183-188.

## Appendix A

Calibration statistical parameters for IHO stations around the North Sea.

| Number | Longitude | Latitude | Station name IHO | Station Code | Country | Statistical Parameters | | |
|---|---|---|---|---|---|---|---|---|
| | | | | | | RMSE | BIAS | R-Squared |
| 1 | 2.92 | 51.24 | Ostend | OS | Belgium | 0.25 | 0.00 | 0.97 |
| 2 | 3.22 | 51.35 | Zeebrugge | ZE | Belgium | 0.41 | 0.05 | 0.90 |
| 3 | 2.61 | 51.58 | Noordhinderl | NO | Belgium | 0.26 | 0.04 | 0.92 |
| 4 | 8.433333 | 55.4666 | Esbjerg | ES | Denmark | 0.13 | -0.01 | 0.93 |
| 5 | -1.61 | 49.66 | Cherbourg | CHB | France | 0.15 | -0.06 | 0.99 |
| 6 | 1.07 | 49.93 | Dieppe | DI | France | 0.32 | -0.02 | 0.98 |
| 7 | 2.38 | 51.06 | Dunkerque | DUK | France | 0.25 | -0.03 | 0.98 |
| 8 | -2.57 | 47.3 | Lecroisic | LES | France | 0.28 | 0.00 | 0.96 |
| 9 | 0.09 | 49.48 | Lehavre | LEV | France | 0.31 | 0.02 | 0.98 |
| 10 | -5.1 | 48.45 | Ouessant | OU | France | 0.29 | -0.10 | 0.97 |
| 11 | -1.07 | 45.58 | Pointedegrave | POG | France | 0.34 | -0.04 | 0.93 |
| 12 | -3.47 | 47.65 | Porttudy | POD | France | 0.21 | -0.06 | 0.97 |
| 13 | -1.24 | 44.64 | Rotondecapferre | ROF | France | 1.67 | 0.18 | -1.28 |
| 14 | -2.0364 | 48.65852 | Sainthelier | SAL | France | 0.31 | -0.08 | 0.99 |
| 15 | -2.11 | 49.16 | Saintpeterport | SAP | France | 0.21 | -0.06 | 0.99 |

| Number | Longitude | Latitude | Station name IHO | Station Code | Country | Statistical Parameters | | |
|---|---|---|---|---|---|---|---|---|
| | | | | | | RMSE | BIAS | R-Squared |
| 16 | -2.53 | 49.45 | Saint-Servani | SAS | France | 0.63 | 0.20 | 0.96 |
| 17 | -1.64 | 43.42 | Socoa | SOC | France | 0.10 | 0.00 | 0.99 |
| 18 | 8.83 | 54.1 | Buesum | BUS | German | 0.98 | 0.19 | 0.36 |
| 19 | 8.73 | 53.86 | Cuxhaven | CU | German | 0.71 | 0.18 | 0.54 |
| 20 | 8.07 | 53.84 | Rotersandleucht | ROD | German | 0.32 | 0.03 | 0.90 |
| 21 | -6.21 | 55.22 | Ballycastlebay | BAL | Ireland | 0.23 | -0.02 | 0.29 |
| 22 | -10.06 | 54.09 | Blacksodquay | BLQ | Ireland | 0.17 | 0.00 | 0.97 |
| 23 | -5.8 | 54.88 | Carrickfergus | CAF | Ireland | 0.42 | -0.01 | 0.78 |
| 24 | -9.19841 | 51.50175 | Castletownshend | CAT | Ireland | 0.20 | -0.01 | 0.95 |
| 25 | -9.07 | 53.25 | Galway | GA | Ireland | 0.27 | -0.03 | 0.95 |
| 26 | -6.069595 | 53.35771 | Howth | HO | Ireland | 0.36 | 0.00 | 0.89 |
| 27 | -8.44 | 54.617 | Killybegs | KIB | Ireland | 0.23 | -0.02 | 0.95 |
| 28 | -9.520934 | 52.62144 | Kilrush | KIR | Ireland | 0.34 | 0.02 | 0.93 |
| 29 | -7.22 | 55.42 | Portmore | POM | Ireland | 0.24 | -0.02 | 0.91 |
| 30 | -6.669446 | 55.208413 | Portrush | POR | Ireland | 0.29 | 0.00 | 0.63 |
| 31 | -6.370031 | 52.27346 | Rosslare | ROL | Ireland | 0.21 | -0.02 | 0.82 |
| 32 | -6.02 | 52.98 | Wicklow | WIL | Ireland | 0.27 | -0.04 | 0.83 |
| 33 | 6.65 | 53.59 | Borkumsuedstrand | BO | Netherlands | 0.20 | 0.04 | 0.94 |

| Number | Longitude | Latitude | Station name IHO | Station Code | Country | Statistical Parameters | | |
|---|---|---|---|---|---|---|---|---|
| | | | | | | RMSE | BIAS | R-Squared |
| 34 | 6.97229 | 53.3294 | Delfzijl | DEF | Netherlands | 0.80 | 0.19 | 0.33 |
| 35 | 4.32 | 52.96 | Haakslv | HA | Netherlands | 0.21 | 0.04 | 0.82 |
| 36 | 4.42 | 52.51 | Katwijk | KA | Netherlands | 0.42 | -0.03 | 0.37 |
| 37 | 3.9 | 52.02 | Maaslv | MA | Netherlands | 0.25 | 0.05 | 0.78 |
| 38 | 3.48 | 51.77 | Schouwenbankl | SCW | Netherlands | 0.27 | 0.05 | 0.84 |
| 39 | 4.86 | 53.44 | Terschellingerba | TE | Netherlands | 0.21 | 0.03 | 0.89 |
| 40 | 5.382 | 53.174 | Vlieland | VL | Netherlands | 0.46 | 0.04 | 0.27 |
| 41 | -5.7 | 43.57 | Gijon | GI | Spain | 0.10 | -0.04 | 0.99 |
| 42 | -3.77 | 43.47 | Santander | SAT | Spain | 0.16 | -0.04 | 0.98 |
| 43 | -2.06 | 57.15 | Aberdeen | ABN | United Kingdom | 0.13 | -0.04 | 0.99 |
| 44 | -4.04 | 52.54 | Aberdovey | ABV | United Kingdom | 0.21 | 0.03 | 0.97 |
| 45 | -1.56 | 55.34 | Amble | AM | United Kingdom | 0.17 | 0.01 | 0.98 |
| 46 | -2.69 | 56.22 | Anstruthereaster | AN | United Kingdom | 0.14 | 0.01 | 0.99 |
| 47 | -5.82924 | 57.43279 | Applecross | AP | United Kingdom | 0.51 | 0.09 | 0.84 |
| 48 | -2.6 | 56.55 | Arbroath | AR | United Kingdom | 0.13 | 0.01 | 0.99 |
| 49 | -2.730904 | 51.523105 | Aust | AU | United Kingdom | 2.02 | 0.87 | 0.63 |
| 50 | 1.44 | 52 | Bawdsey | BAW | United Kingdom | 0.19 | 0.02 | 0.96 |
| 51 | -1.994733 | 55.78422 | Berwick | BE | United Kingdom | 0.22 | 0.01 | 0.97 |

| Number | Longitude | Latitude | Station name IHO | Station Code | Country | Statistical Parameters | | |
|---|---|---|---|---|---|---|---|---|
| | | | | | | RMSE | BIAS | R-Squared |
| 52 | -0.15 | 54.57 | Blyth | BLY | United Kingdom | 0.49 | 0.00 | 0.86 |
| 53 | -0.19 | 54.08 | Bridlington | BRL | United Kingdom | 0.20 | -0.01 | 0.98 |
| 54 | -2.76 | 50.69 | Bridport | BRP | United Kingdom | 0.19 | 0.01 | 0.97 |
| 55 | -0.12 | 50.81 | Brighton | BRT | United Kingdom | 0.33 | 0.03 | 0.97 |
| 56 | -5.13 | 55.58 | Brodickbay | BRB | United Kingdom | 0.30 | 0.01 | 0.86 |
| 57 | -3.5 | 57.7 | Burghead | BUH | United Kingdom | 0.25 | 0.01 | 0.93 |
| 58 | -5.58 | 55.42 | Campbeltown | CAB | United Kingdom | 0.25 | 0.01 | 0.88 |
| 59 | -2.48 | 50.56 | Chesilbeach | CHS | United Kingdom | 0.14 | 0.00 | 0.98 |
| 60 | -5.93 | 55.83 | Craighouse | CR | United Kingdom | 0.24 | 0.01 | -0.16 |
| 61 | 1.42 | 51.19 | Deal | DEA | United Kingdom | 0.29 | -0.01 | 0.97 |
| 62 | -4.47 | 54.13 | Douglas | DO | United Kingdom | 0.36 | -0.07 | 0.96 |
| 63 | -2.52013 | 56.00684 | Dunbar | DUB | United Kingdom | 0.17 | 0.01 | 0.98 |
| 64 | -2.93702 | 56.4533 | Dundee | DUD | United Kingdom | 0.31 | 0.01 | 0.95 |
| 65 | 0.97 | 50.9 | Dungeness | DUS | United Kingdom | 0.36 | 0.02 | 0.97 |
| 66 | 0.3 | 50.76 | Eastbourne | EA | United Kingdom | 0.38 | 0.01 | 0.97 |
| 67 | -2.78 | 56.08 | Fidraisland | FI | United Kingdom | 0.19 | 0.01 | 0.98 |
| 68 | -4.634 | 50.312 | Fowey | FO | United Kingdom | 0.15 | 0.01 | 0.99 |
| 69 | -4.83 | 55.96 | Gourockgreenock | GO | United Kingdom | 0.38 | -0.09 | 0.83 |

| Number | Longitude | Latitude | Station name IHO | Station Code | Country | Statistical Parameters | | |
|---|---|---|---|---|---|---|---|---|
| | | | | | | RMSE | BIAS | R-Squared |
| 70 | 1.34 | 51.76 | Gunfleetlighthou | GU | United Kingdom | 0.22 | 0.03 | 0.96 |
| 71 | 1.12 | 51.39 | Hernebay | HEB | United Kingdom | 0.29 | 0.05 | 0.95 |
| 72 | -2.93 | 54.04 | Heys | HES | United Kingdom | 0.58 | -0.01 | 0.95 |
| 73 | -3.21 | 53.37 | Hilbreisland | HIL | United Kingdom | 0.50 | -0.03 | 0.96 |
| 74 | -3.12 | 51.24 | Hinkleypoint | HIP | United Kingdom | 1.40 | 0.50 | 0.80 |
| 75 | -0.19 | 53.64 | Imming | IM | United Kingdom | 0.64 | 0.13 | 0.88 |
| 76 | -4.16 | 57.68 | Invergordon | ING | United Kingdom | 0.21 | 0.01 | 0.97 |
| 77 | -4.25 | 57.5 | Inverness | INS | United Kingdom | 0.29 | 0.01 | 0.94 |
| 78 | -6.39 | 56.32 | Iona | IO | United Kingdom | 0.32 | 0.01 | 0.89 |
| 79 | -4.36062 | 54.69253 | Isleofwhithorn | IS | United Kingdom | 0.36 | -0.01 | 0.96 |
| 80 | -2.9579 | 58.99678 | Kirkwal | KIW | United Kingdom | 0.19 | 0.04 | 0.93 |
| 81 | -5.710012 | 57.2783 | Kyleakin | KY | United Kingdom | 0.30 | 0.00 | 0.95 |
| 82 | -3.15771 | 56.00178 | Leith | LET | United Kingdom | 1.75 | 0.01 | -1.51 |
| 83 | -7.03195 | 57.754836 | Leverburgh | LEB | United Kingdom | 0.26 | 0.00 | 0.94 |
| 84 | 0.54 | 50.79 | Littlehampton | LIH | United Kingdom | 0.44 | 0.01 | 0.92 |
| 85 | -3.01 | 53.42 | Liverpool | LIP | United Kingdom | 1.08 | 0.19 | 0.82 |
| 86 | -5.21 | 49.95 | Lizardpoint | LIZ | United Kingdom | 0.12 | -0.04 | 0.99 |
| 87 | -5.301251 | 58.144334 | Lochinver | LO | United Kingdom | 0.21 | 0.01 | 0.97 |

| Number | Longitude | Latitude | Station name IHO | Station Code | Country | Statistical Parameters | | |
|---|---|---|---|---|---|---|---|---|
| | | | | | | RMSE | BIAS | R-Squared |
| 88 | -4.64 | 51.15 | Lundyisland | LU | United Kingdom | 0.25 | -0.03 | 0.98 |
| 89 | -5.63 | 57.85 | Melloncharlesl | ME | United Kingdom | 0.22 | 0.01 | 0.97 |
| 90 | -5.03 | 51.7 | Milfordhavenwa | MI | United Kingdom | 0.17 | -0.04 | 0.99 |
| 91 | -0.95 | 50.67 | Nabtower | NA | United Kingdom | 0.23 | -0.02 | 0.96 |
| 92 | -5.53 | 50.1 | Newlyn | NE | United Kingdom | 0.15 | -0.04 | 0.99 |
| 93 | -3.37 | 50.6 | Orcombepoint | OR | United Kingdom | 0.19 | 0.02 | 0.97 |
| 94 | -1.73 | 57.49 | Peterhead | PE | United Kingdom | 0.28 | -0.01 | 0.90 |
| 95 | -1.93 | 50.66 | Pooleharbourent | POO | United Kingdom | 0.21 | 0.02 | 0.70 |
| 96 | -5.418386 | 56.554613 | Portappin | POI | United Kingdom | 0.32 | 0.01 | 0.89 |
| 97 | -3.69 | 51.45 | Porthcawl | POW | United Kingdom | 0.46 | 0.00 | 0.97 |
| 98 | -6.53 | 55.68 | Portnahavenando | POH | United Kingdom | 0.29 | -0.15 | 0.55 |
| 99 | -4.68 | 58.5 | Portnancon | POC | United Kingdom | 0.35 | 0.02 | 0.91 |
| 100 | -5.13 | 54.81 | Portpartrick | POP | United Kingdom | 0.25 | -0.05 | 0.94 |
| 101 | 0.28 | 52.92 | Roaringmiddle | ROM | United Kingdom | 0.60 | -0.06 | 0.90 |
| 102 | -3.78 | 50.21 | Salcombebe | SAC | United Kingdom | 0.17 | -0.01 | 0.98 |
| 103 | -6.79 | 56.48 | Scarinishtiree | SCN | United Kingdom | 0.25 | 0.00 | 0.94 |
| 104 | -3.55 | 58.61 | Scrabster | SCS | United Kingdom | 0.27 | 0.00 | 0.94 |
| 105 | 1.07 | 51.5 | Shiveringsands | SH | United Kingdom | 0.31 | 0.01 | 0.95 |

| Number | Longitude | Latitude | Station name IHO | Station Code | Country | Statistical Parameters | | |
|---|---|---|---|---|---|---|---|---|
| | | | | | | RMSE | BIAS | R-Squared |
| 106 | 0.37 | 53.14 | Skegness | SK | United Kingdom | 0.37 | -0.01 | 0.95 |
| 107 | 0.75 | 51.52 | Southend | SOE | United Kingdom | 0.46 | 0.02 | 0.91 |
| 108 | 1.68 | 52.32 | Southwold | SOW | United Kingdom | 0.15 | 0.02 | 0.94 |
| 109 | -5.47 | 50.23 | Stives | STV | United Kingdom | 0.17 | -0.01 | 0.99 |
| 110 | -2.15 | 56.95 | Stonehaven | STH | United Kingdom | 0.12 | 0.00 | 0.99 |
| 111 | -4.69 | 55.55 | Troon | TR | United Kingdom | 0.33 | 0.01 | 0.86 |
| 112 | -5.17437 | 57.890211 | Ullapool | UL | United Kingdom | 0.30 | 0.01 | 0.94 |
| 113 | -8.56 | 57.81 | Villagebay | VI | United Kingdom | 0.17 | 0.00 | 0.96 |
| 114 | -1.19 | 54.68 | Westhartlepool | WE | United Kingdom | 0.21 | -0.08 | 0.97 |
| 115 | -0.60656 | 54.493206 | Whitby | WHB | United Kingdom | 0.13 | 0.00 | 0.99 |
| 116 | -2.581 | 57.68128 | Whitehills | WHH | United Kingdom | 0.49 | -0.08 | 0.72 |
| 117 | -3.05 | 58.43 | Wick | WIK | United Kingdom | 0.12 | 0.00 | 0.98 |
| 118 | 1.705933 | 52.73091 | Winterton | WIT | United Kingdom | 0.16 | -0.01 | 0.96 |
| 119 | -3.581184 | 54.646892 | Workington | WO | United Kingdom | 0.38 | 0.00 | 0.97 |
| 120 | -4.48 | 53.43 | Wylfahead | WY | United Kingdom | 0.26 | -0.08 | 0.98 |
| 121 | -1.494152 | 50.710439 | Yarmouth | YA | United Kingdom | 0.24 | 0.02 | 0.84 |